



First-day road log: From Bernalillo to San Ysidro, southern Nacimiento Mountains, Guadalupe Box, Jemez Springs, Valles Caldera, and Los Alamos

Margaret Anne Rogers, Barry S. Kues, Fraser Goff, Frank J. Pazzaglia, Lee A. Woodward, Spencer G. Lucas, and Jamie N. Gardner

1996, pp. 1-39. <https://doi.org/10.56577/FFC-47.1>

in:
Jemez Mountains Region, Goff, F.; Kues, B. S.; Rogers, M. A.; McFadden, L. S.; Gardner, J. N.; [eds.], New Mexico Geological Society 47th Annual Fall Field Conference Guidebook, 484 p. <https://doi.org/10.56577/FFC-47>

This is one of many related papers that were included in the 1996 NMGS Fall Field Conference Guidebook.

Annual NMGS Fall Field Conference Guidebooks

Every fall since 1950, the New Mexico Geological Society (NMGS) has held an annual [Fall Field Conference](#) that explores some region of New Mexico (or surrounding states). Always well attended, these conferences provide a guidebook to participants. Besides detailed road logs, the guidebooks contain many well written, edited, and peer-reviewed geoscience papers. These books have set the national standard for geologic guidebooks and are an essential geologic reference for anyone working in or around New Mexico.

Free Downloads

NMGS has decided to make peer-reviewed papers from our Fall Field Conference guidebooks available for free download. This is in keeping with our mission of promoting interest, research, and cooperation regarding geology in New Mexico. However, guidebook sales represent a significant proportion of our operating budget. Therefore, only *research papers* are available for download. *Road logs*, *mini-papers*, and other selected content are available only in print for recent guidebooks.

Copyright Information

Publications of the New Mexico Geological Society, printed and electronic, are protected by the copyright laws of the United States. No material from the NMGS website, or printed and electronic publications, may be reprinted or redistributed without NMGS permission. Contact us for permission to reprint portions of any of our publications.

One printed copy of any materials from the NMGS website or our print and electronic publications may be made for individual use without our permission. Teachers and students may make unlimited copies for educational use. Any other use of these materials requires explicit permission.

This page is intentionally left blank to maintain order of facing pages.

FIRST-DAY ROAD LOG, FROM BERNALILLO TO SAN YSIDRO, SOUTHERN NACIMIENTO MOUNTAINS, GUADALUPE BOX, JEMEZ SPRINGS, VALLES CALDERA, AND LOS ALAMOS

MARGARET ANNE ROGERS, BARRY S. KUES, FRASER GOFF, FRANK J. PAZZAGLIA, LEE A. WOODWARD,
SPENCER G. LUCAS and JAMIE N. GARDNER

THURSDAY, SEPTEMBER 26, 1996

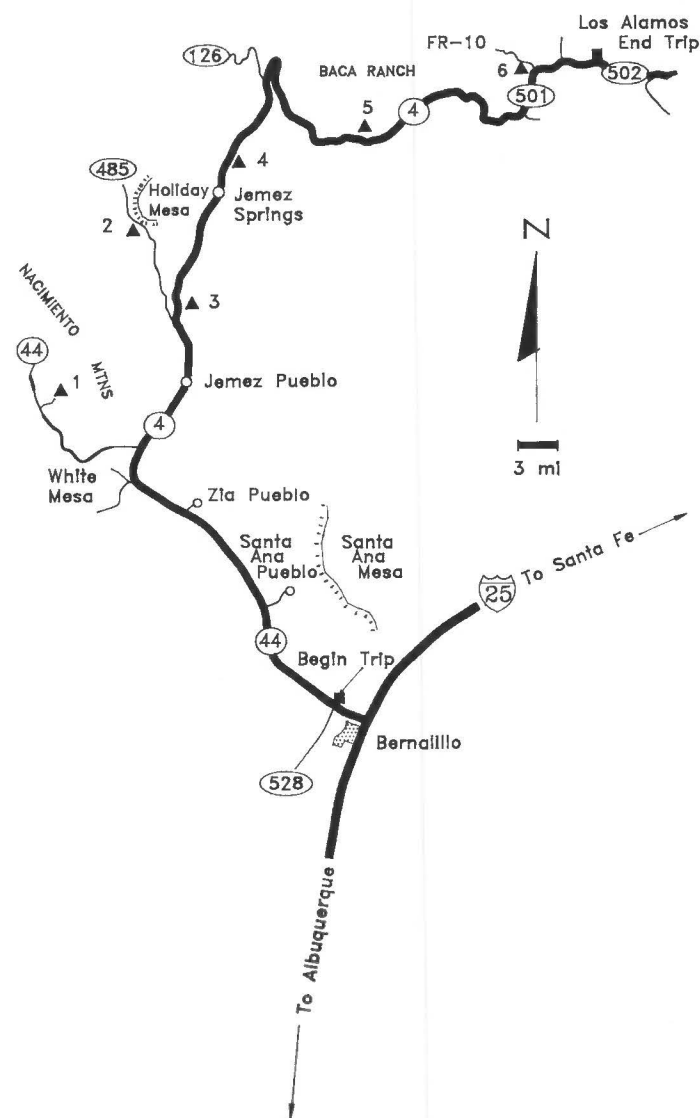
Assembly point: Corrales Road at NM-44, Bernalillo
Time: 7:00 AM
Distance: 113.8 miles
Stops: 6

Summary

The First-Day road log begins on the west side of Bernalillo at the NM-44/Corrales Road (NM-528) junction. To get to the rendezvous point from Albuquerque, take I-25 north. Leave the interstate at Exit 242, the second Bernalillo exit, which is 16 mi from the I-25/I-40 interchange. At the stoplight, turn left onto NM-44 heading west, cross above I-25, and continue through stoplights at NM-313 (Camino del Pueblo, 0.7 mi) and Don Tomas Road (1.2 mi), cross the Rio Grande (1.4 mi), note road to Coronado State Park to right (1.7 mi), and line up (as close together as possible) along right side of NM-44 at the Corrales intersection (2.5 mi). Corrales Road (NM-528) leads south to Rio Rancho.

Today's trips head northwest on NM-44 mainly through Miocene Zia Formation exposures along the west side of the Jemez River, past Mesa Blanca (White Mesa) to San Ysidro, then skirts the southern end of the Nacimiento Mountains to Stop 1. Here, near the range-bounding Pajarito fault, we will observe and discuss the structure, tectonics and stratigraphy of the Nacimientos, large travertine mounds developed around hot springs, and other Quaternary features of the mountain front. Returning to San Ysidro, the trip proceeds north on NM-4 through Jemez Pueblo and turns northwest on NM-485 to Guadalupe Box. At Stop 2, Precambrian gneiss, overlain by an excellent Mississippian-Pennsylvanian sequence will be examined, as well as the Rio Guadalupe's erosion through the Precambrian. Surrounding mesas display thick Pleistocene Bandelier Tuff resting on paleotopography formed in Permian Yeso strata.

Returning to NM-4, the trip pauses, if time allows, at optional Stop 3, for a superb view of the Bandelier Tuff on Guadalupe Mesa, discussions of the geomorphic history of the Jemez River, and stratigraphy and paleontology of the Permian Abo and Yeso Formations. Proceeding north, we pass through Jemez Springs town and down-section into the Pennsylvanian Madera Forma-



tion, stopping next (Stop 4) at Soda Dam, an unusual travertine dam deposited by hot springs across the Jemez River. Here we will learn more about the relationships of the hydrothermal features in San Diego Canyon to the Valles caldera, examine the structure along the Jemez fault system, and observe and discuss the stratigraphy and paleontology of the Madera Formation.

Continuing north on NM-4, we leave Paleozoic sedimentary rocks and pass into a terrain dominated by the youngest eruptions of the Valles caldera, turning east toward Los Alamos. At Stop 5

we will view the very young (50–60 ka) El Cajete pumice deposits, then turn north on NM-501 for the final stop of the day, an overview of the Pajarito Plateau and its geology and structure. Continuing on to Los Alamos, we complete Day 1's trip with a banquet at the historic Fuller Lodge.

We thank Hedy Dunn and Georgia Strickfaden of the Los Alamos Historical Society for some of the comments provided for the last 3 mi of the road log.

Mileage

0.0 Junction of NM-44 and NM-528. View to north shows Jemez Mountains on skyline at 2:00. At 3:00 to 4:00, Canjilon Hill, about 1 mi south of the confluence of the Jemez River and Rio Grande, is in the middle distance. The south end of Santa Ana Mesa rises behind it.

Canjilon Hill is a well-preserved tuff-breccia diatreme, oval in shape, about 0.8 mi long and 200 ft high. The diatreme is the root of a much larger tuff ring or maar that probably developed on the same surface as the San Felipe volcanic field that covers Santa Ana Mesa (Kelley and Kudo, 1978). Kudo et al. (1977) reported a K-Ar age of 2.6 Ma for Canjilon Hill, slightly older than the 2.5 Ma age (Bachman and Mehnert, 1977) of the basal San Felipe volcanic flow. These ages are the same within the uncertainties.

Santa Ana Mesa, visible for many miles to the north and east of NM-44, covers an area of about 40 mi² between the Rio Grande and the Jemez River. The slopes are eroded exposures of Santa Fe Group strata, and the top is capped by basalt flows, tuffs, and cinder cones of the San Felipe volcanic field (Kelley and Kudo, 1978).

Our trip begins in the northern Albuquerque basin, characterized as a down-to-the-east half-graben (Fig. 1.1). Recent seismic reflection data places a major westward dipping listric normal structure, the Rio Grande fault, beneath the Rio Grande (Russell and Snelson, 1994). It is unclear if or where this fault actually breaks the land surface. At least 200 ft of offset of a Guaje Pumice (1.6 Ma) layer in the upper portion of the Santa Fe Group east of the Rio Grande constrains the amount of Pleistocene deformation on this structure.

The town of Bernalillo was founded in 1695, although Spanish influence dates from 1540, when Coronado's party wintered at a Tiguex village (Kuaua pueblo, excavated in the 1930s and included within Coronado State Park) in the area. Don Diego de Vargas, who led the Reconquest of

New Mexico after the Pueblo Revolt of 1680, died here in 1704, after a battle with Apache Indians in the Sandia Mountains (Pearce, 1965). The town became an important trading center, approaching Albuquerque's population in the mid- to late 19th century (in 1880, Albuquerque had 2300 residents; Bernalillo 1200), and was county seat of a much larger Bernalillo County when it was created in 1852. In 1880, the Santa Fe Railroad, after laying its tracks through Bernalillo with the intention of locating its yards and shops there, was thwarted by a powerful landowner; and the railroad built them in Albuquerque instead. Albuquerque boomed while Bernalillo became a brief stop on the line and remained a small town (Chilton et al., 1984). It became the county seat of Sandoval County when the county was created in 1903.

To the south along NM-528 sprawls fast-growing Rio Rancho, essentially a suburb of Albuquerque but now the 5th largest city in the state. **0.1**

0.1 Road ascends West Mesa, underlain by the Santa Fe Group, for about the next 4 mi. West Mesa is the divide between the Rio Grande rift axial drainage from the Rio Puerco axial system to the west. Incision of the Rio Grande to its present elevation probably began in the middle Pleistocene (Hawley et al., 1982), following a decrease in sediment yield from the Jemez Mountains as well as an increase in mean discharge following integration of the San Luis basin drainage to the north (Wells, et al., 1987). The West Mesa was already abandoned as an active fluvial surface prior to the extrusion of basalt to form the Albuquerque volcanoes to the south, which are thought to date from between 250 and 80 ka (Geissman et al., 1990). Important late Quaternary deposits on the West Mesa landscape include minor inset terraces along the major washes and several generations of late (?) Pleistocene and Holocene dunes. **1.5**

1.6 NM Highway Department Historic Marker on left for Bernalillo. **0.3**

1.9 Water tank on left. Roadcut in sand and gravel of the upper Zia Sandstone, known to earlier writers as the "middle red member" of the Santa Fe Formation. Bryan and McCann (1937, 1938) divided Neogene basin fill of the northern Albuquerque basin into three informal members of the Santa Fe Formation—the "lower gray", "middle red" and "upper buff" members. Kelley (1977) replaced the informal name upper buff member with Ceja Member, and Galusha (1966) introduced the term Zia Sand Formation, subsequently

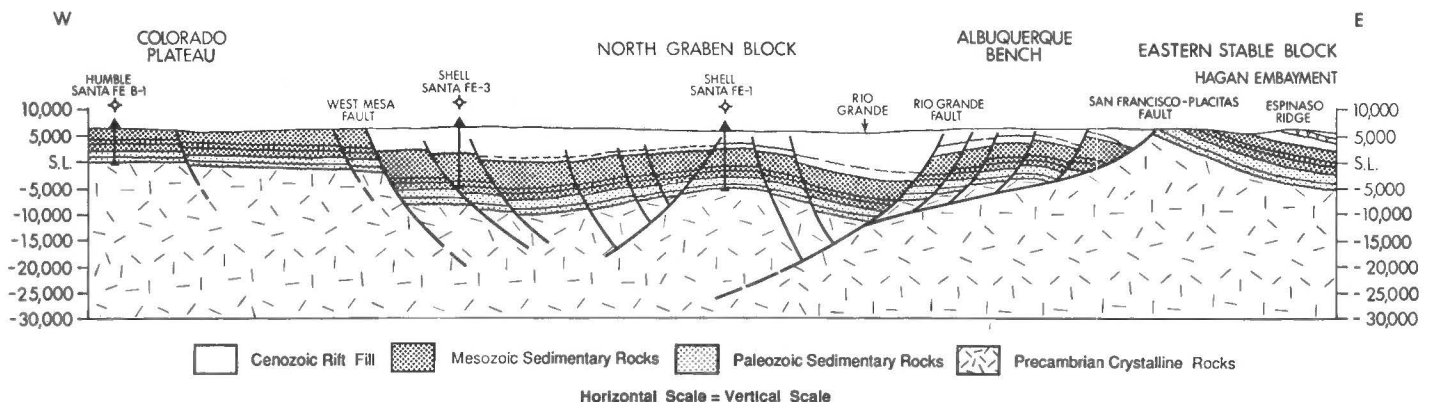


FIGURE 1.1. East-west structure cross section through the northern Albuquerque basin.

modified to Zia Formation by Lucas and Ingersoll (1981) and Tedford (1982), for the lower gray member and most of the middle red member. Tedford (1982) included the remainder of the middle red member in the Zia Formation, which currently consists of four members (in ascending order): Piedra Parada, Chamisa Mesa, Canada Pilares, and unnamed members. Fossil mammals from the Zia Formation and overlying Ceja Formation of the Santa Fe Group provide the best current means for age correlation of these units. The Zia Formation ranges in age from late Arikareean (early Miocene) to Clarendonian (late Miocene), whereas the few fossil mammals from the Ceja Formation indicate a Blancan (Pliocene) age (Tedford, 1981).

The Santa Fe Group in this area is part of a large fan-delta complex that prograded into the Albuquerque basin from the northwest (Hawley et al., 1995). This fan-delta contains axial stream facies of the paleo-Jemez River and Rio Puerco, which constitute an excellent and productive aquifer beneath Rio Rancho and the northern portion of the West Mesa. **0.3**

- 2.2 Exposures of upper Zia ("middle red member") Formation in roadcut to right. **1.1**
- 3.3 Roadcut in upper Zia Formation. **0.2**
- 3.5 Small road to left. **0.5**
- 4.0 Road crests Loma Barbon (Billy Goat Hill), through roadcuts in the upper Zia Formation, consisting here of east-dipping, reddish and tan, poorly indurated sandstone. **0.1**
- 4.1 Excellent Zia badlands exposures in arroyo to the right (north) (Fig. 1.2) are capped with eolian material. Road crosses poorly exposed south end of Santa Ana fault (Kelley, 1977). Good view to right in distance at 3:00 of Santa Ana Mesa, capped with 2.5 Ma basalts above Santa Fe Group sediments. The basalts probably flowed down paleovalleys. Widespread topographic inversion has resulted in the former valley lows now sitting high in the landscape. Kelley (1977) speculated that the Santa Ana basalts were extruded upon the Ortiz pediplane (Bryan and McCann, 1936, 1938), a widespread, fluvially cut surface extending from Mesa Prieta to the west to the Ortiz Mountains to the east. Our present understanding of the age of basalts or sediments overlying this surface indicates that it is diachronous, casting doubt on the appropriateness of

correlating valley bottoms of concordant elevations across wide areas. The step-like nature of Santa Ana Mesa is caused by down-to-the-east normal faults. **0.3**

- 4.4 The southern end of the Nacimiento uplift is visible on the far horizon. The high, isolated peak at 12:00 is Pajarito Peak (9042 ft). On the skyline, peaks of the Sangre de Cristo range are visible at 3:00. To the left is a line of low hills developed in the Zia Formation.
- To the southwest about 2 mi, the Shell Santa Fe Pacific No. 1 well was drilled in 1972. It was abandoned at a depth of 11,045 ft, after penetrating 90 ft of Precambrian basement rocks. Pennsylvanian through Cretaceous (Mesa Verde Group) strata were reported below 3,644 ft of Cenozoic (Galisteo Formation and Santa Fe Group) units. The well was drilled on a structural high, the Ziana anticline, formed by Santa Fe Group beds drape-folded over a north-trending horst at depth (Black and Hiss, 1974; Black, 1989). **0.2**
- 4.6 Milepost (MP) 7. **0.5**
- 5.1 Entering Santa Ana Pueblo lands; folded rocks in the southern Nacimiento uplift ahead at 12:00; Redondo Peak (11,254 ft), the resurgent dome of the Valles caldera, is the highest peak in the distance at 1:00, rising above several closer, lower features (Chamisa Mesa, Pico Butte, Loma Creston) from 12:00 to 1:00; basalt-capped Santa Ana Mesa at 2:00 to 3:00. **1.0**
- 6.1 Crossing the north-trending down-to-the-east Santa Ana fault (Kelley, 1977). Highway descends next 0.6 mi through Zia Sandstone exposures, consisting of fine, light gray eolian sands with zeolite cementation forming thin resistant layers typical of the Zia. To left, note whitish bentonite beds along arroyo. **0.6**
- 6.7 Cross unnamed arroyo; excellent view to right (4:00 to 5:00) of prominent, 2-ft-thick white ash bed (Fig. 1.3) in south arroyo wall. **0.2**
- 6.9 Prominent roadcuts to left and right in Zia Formation (Fig. 1.4), consisting of poorly indurated light, fine-grained sandstone with thin, resistant cemented beds. Zia sandstone exposures continue along highway for next 0.7 mi. **0.8**
- 7.7 On right, NM Highway Department Historic Marker for Pueblo of Santa Ana and pueblo viewpoint. Route SP-74, leading northeast to the Jemez River valley and Santa Ana



FIGURE 1.2. View to northeast across badlands of Zia Formation at mile 4.1; Santa Ana Mesa in background.



FIGURE 1.3. Ash bed in south wall of unnamed arroyo, just east of NM-44 at mile 6.7.

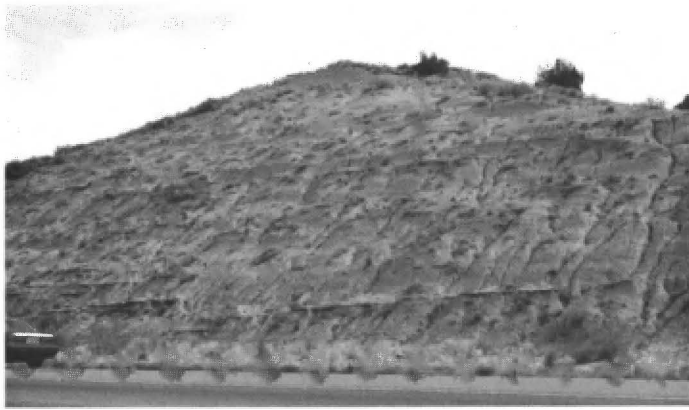


FIGURE 1.4. Roadcut in Zia sandstones at mile 6.9

Pueblo, just beyond the viewpoint. View to north of Chamisa and Borrego Mesas; Redondo Peak on the far horizon at 2:00. NM-44 parallels the Jemez River (no more than a mile away to the north) from here to the junction with NM-4 in San Ysidro. The historical marker notes: "The Keres-speaking pueblo of Santa Ana was established on its present site in 1693, as part of Diego de Vargas' reconquest of New Mexico. The spot, exposed to flooding, was poorly suited for farming, and today the residents live on their farms along the Rio Grande instead of the pueblo, which is used as a ceremonial site. The original pueblo dates from pre-Spanish times; it was destroyed after the Reconquest in 1687 and rebuilt soon afterwards. Most Santa Anans now live in a separate town, sometimes called Santa Ana Pueblo Two, just north of Bernalillo on the east side of the Rio Grande. Santa Ana is one of the smallest pueblos with about 600 members." **0.3**

- 8.0 Low exposures of Zia Formation along highway for the next 0.5 mi. A dune field may be seen about 0.5 mi north of the highway, at 3:00, along the southwest side of the Jemez River valley. The anastomosing channels of the river are the source for these sands. **0.6**
- 8.6 MP 11. **0.8**
- 9.4 Highway crosses red bridge over small arroyo; eroded ridge of Zia Formation here with basal portion of the Santa Fe Group just beyond, to the north. To left, low hills, and in distance a line of sharp-crested hills of Zia. **0.6**
- 10.0 Bridge over arroyo. **0.5**
- 10.5 Road crosses approximate location of Ziana anticline axis (Kelley, 1977). **0.4**
- 10.9 Entering Zia Pueblo lands. **0.6**
- 11.5 Bridge over arroyo, one of several unincised, north-flowing tributaries of the Jemez River. Most tributary washes to the Rio Jemez, Rio Salado and Rio Puerco are steep-walled arroyos, but others are clearly unincised. The internal and external mechanisms for triggering channel incision and aggradation still are not clearly understood. In general, most incised rivers in the desert Southwest reflect a period of valley incision between 1880 and 1920. A heated controversy has erupted involving the relative roles that climate change and anthropogenic activities (grazing) play in triggering an incision cycle. **0.3**
- 11.8 Folded rocks in Nacimiento uplift at 12:00; at 2:30, Chamisa Mesa, capped with Paliza Canyon Formation basalt of the Jemez volcanic field. Jemez Mountains on skyline to north. **0.8**
- 12.6 MP 15. **0.1**
- 12.7 Low, eroded roadcuts expose the Zia Formation for next 0.3 mi. **0.8**
- 13.4 Road crosses crest of low rise. View ahead includes White Mesa (11:30), the southern end of the Nacimiento uplift (11:30-12:30), and Chamisa Mesa (2:30). The view of the southern Nacimientos is dominated by a large, southeast-plunging, flat-bottomed syncline, its structure easily visible from here. Most of the surface of the syncline is the light tan sandstones of the Upper Triassic Agua Zarca Formation (base of the Chinle Group). The well-exposed eastern limb of the syncline displays, in ascending order, the reddish Permian Abo Formation, red-orange Yeso Formation, and light tan Glorieta Formation, overlain by a thin band of reddish Triassic Moenkopi Formation strata beneath the Agua Zarca. The Moenkopi Formation was originally mapped in this region as the Permian Bernal Formation (see Lucas and Hayden, 1991).
- Chamisa Mesa is a prominent isolated feature about 8.5 mi NNE of here. The lower part is developed in the Chamisa Mesa Member of the Zia Formation, typically a light gray eolian sandstone unit bearing mammal fossils from several productive horizons of early to middle Hemingfordian (early Miocene, about 18-20 Ma) age (Galusha, 1966; Gawne, 1976, 1981; Tedford, 1981). Chamisa Mesa is capped with Paliza Canyon basalt of the Jemez volcanic field, dated at 10.4 Ma (Bailey and Smith, 1978). **1.3**
- 14.7 Road crosses inferred trace location of down-to-the-east Zia fault (Kelley, 1977). **0.5**
- 15.2 Store and service station to left; small Zia Pueblo housing development to right. **0.3**
- 15.5 Road to Zia Pueblo on right. Zia Pueblo, built on a bluff east of the Jemez River, was visited by Coronado's expedition in 1541, and its church was built before 1613 (the present structure dates from 1692). Mid-16th century estimates suggest that as many as 5000 Zians lived in the area (Chilton et al., 1984), but the number declined steadily during Spanish colonial time. The Pueblo participated in the revolt of 1680 and suffered greatly during the reconquest. In 1688, Domingo Jironza de Cruzate led a small group of Spanish soldiers into battle with a large group of Indians from various Keres pueblos that had assembled at Zia. In the battle about 600 Indians were killed and 70 more taken to be sold as slaves. The Pueblo was sacked and burned. By 1890 the Zia population was below 100 and there were doubts that the tribe would survive, but the number by 1990 had increased to 637. The Zia sun symbol is the official insignia of New Mexico, appearing on the state flag, license plates and in the emblem of N.M.G.S. The Pueblo has recently sought to collect a multi-million dollar royalty from the state for past and future use of the symbol, but the attempt, perhaps quixotic, was unsuccessful. **0.7**
- 16.2 Ridge of Zia sandstone continues in distance to the south. **0.3**
- 16.5 MP 19. **0.5**
- 17.0 Good view of White Mesa (Mesa Blanca) at 12:00 (Fig. 1.5), with southern Nacimiento syncline (Kelley, 1977; Woodward, 1987) and exposed Permian and Triassic strata of the east limb at 12:30-1:00. Mesa Blanca is capped by white Jurassic Todilto gypsum over Entrada sandstone over



FIGURE 1.5. View of White Mesa from mile 17.0. The white cap is gypsum of the Tonque Arroyo Member of the Todilto Formation above the thin dark gray limestone of the Luciana Mesa Member. Upper walls of mesa are Entrada Formation, above slopes of Triassic Petrified Forest Formation.

red Chinle strata. Nacimiento Peak at 1:00, in the Nacimiento uplift. On skyline, high peak at 2:30 is Redondo Peak. At 3:00 can be seen Chamisa and Borrego Mesas. **0.7**

17.7 Historic Marker to right describes Vasquez de Coronado's Route. It notes: "Francisco Vasquez de Coronado, preparing to spend his second winter in New Mexico, sent out expeditions from Tiguex, near Bernalillo, in the fall of 1541 to gather supplies. Captain Francisco de Barrionuevo went as far west as Jemez Pueblo, then visited others as far north as the Rio Chama." **0.4**

18.1 White Mesa at 12:00; southern Nacimientos syncline at 1–2:00; Mid-American Pipeline System pumping station to left. New Mexico's largest gypsum mine operates on the top of White Mesa, excavating from the upper, Tonque Arroyo Member of the Jurassic Todilto Formation. White Mesa is situated near the south-plunging axis of the large syncline floored with the Triassic Agua Zarca Formation of the Chinle Group. Thus, the stratigraphic section of the mesa begins with the upper part of the Chinle Group (Petrified Forest Formation) on its northern edge, overlain by Middle Jurassic Entrada and Todilto Formations. The Todilto covers the southern dip slope of the mesa; to the south a thick, generally south-dipping Mesozoic–Cenozoic section is exposed. This section includes the Jurassic Summerville and Morrison Formations, Cretaceous Dakota and Mancos Formations and Mesa Verde Group, overlain by Eocene Galisteo Formation, Miocene Zia Formation and finally by the Pliocene Santa Fe Group. As we approach White Mesa, the Jurassic section is very visible, but most of the younger units (Mesa Verde and overlying units) are out of view, over the ridge of Zia Formation visible to the west of the highway. **0.3**

18.4 Cross bridge over Arroyo Piedra Parada. To the left, note the red beds of the Summerville Formation, overlain by yellow-brown sandstones of the Salt Wash Member of the Morrison Formation, capped by green and salmon-banded claystones of the Brushy Basin Member of the Morrison. These identifications follow the stratigraphy of Anderson and Lucas (1992, 1995), contrary to an earlier view, which called the red beds Recapture Member overlain by sandstones of the Westwater Canyon Member of the Morrison Formation (see following minipaper).

About 3 mi down the arroyo to the southwest is the type section of the Zia Sandstone, and of its lower member, the Piedra Parada Member (Galusha, 1966; Gawne, 1981), which rests disconformably on strata of the Eocene Galisteo Formation. The Piedra Parada Member is predominantly gray, cross-bedded sand with local sandstone ledges and concretionary zones, representing dune sand deposition. Fossil mammals, some described by Gawne (1975, 1976) indicate a latest Arikareean (early Miocene, ca. 20–21 Ma) age. The upper (Chamisa Mesa) member of the Zia in this area, and at the type locality near Chamisa Mesa, is of Hemingfordian (late early Miocene) age. Total thickness of the Zia Formation in this area is about 1000 ft.

The Galisteo Formation along Arroyo Piedra Parada unconformably overlies the Upper Cretaceous Menefee Formation and attains a total thickness of more than 575 ft. Petrified logs, large titanotheres, artiodactyls and turtles indicating a late Eocene age have been recovered from these exposures (Lucas, 1982). **0.3**

CONTRASTING DEPOSITIONAL ENVIRONMENTS OF THE MORRISON FORMATION AND SAN RAFAEL GROUP IN NORTHERN NEW MEXICO

Orin J. Anderson¹, Spencer G. Lucas² and Lee A. Woodward³

¹New Mexico Bureau of Mines and Mineral Resources, Socorro, NM 87801;

²New Mexico Museum of Natural History and Science, Albuquerque, NM 87104;

³Department of Earth and Planetary Sciences, University of New Mexico, Albuquerque, NM 87131

In this unique area of New Mexico, three physiographic provinces come together; the Southern Rocky Mountains, the Colorado Plateau, and the Basin and Range (Rio Grande rift section). The Colorado Plateau portion offers excellent outcrops of Mesozoic sedimentary rocks. Of interest here is the Jurassic System, which is further divided into the Middle Jurassic San Rafael Group (Entrada Sandstone, Todilto Formation and Summerville Formation), and the overlying Upper Jurassic Morrison Formation.

The upper part of the San Rafael Group (that portion above the Todilto), can in many areas be assigned to the Summerville Formation and the overlying Bluff Sandstone, although intertonguing of the two is common. The Summerville consists of parallel-bedded, fine-grained sandstones alternating with maroon siltstones or mudstones. Bedding is thin, generally less than 0.5 m thick, and the unit commonly weathers to a finely ribbed slope or cliff. The Bluff Sandstone is a thicker-bedded unit composed of well sorted, fine-grained sandstone. It is crossbedded on a wide variety of scales and is largely an eolianite with fluvially reworked zones. Color varies from red to tan and light gray. In this area, however, recognizing and mapping both the Summerville and Bluff is difficult. Summerville lithologies predominate in the lower part and Bluff lithologies dominate above, although intertonguing is extensive.

Of greater importance in the Jurassic section locally is the correct placement of the contact between San Rafael Group and Morrison strata. Some previous work, particularly that of the U.S. Geological Survey, advocated the inclusion of Summerville-Bluff strata in the Morrison Formation as was done in the Chama embayment and Ghost Ranch areas. Flesch (1974), and unpublished mapping on Ojito Spring Quadrangle, correctly recognized a Summerville lithology overlying the Todilto Formation. He, however, accepted U.S. Geological Survey practice of including the overlying eolian-dominated strata as part of the "Recapture Member" of the Morrison.

We contend the lithology of the unit referred to by previous workers as "Recapture Member" relates to San Rafael Group strata. The San Rafael Group was deposited under arid conditions—sābkhā, arid coastal plain,

sand-sheet and interdunal environments. The logical base of the Morrison Formation in the local section, as well as regionally, is placed by us at the horizon of maximum lithologic contrast and above the highest occurrence of eolianites or sabkha-type sediments. That horizon is marked by a regional scour surface and an unconformity, as indicated by thin but laterally extensive pedogenic carbonate development. The overlying sandstone is typically fluvial, containing pebbly facies, rip-up clasts, woody-trash impressions, thin sets of trough crossbeds, and vertebrate (dinosaur) body fossils. This sandstone forms the mappable base of the Morrison Formation throughout the San Juan Basin. As it is similar in lithology and stratigraphic position to the Salt Wash Member of the Morrison in eastern Utah, we advocate usage of the name Salt Wash Member for basal Morrison sandstones in New Mexico (Anderson and Lucas, 1995). The name "Westwater Canyon Member" previously used for this sandstone, is a junior synonym for Salt Wash Member, and thus the name "Westwater Canyon" should be abandoned (Anderson and Lucas, 1995). Moreover, the name "Westwater Canyon" was not used in a consistent sense by the original user (H. E. Gregory), having been applied to both a basal sandstone and a medial sandstone in the Morrison of southeastern Utah.

Repositioning the base of the Morrison Formation as advocated here places the San Rafael Group–Morrison contact at a tectonosequence boundary. This boundary corresponds to a significant tectonic reorganization of the Jurassic Western Interior basin, where San Rafael Group eolian and sabkha deposits with source areas to the NE and SW are succeeded by Morrison fluvial and lacustrine deposits derived from a volcanically active uplift to the west.

18.7 Unpaved road to left leads southwest along the south side of White Mesa toward Mesa Prieta; sign announces Zia Pueblo land, no trespassing but passage along the road to BLM land beyond is allowed. Continue straight on NM-44. Eroded, greenish brown hills of the Upper Cretaceous Dakota/Mancos strata are along highway to left, at the base of White Mesa, for next 0.8 mi. The Cretaceous shales are in contact, along the north-trending San Ysidro fault, with the Jurassic Morrison, Entrada, and Todilto Formations to the west that underlie White Mesa. The San Ysidro fault is normal, downthrown to the east, dips east, and appears to be listric (Woodward, 1987).

The unpaved road to Mesa Prieta divides immediately, the west branch ascending to the gypsum mine on White Mesa, and the south branch heading towards Mesa Prieta, 14 mi to the west. This road was logged in detail for part of its distance by Siemers (1975) and Woodward et al. (1989), and the San Ysidro 7.5' quadrangle, into which we have just driven, was mapped by Woodward and Ruetschilling (1976). Generally, the road winds through well-exposed Jurassic Morrison Formation and intertonguing Cretaceous Dakota and Mancos Formations. The butte visible about 1.2 mi to the west at 9:00 is composed of green, gray and red claystone and yellowish sandstones of the Morrison Formation. About 3 mi down the road from NM-44 a partial skeleton of the large sauropod dinosaur *Camarasaurus* was excavated from the Brushy Basin Member of the Morrison in 1978 (Rigby, 1982; Lucas and Hunt, 1985), and a partial skeleton of *Diplodocus* was reported from the same member in this area by Hunt and Lucas (1993). A little farther on, the road skirts the south end of the small, south-plunging Tierra Amarilla anticline, long a favorite mapping area for University of New Mexico field geology classes. In this area, the giant sauropod *Seismosaurus* was discovered in the Brushy Basin Member (Gillette, 1991). Often touted as the largest known dinosaur, with an estimated length in excess of 140 ft, more recent estimates suggest that *Seismosaurus* was

"only" about 110 ft long and thus large, but not the largest known dinosaur. About 6 mi west of NM-44, the road passes through the Juana Lopez Member and Semilla Sandstone-equivalent shales and sandstones of the Mancos Shale, the site of the shark-tooth deposits described in following minipaper. 0.4

SELACHIAN FAUNA FROM THE UPPER CRETACEOUS (TURONIAN) MANCOS SHALE, NEAR SAN YSIDRO, NEW MEXICO

Thomas E. Williamson¹ and Barry S. Kues²

¹New Mexico Museum of Natural History and Science, 1801 Mountain Road, NW, Albuquerque, NM 87104-1375; ²Department of Earth and Planetary Sciences, University of New Mexico, Albuquerque, NM 87131-1116

A selachian fauna of relatively low diversity was recovered from New Mexico Museum of Natural History (NMMNH) locality 3271, about 10 km west of San Ysidro, Sandoval County, along the west side of Canada de las Milpas, in NE $\frac{1}{4}$ SE $\frac{1}{4}$ SE $\frac{1}{4}$ sec. 32, T15N, R1E. The teeth and other elements of this fauna were collected from anthills constructed near the contact of a dark gray fissile shale interval of the Mancos Shale and a small, sandstone-capped cuesta questionably identified as the Semilla Sandstone Member of the Mancos by Siemers (1975). The Semilla Sandstone Member, and locally the overlying Juana Lopez Member, crop out in this area (Cobban and Hook, 1980); Semilla Sandstone bodies in the nearby Bernalillito Mesa area pinch out in all directions into time-equivalent shales of the Mancos (LaFon, 1981). The selachian remains from this locality thus come from strata approximately coeval with the Semilla Sandstone, and are of late middle Turonian age (Cobban and Hook, 1980, 1989).

The fauna described here consists mainly of isolated, partial tooth crowns. In addition to the selachian teeth are two small calcified vertebral centra of an unidentified selachian, as well as numerous isolated teeth of teleost fish. At least seven selachian taxa occur in this fauna.

Scapanorhynchus raphiodon (Agassiz) (Figs. 1.6 A–D), represented by numerous tooth fragments, is the most common selachian in this fauna. Unfortunately, few of the teeth preserve the roots. The anterior teeth of *S. raphiodon* (Figs. 1.6 A, B) are distinguished by crowns with narrow blades that are striated over their lingual surfaces. A few fragments of lateral teeth can also be identified within the fauna (Figs. 1.6 C, D). These generally have smooth lingual surfaces and roots with a large, lingual groove.

Cretodus semiplicatus (Agassiz) (Figs. 1.6 J, K) is represented by a single, highly weathered, fragmentary tooth. This specimen is massive, with large, triangular lateral denticles, a relatively short, triangular central blade, and thick massive roots with a bulbous lingual protuberance. Much of the enamel is missing but a remnant of striations is preserved on the lingual surface of the central blade.

A single fragmentary tooth, consisting of the crown and part of the root, is referred to *Cretolamna appendiculata* (Agassiz) (Figs. 1.6 H, I). The crown is triangular in profile; the lingual surface lacks a nutrient groove but possess a small nutrient pore.

Squalicorax falcatus (Agassiz) is represented by numerous tooth fragments (e.g., Figs. 1.6 E–G). The teeth of *S. falcatus* are easily identified by their leaf-shaped blades with serrated edges and the apex of the crown (Fig. 1.6 G) is acutely pointed. The distal blade is separated from the main cusp by a deep notch. The mesial cutting edge is only weakly convex and lacks the distinctive "mesial hump" of *S. kaupii* Agassiz.

The "sawfish" *Ischyrrhiza schneideri* Slaughter and Steiner (Figs. 1.6 L, M) is represented by a single oral tooth and a fragment of a rostral tooth. The rostral tooth fragment preserves the base of the crown and the distal portion of the root. The tooth is oval in cross section and orthodont. The oral tooth is bilobed and symmetrical with a single central cusp and low shoulders. The attachment surface is flat, transverse and divided by a deep nutrient groove. The labial face of the crown is smooth and extends proximally to a bulbous labial flange. The lingual flange is small.

Two specimens (e.g., Fig. 1.6 N) are referred to the sclerorhynchid ray *Ptychotrigon triangularis* (Reuss). The teeth of *P. triangularis* are trian-

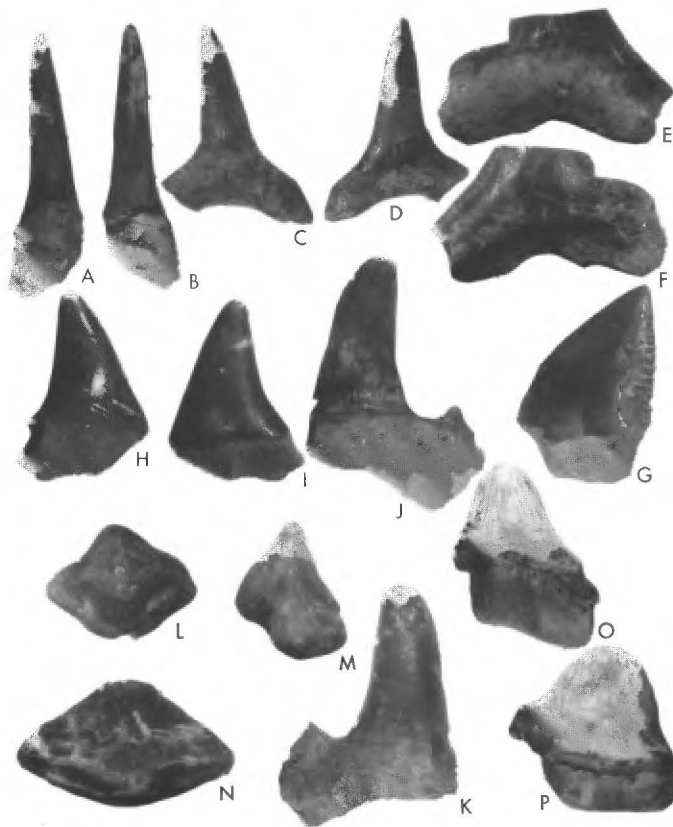


FIGURE 1.6. Selachian fossils from the Mancos Shale. A, B, *Scapanorhynchus raphiodon*, NMMNH P-26048, anterior tooth in lingual (A) and labial (B) view, x2.3. C, D, *Scapanorhynchus raphiodon*, NMMNH P-26047, lateral tooth in lingual (C) and labial (D) views, x2.3. E, F, *Squalicorax falcatus*, NMMNH P-26052, in lingual (E) and labial (F) views, x3.8. G, *Squalicorax falcatus*, NMMNH P-26053 in labial view, x3.8. H, I, *Cretolamna appendiculata*, NMMNH P-26045, in lingual (H) and labial (I) views, x3.8. J, K, *Cretodus semiplicatus*, NMMNH P-26044, in lingual (J) and labial (K) views, x3.8. L, M, *Ischyrrhiza schneideri*, NMMNH P-26061, in occlusal (L) and lateral (M) views, x8.2. N, *Ptychotrigon triangularis*, NMMNH P-26063, in occlusal view, x5.7. O, P, *Ptychodus* cf. *P. whipplei*, NMMNH P-26055, in posterior (O) and lateral (P) views, x2.3.

gular and symmetrical in occlusal view with several transverse ridges. The labial flange has a few labially directed ridges. The attachment surface of the teeth is flat and divided by a deep nutrient groove.

Several nearly complete and numerous fragmentary teeth are tentatively identified as *Ptychodus* cf. *P. whipplei* Marcou (Figs. 1.6 O, P). These possess a central, high, steep-sided crown. The central crown is marked by prominent transverse ridges that extend down the lateral sides. The crown margin is rugose. These closely resemble the teeth of *P. whipplei*, but the central crowns of most of the *Ptychodus* teeth from NMMNH 3271 are generally much wider than is typical in *P. whipplei*. Therefore, referral to this species is best considered tentative.

The selachian fauna from NMMNH 3271 closely resembles the selachian fauna recovered from the middle Turonian, lower sandstone member of the Toreva Formation of Black Mesa, Arizona (Williamson et al., 1993). The NMMNH 3271 fauna differs only in lacking the heterodontid shark *Hybodus*. The taxonomic similarities between these two faunas reflect similarity of age and environmental setting, and geographic proximity.

Several selachian taxa within this fauna have biostratigraphic utility. Welton and Farish (1993) documented the stratigraphic ranges of many selachians in Cretaceous marine deposits of Texas. They reported a Cenomanian range for *Cretodus semiplicatus*, a Cenomanian–Santonian range for *Squalicorax falcatus*, and a Turonian–Coniacian range for *Scapanorhynchus raphiodon*, *Ptychodus whipplei* and *Ischyrrhiza texana* (= *I. schneideri*). The presence of *Cretodus semiplicatus* in this fauna, as well as in Coniacian deposits of the Mancos Shale in New Mexico

(Williamson and Lucas, 1992) and Turonian deposits of Black Mesa, Arizona (Williamson et al., 1993), indicates a significant range extension for this taxon upward into at least the Turonian. The presence of other key taxa in this fauna (*S. raphiodon*, *P. whipplei* and *I. schneideri*) is consistent with the stratigraphic ranges reported by Welton and Farish (1993).

19.1 Jemez River valley at 2:00. 0.2

19.3 Low, eroded, greenish hills to left, along the base of White Mesa, were mapped as Dakota Formation by Woodward and Ruetschilling (1976) and Woodward (1987), but Siemers (1975) considered it to be Mancos. The lithology includes both sandstone and dark shales, and it probably represents part of the Dakota–lower Mancos intertonguing sequence. These Cretaceous strata are in contact along the San Ysidro fault with the pinkish to gray Jurassic Morrison and Todilto Formations immediately to the west (Fig. 1.7). The landscape around White Mesa preserves numerous remnants of pediments mantled with pink gypsiferous alluvium, colluvium, and eolian sediment. 0.4

19.7 View to left of steep northeastern face of White Mesa (Fig. 1.8). The low red/maroon hills and lower slopes of the mesa are the Upper Triassic Petrified Forest Formation (Chinle Group). These are overlain unconformably by the light tan, yellow and pink Jurassic Entrada Sandstone near the top. The mesa is capped by the thin, dark gray lower limestone unit (Luciano Mesa Member, see Lucas et al., 1995) of the Jurassic Todilto Formation. The flat surface at 11:30 in front of the plunging syncline is underlain by travertine-cemented gravels. Road follows trace of San Ysidro fault for approximately 0.4 mi. 0.4



FIGURE 1.7. View to west along base of White Mesa, showing trace of San Ysidro fault, separating greenish-gray Upper Cretaceous Dakota/Mancos sequence (to left) from Jurassic, pinkish to gray Entrada and Todilto Formations (rather flat-topped ridge to right).

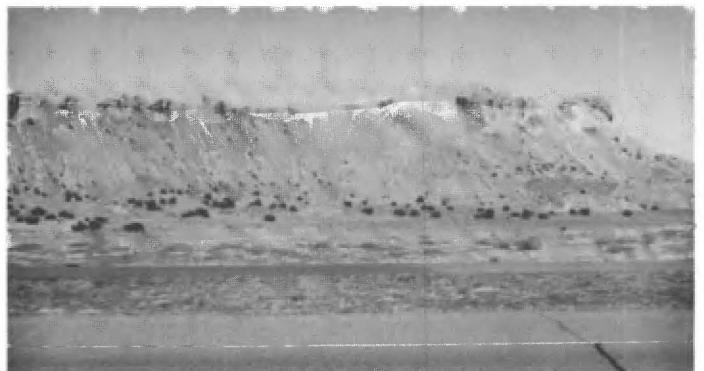


FIGURE 1.8. View to west (left) of northeastern side of White Mesa at mile 19.7.

- 20.1 The shallow, plunging syncline of the southern end of the Nacimiento uplift is now in full view just ahead (Fig. 1.9). The central, exposed portion of the syncline is the tan, Upper Triassic Agua Zarca Formation (Chinle Group); reddish Petrified Forest Formation exposures occur along the southernmost margin of the syncline, adjacent to NM-44. The east limb of the syncline, uplifted along a north-trending fault, displays, in descending order, Agua Zarca, Moenkopi, Glorieta, Yeso and Abo Formations. Low mounds along the south bank of the Rio Salado ahead are vegetated dunes. **0.2**
- 20.3 Cross Rio Salado, which joins the Jemez River a short distance to the east. **0.2**
- 20.5 Enter village of San Ysidro, named for St. Isidore, a Spanish prelate and scholar of the late 6th and early 7th centuries, who has been adopted as the patron saint of farmers. San Ysidro was settled by the Spanish in 1699, although an official grant to the area was not awarded until 1786. Much of this grant was bought in 1936 by the federal government and deeded to Zia Pueblo (Chilton et al., 1984). Present population of the village is about 230. **0.3**
- 20.8 Thriftway store to right; Circle K just beyond to left. **0.3**
- 21.1 Junction of NM-4 to right, which heads towards Jemez Springs. **Bear left** and continue on NM-44, along the west side of the Nacimiento uplift. Travertine and travertine-cemented gravels are an important geomorphic component of this landscape. The travertine is known to be generated by hydrothermal waters along faults. The regional ground water flow system of the Jemez Mountains is to the southwest, down San Diego Canyon. At 3:00, this travertine-capped surface is cut by the San Ysidro Fault. There is no discernable offset of the travertine deposit. We will have a more detailed discussion of travertine, its origin and age, at Stop 1. **0.4**
- 21.5 Milepost 24. To right are upper Triassic red beds of the lower part of the Petrified Forest Formation of the Chinle Group. These beds, locally mottled blue and gray, are equivalent to the Salitral Formation to the north, in the Chama basin. However, in the San Ysidro area, the Poleo Formation—a medial Chinle sandstone complex that separates the Salitral and Petrified Forest Formations in the Chama basin—is absent, so separating the Salitral and Petrified Forest Formations, both mudstone dominated, is problematic here. For that reason, the thick, mudstone-dominated section of the Chinle Group in this area is simply mapped as the Petrified Forest Formation (Woodward, 1987; Lucas and Hunt, 1992). **0.1**
- 21.6 San Ysidro fault at 3:00 with Cretaceous Dakota Formation to east and Triassic Petrified Forest Formation (Chinle Group) to the west, capped with travertine-cemented terrace gravel. Numerous travertine deposits occur along the western margin of the Rio Grande rift in this area. **0.1**
- 21.7 Cliff at 9:00 formed on Petrified Forest, Entrada, and Todilto Formations, in ascending order. **0.5**
- 22.2 Cross bridge. **0.3**
- 22.5 Historic Marker on right noting the eastern edge of the Colorado Plateau. Landslides, colluvium, and other mass-movement hillslope deposits are visible at 9:00 on the flanks of White Mesa. Numerous terraces, pediments, and travertine-capped surfaces extend north of the highway. Notice the travertine mound at about 2:00 on the Agua Zarca Ridge to the north. Thick (~100 ft) alluvial fills occur along this portion of the course of the Rio Salado (to the south (left) between the highway and White Mesa). The alluvium fills a rugged paleotopography developed in the Petrified Forest Formation. **1.5**
- 24.0 San Ysidro warm spring at 3:00 is part of a Known Geothermal Resource Area (KGRA). Reservoir temperatures are probably less than 100°C and thus not suitable for generating electricity. **0.3**
- 24.3 Petrified Forest Formation of Chinle Group at 3:00, capped by travertine. Crossing faults of the Rio Puerco fault zone. Some of these faults offset travertine-cemented Quaternary gravels. **0.1**
- 24.4 "C" spring (about 25°C) is on right. This is another one of the many tepid, mineralized springs of the Nacimiento fault zone. The chemical and isotopic composition of these springs indicate that they are not related to the geothermal system of Valles caldera but part of a unique aquifer localized within this sector of the San Juan basin (Vuataz and Goff, 1986; Shevenell et al., 1987). **0.9**
- 25.3 Agua Zarca Formation of Chinle Group at 3:00. Cross Pajarito reverse fault (Woodward, 1987) that bounds west side of Nacimiento uplift. (Fig. 1.10). Here the fault places Triassic Agua Zarca Formation to the east against Jurassic Todilto and Morrison Formations to the west. This Pajarito fault is not to be confused with the Pajarito fault on the east side of the Pajarito Plateau, which is the present western structural boundary for the Española basin. **0.5**



FIGURE 1.9. View from San Ysidro of uplifted east edge of southern Nacimiento Mountains. The lower reddish strata are the Permian Abo and Yeso Formations, overlain by gray Glorieta, and Triassic Moenkopi and Agua Zarca Formations.



FIGURE 1.10. Southern end of Pajarito (or southern Nacimiento) fault, which juxtaposes uplifted Agua Zarca sandstones (to right) against down-dropped Jurassic (Entrada, Todilto, Morrison) strata to left (west).

- 25.8 Roadcuts in Entrada Sandstone overlain by Todilto Formation. Six small oil fields in the southeastern part of the San Juan Basin have produced small amounts of oil from the eolian Entrada Sandstone (Vincelette and Chittum, 1981). Organic-rich, laminated limestone of the basal member of the Todilto Formation was probably the source of the oil. Notice well-developed Quaternary pediment at 9:00. **0.2**
- 26.0 We begin to move up the axis of an en-echelon fold developed in the footwall of the Pajarito fault. The fold is a northwest out-plunging anticline cored by the Chinle Group. The en-echelon folds have complex geometries attributed to polygenetic phases of deformation. The northwest-oriented, plunging folds formed first. Their eastern boundaries were then refolded and then ultimately cut by the Pajarito fault as the tip line of that fault extended southward. Further folding occurred locally in response to drag on the uplifting hanging wall. **0.4**
- 26.4 The Morrison Formation lies in the core of a northwest trending syncline, one of the en-echelon folds. At 10:00 is a broad north-trending anticline cored by the Agua Zarca Formation. This structure is used by PNM as a gas storage facility. At 8:00, the syncline east of the gas-storage anticline has a faulted western limb. This fault, the Las Milpas Fault, is a part of an arcuate group of northeast-trending normal faults of the Rio Puerco fault zone. These faults locally mark the westernmost boundary of the Rio Grande rift. **0.3**
- 26.7 The top of Cabezon peak, a Pliocene volcanic neck along the Jemez lineament is visible at 10:00. Road turns toward the north and follows Arroyo Peñasco on the left. **0.2**
- 26.9 Small caves in a gypsum karst system occur in the Todilto Formation here at 9:00. Several miles of passages can be accessed via a sink hole in the large gully immediately west of the bridge ahead. **0.4**
- 27.3 Cross Arroyo Peñasco. Todilto Formation is exposed north of bridge. **0.3**
- 27.6 Cliff at 9:00 formed on Todilto, which is underlain by slope formed on Entrada. **0.8**
- 28.4 On the hill to the left is the reference section of the Luciano Mesa Member of the Todilto Formation of Lucas et al. (1995, fig. 6). Here, the Luciano Mesa Member is 9 ft of laminar limestone and calcarenite. **0.3**
- 28.7 We are continuing in the Arroyo Peñasco drainage, a major tributary to the Rio Salado. Several distinct pediment and terrace surfaces occur along this portion of the drainage. **0.2**
- 28.9 **OPTIONAL STOP** along east side of highway, useful if access to Stop 1 through Zia Pueblo land is not available. The geology of this area is portrayed on Figure 1.11. Fine exposures of the lower Mesozoic section along this portion of the Colorado Plateau are visible at 11:00 ahead (Fig. 1.12). The Triassic Petrified Forest Formation of the Chinle Group is exposed at the base of the outcrop and extends up to about 7 ft above the prominent sandstone ledge. This grayish-red unit of sandstone and conglomerate correlates with the Correo Member of the Petrified Forest Formation in the Lucero uplift to the south. An indistinct unconformity separates the Triassic rocks from the overlying, lighter-colored Jurassic Entrada Sandstone. The Entrada is conformably overlain by approximately 7 ft of laminated petroliferous limestone, and 20 to 35 ft of gypsum of the Todilto Formation. Deposition of the Todilto Formation occurred in response to the evaporation of a large lake that spanned much of the Four Corners region in the Jurassic. Slow as you approach turn off to Stop 1. **0.3**
- 29.2 **Turn right** on dirt road. Proceed through gate and stay straight on main road. This road crosses Zia land, and permission to pass must be obtained from Zia Pueblo. The Pajarito fault and uplifted hanging wall lie straight ahead. You are in the Arroyo Peñasco drainage on the Qt4 valley floor surface (of Formento-Trigilio and Pazzaglio, this volume). **0.2**
- 29.4 Bear to the left and ascend a steep grade up to the top of the Qt2 terrace. Notice exposures along the way reveal that Qt2 is a fill terrace underlain by stratified alluvial sands and gravels interbedded with travertine flowstone. **0.5**
- 29.9 Stay to right on main dirt road. Excellent view straight ahead of the Pajarito fault and uplifted hanging wall to the east. Stratigraphy in hanging wall is from base to top: Precambrian granites and gneisses, Pennsylvanian Madera Formation, Permian Abo, Yeso, and Glorieta Formations, Triassic Moenkopi Formation, and finally the Triassic Agua Zarca Formation of the Chinle Group (Fig. 1.13). Notice concave-up Quaternary pediment-fan complexes sloping towards you on the uplifted hanging wall. Offset of the Quaternary deposits reflects a complex combination of landsliding and Quaternary reactivation of the Pajarito fault. The dirt road leading north that we have just passed takes you out to the base of the steep Agua Zarca ridge at 10:00. Here a line of impressive constructional travertine mounds are located over faults. Research of Gardner et al. has shown that the faults intercept San Juan basin ground waters (see following minipaper). Modern potentiometric head indicates that flows must have been much greater in the past. **0.2**
- 30.1 Cross small check dam. Notice tight synclinal drag-fold of the Todilto Formation at 2:00 along Pajarito fault. **0.2**
- 30.3 Stay straight, road to left accesses spring mounds in front of the Agua Zarca Formation ridge. **0.1**
- 30.4 Nice view of landslide/fault scarps at 12:00 on the Quaternary pediment fan complexes. Notice by looking at 7:00 how the Qt2 surface you are now on appears to be backtilted towards the mountain front. **0.1**
- 30.5 Stay straight, descend the Qt2 tread. At 12:00 the active travertine mound is on a fault in the Petrified Forest Formation. This mound is sacred to the Zia people. Do not trespass. **0.2**
- 30.7 **Turn left** at T in road. **0.1**
- 30.8 Continue straight, notice a large, active travertine spring mound at 12:00. This is called swimming pool spring and it is located directly above the Pajarito fault. The pipe feeding the mound is greater than 150 ft deep. **0.1**
- 30.9 Excellent view of northeast striking fault in headwaters of Arroyo Peñasco drainage at 12:30 that offsets Mesozoic strata. **0.1**
- 31.0 Bear right into parking/staging area. Follow student parking directions. Proceed on foot to the east to **STOP 1**. Assemble at base of travertine exposure and Pajarito fault. Following brief introduction to geology/hydrology of this stop, use the map of Figure 1.14 to visit (1) exposures of Pajarito fault, (2) exposures of offset Quaternary alluvium and travertine, (3) an extinct travertine mound, and (4) Proterozoic rocks in the hanging wall of the Pajarito fault. Refer to paper by Formento-Trigilio and Pazzaglia (this volume) for detailed discussion of this site. The following minipapers summarize the tectonics of the Nacimiento Mountains and the travertine springs in this area.

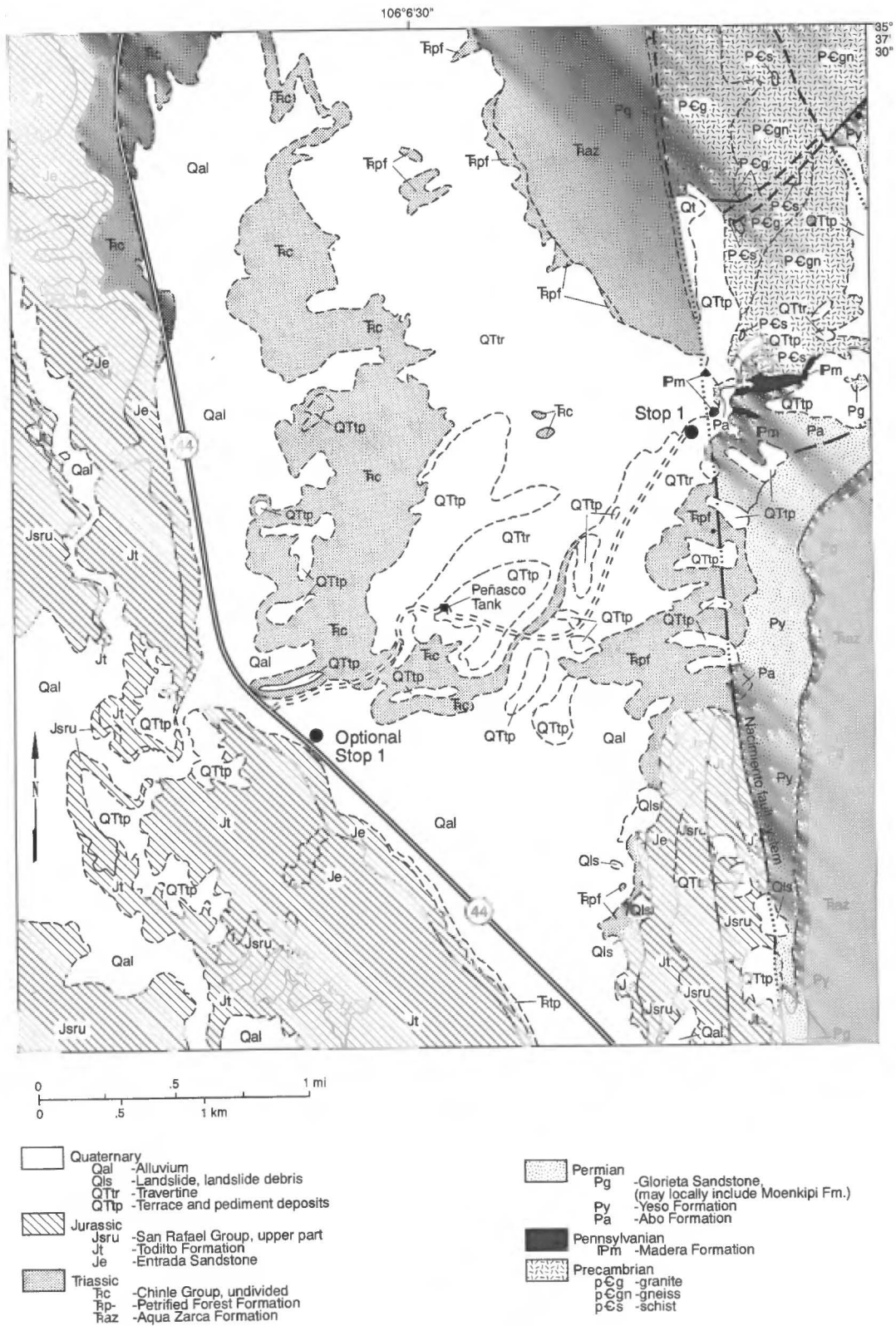


FIGURE 1.11. Geology of the southern part of the Nacimiento fault system (Pajarito fault) in the area of Optional Stop and Stop 1 based on Woodward, 1987 and unpublished mapping by G. A. Flesch; courtesy of Orin Anderson.



FIGURE 1.12. Mesozoic outcrop to west (left) of Optional Stop, consisting of Petrified Forest Formation (Chinle Group), overlain by Jurassic Entrada and Todilto Formations.



FIGURE 1.13. View to east of uplifted hanging wall of Pajarito fault, just south of Stop 1, consisting of Permian Abo, Yeso, and Glorieta, and Triassic Agua Zarca Formations. Lighter exposures in right middle-ground are Jurassic strata down-dropped west of the fault.

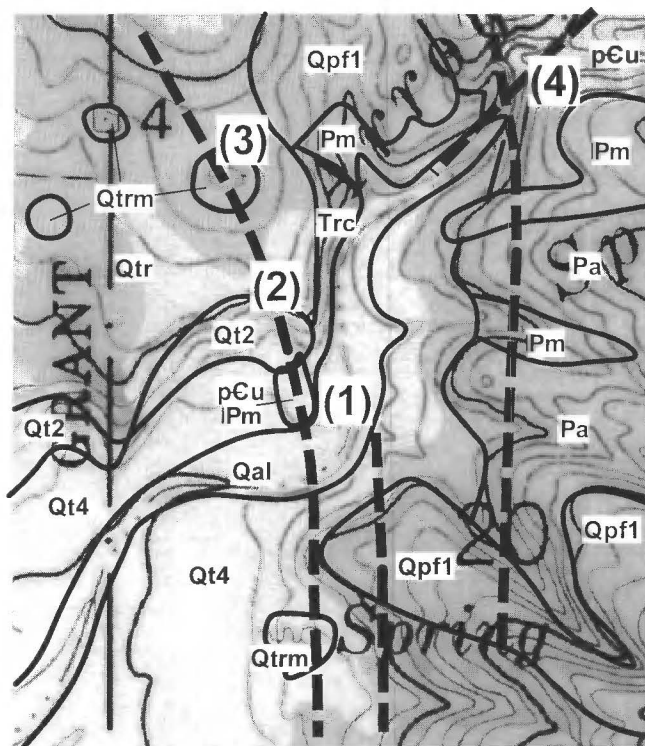
TECTONICS OF NACIMIENTO UPLIFT AND ADJACENT AREAS

Lee A. Woodward

Department of Earth and Planetary Sciences, University of New Mexico, Albuquerque, NM 87131

The Nacimiento uplift trends north and is about 50 mi long and 6 to 10 mi wide (Fig. 1.15). In general, it consists of an uplifted block that is tilted eastward and is bounded on the west mainly by reverse and thrust faults (Woodward, 1987). There is at least 10,000 ft of structural relief between the highest part of the uplift and the adjacent San Juan basin. East of the range-marginal faults, an anticlinal bend occurs locally on the west side of the uplift where Phanerozoic strata are preserved. A synclinal bend that locally has an inverted limb is present to the west of the bounding faults and marks the eastern margin of the San Juan basin.

Three separate, northerly striking faults bound the west side of the uplift. These faults are collectively called the Nacimiento-Gallina fault system and are from south to north, the Pajarito, Nacimiento, and Gallina faults (Woodward et al., 1992). The fault system continues to the north and is defined by the Tierra Montañosa fault. The Pajarito fault is a vertical to high-angle reverse fault dipping 90° to 76°E; maximum stratigraphic separation is about 3600 ft. The Nacimiento fault is an east-dipping reverse and thrust fault along most of its trace on the west side of the uplift, but changes northward to a vertical fault and at its north end is a west-dipping normal fault. Along most of its trace the Nacimiento fault is an upthrust that is steep at deep structural and stratigraphic levels, but flattens upward and has westward movement of the hanging wall block



STOP 1.

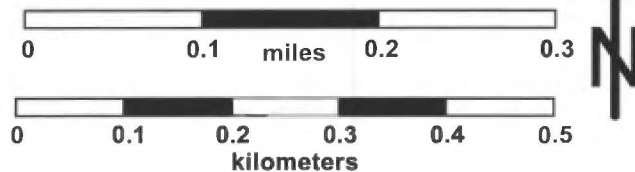


FIGURE 1.14. Map of Stop 1 outcrops (1) to (4).

over the San Juan basin. Maximum stratigraphic separation on the Nacimiento fault is about 4000 ft, but structural relief between the Nacimiento uplift and the San Juan basin is at least 10,000 ft because of the anticlinal and synclinal bends adjacent to the fault. The Gallina fault is nearly vertical and strikes north-northeasterly, parallel to and west of the northern part of the Nacimiento fault. At most localities the Gallina fault is downthrown on the west, but at one locality it is down on the east side. This appears to be due to differential folding during faulting when the west side of the fault, the block forming the San Juan basin, was downbuckled and underwent minor right slip (Woodward et al., 1992).

The northern end of the uplift is a broad, faulted anticline that plunges 10° to 20° northward and merges through a saddle with the Gallina-Archuleta arch (Fig. 1.15). The uplift terminates at the south end where folds plunge to the south beneath an unconformable cover of Tertiary strata.

Within the uplift are high-angle faults striking east, northwest, and northeast. These faults separate differentially uplifted segments within the Nacimiento uplift. Other structures within the uplift include second-order, east-tilted fault-blocks bounded by north-trending normal faults near the north end of the uplift. A graben occurs near the crest of the southern part of the uplift. Neogene volcanic rocks of the Jemez volcanic field lap unconformably onto the east side of the uplift. Late Cenozoic normal faults forming the west side of the Albuquerque basin of the Rio Grande rift cut the southeast part of the uplift. These faults are well exposed from San Ysidro northward to Guadalupe Box and to Soda Dam north of Jemez Springs.

Right shift in Precambrian basement rocks along the eastern margin of the Colorado Plateau in late Paleocene to mid-Eocene time created northwest-trending echelon folds in the overlying Phanerozoic strata. This

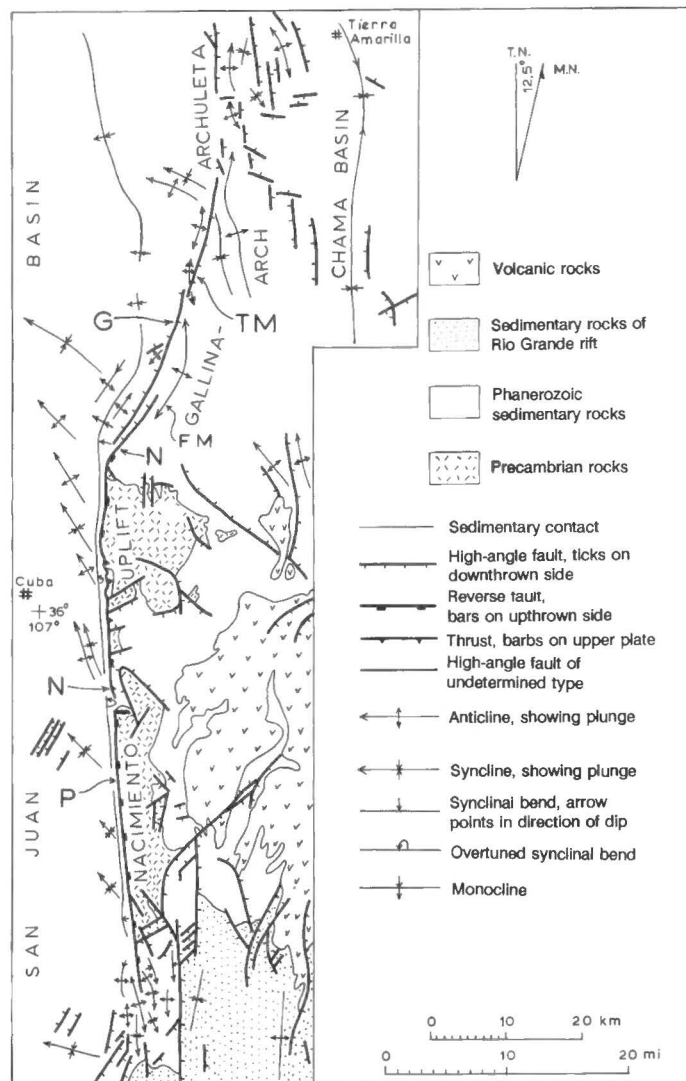


FIGURE 1.15. Generalized tectonic map of the Nacimiento uplift and adjacent areas. P = Pajarito fault; N = Nacimiento fault; TM = Tierra Montanosa fault; FM = French Mesa anticline. Modified from Woodward et al. (1992)

was followed by development of a west-facing monocline that was cut by the Pajarito and Nacimiento reverse faults. As the San Juan Basin subsided it was differentially folded relative to the Gallina–Archuleta arch, resulting in a component of right slip along the Gallina fault. This differential folding resulted in variable offset along the Gallina fault with nonmatching folds on opposite sides of the fault. The axes of the folds do not predate fault movement and therefore cannot be used to determine the amount of strike slip. Right shift of the Colorado Plateau dies out at the north end of the Gallina fault. The tilted fault-blocks and the graben within the uplift probably developed as a result of east-west extension as the uplift rose and yielded westward along the Pajarito and Nacimiento reverse and thrust faults.

Laramide right slip along the Nacimiento fault was estimated to be a maximum of 3 mi (Baltz, 1967) and the southern continuation of this fault system, the Rio Puerco fault zone, was calculated to have about 1.25 mi on the basis of detailed mapping (Slack and Campbell, 1967). Karlstrom and Daniel (1993) suggested 43–49 mi of right slip on the Nacimiento fault system, but Woodward (1994) disagreed with some of the evidence that yielded this figure. Some of the rise of the Nacimiento uplift is probably post-Miocene and may be related to development of the late Cenozoic Rio Grande rift. The distribution of the Pedernal chert member of the Abiquiu Formation (Miocene) along the northern and highest part of the uplift supports this hypothesis.

TRAVERTINE MOUND SPRINGS ALONG THE EASTERN MARGIN OF THE SAN JUAN BASIN, SANDOVAL COUNTY, NEW MEXICO

Rebecca D. Gardner, Laura J. Crossey, Armand Groffman
and Joseph Sterling

Department of Earth and Planetary Sciences, University of New Mexico,
Albuquerque, NM 87131-1116

Sotuknang told the people as they stood at their Place of Emergence on the shore of the present Fourth World, "The name of this Fourth World is Tuwaqachi, World Complete. It is not all beautiful and easy like the previous worlds. It has height and depth, heat and cold, beauty and barrenness; it has everything for you to choose from. What you choose will determine if this time you can carry out the plan of Creation on it or whether it must in time be destroyed too."
Frank Waters, *Book of the Hopi*

Place of Emergence, Sipapu; Nacimiento, sacred birth; Ojos del Espiritu Santo, springs of the Holy Spirit: Pueblo and Spanish cultures gave these names to a wonderful series of springs that issue forth in the region where the San Juan basin intersects the Nacimiento uplift, the Jemez volcanic field, and the Rio Grande rift. Springs and associated travertine (calcium carbonate, CaCO_3) deposits are numerous in this region. Water characteristics and structural relationships define three ground-water provinces (Craig, 1992). West of the Jemez fault is the Jemez Valley province; between the Nacimiento–Pajarito fault and the Jemez fault is the Nacimiento Mountain province; and west of the Nacimiento–Pajarito fault lies the San Juan basin province. Here, we describe the springs and associated travertine deposits that issue from the San Juan basin ground-water province.

Some of the more remarkable travertine deposits and associated saline warm springs are located immediately north and south of the Rio Salado. Issuing as point sources, these springs have encircled themselves with layers of CaCO_3 forming tall, conical structures. Measurements of two of the tallest structures show that they rise 65 to 80 ft and have circular bases approximately 300 ft in diameter. From the top of these mounds one looks down into huge cisterns nearly 65 ft across and 65 ft deep. At the bottom of these cisterns are small, 10-ft-wide openings filled with actively degassing springs.

Fifteen well-defined travertine mounds are found in Arroyo Peñasco and along the base of the sandstone hogback (Triassic Agua Zarca Formation, Chinle Group) that flanks the southwestern end of the Sierra Nacimiento, west of the Pajarito fault (see Fig. 1.16, and map in Formento-Trigilio and Pazzaglia, this volume). These lands belong to the Pueblos of Zia and Jemez. Some of these mounds are completely dry, whereas others contain springs in various stages of activity. Several springs are overflowing their rims, degassing CO_2 and actively depositing CaCO_3 on their flanks. Other springs, such as those described above, are actively discharging and degassing CO_2 , but are doing so at great depths below their rims. Finally, a few mounds contain stagnant water in the bottom of their cisterns with no signs of degassing. Traces of former mounds or spring conduits include broken blocks of travertine and circular regions filled with sediment, vegetation, or desert pavement (see Clark, 1929; Harrington, 1948; Craig, 1992).

The mound springs represent the latest travertine depositing episode in this region. Stratigraphic relationships suggest that several episodes of travertine deposition have occurred. The travertine mounds paralleling the hogback are superimposed on a thick (15–30 ft) platform of horizontally-deposited sheets of travertine. These sheet travertines unconformably overlie the Triassic Petrified Forest Formation (Chinle Group) and currently cover a 2 mi² area west of the hogback. This unit has been truncated by Arroyo Cuchillo to the west and Arroyo Peñasco to the south. The contact between the Petrified Forest and the sheet travertines consists of CaCO_3 -cemented terrace gravel (Qtz.p) possibly middle to late Pleistocene in age (Formento-Trigilio and Pazzaglia, this volume).

These sheet travertines appear to have been deposited by springs issuing from a line source (e.g., a fault, fracture, or geologic contact) along their eastern boundary, upslope of the mound structures. Although this boundary parallels the Pajarito fault, no faults are found in the immedi-

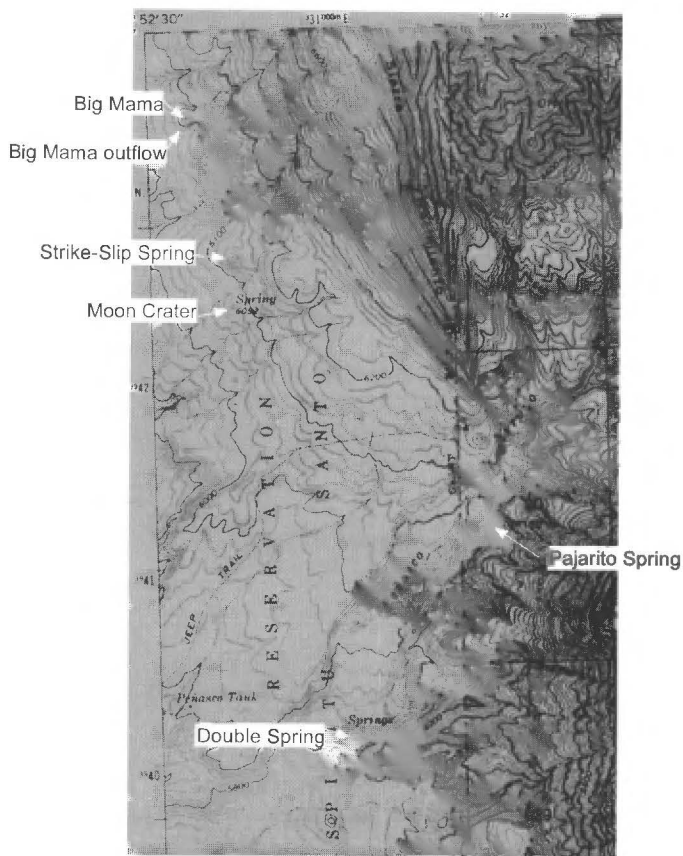


FIGURE 1.16. Travertine mound sampling locations along southwestern slopes of the Nacimiento Mountains, USGS San Ysidro 7.5 min quadrangle map.

ate vicinity. Formento-Trigilio and Pazzaglia (this volume) found evidence for Quaternary faulting of the Qt₂p terrace in Arroyo Peñasco and suggest that the mound structures are aligned on inferred en echelon oblique-slip faults. These faults may account for the change from sheet deposition to mound construction. The most obvious line source for the travertine sheet deposits, however, appears to be the geologic contact between the red shale of the Petrified Forest Formation and the gray sandstone of the Agua Zarca.

Rogers et al. (1988) noticed this relationship and that all of the travertine depositing springs of the San Juan basin ground-water province are situated on top of the Petrified Forest Formation. They also noted that these springs are associated with anticlinal structures; the mound springs of Arroyo Peñasco with a minor southward plunging, SSW-striking anticline, the mound and sheet travertines with the NNW-striking Rio Salado anticline, and the mound springs south of the Rio Salado with the Tierra Amarilla anticline. They suggested the following model: southeasterly flowing deep basin waters of the San Juan basin are forced upward by hydraulic head into the large scale anticlinal structures along the eastern boundary of the San Juan basin. The warm deep basin water is concentrated in the Agua Zarca sandstone aquifer via extensional fractures in the anticlines or by faults related to the Nacimiento uplift. The overlying impermeable Petrified Forest shale traps the water until the stratigraphic contact is exposed, as is the case along the hogback monocline, or until

the Petrified Forest is extensionally fractured, such as along the Tierra Amarilla anticline.

This model also accounts for the anomalous temperatures and high total dissolved solids (TDS) measured at the mound springs and in the two artesian Kaseman Test wells drilled in 1926 (Clark, 1929; Renick, 1931; Craig, 1984, 1992). The Kaseman Tests, located along NM-44, were petroleum exploration wells drilled into the Rio Salado anticline. The first well yielded hot (40°C) saline water under pressure from the Agua Zarca Formation at a depth of 540 ft. The second well, never capped and now known as Warm Springs, was drilled to a depth of 2000 ft. It encountered hot, 40 to 60°C, saline water from Triassic, Permian and Pennsylvanian units. Flow from these artesian wells apparently caused water levels to drop in many of the mound springs (Clark, 1929). Water sampled from Warm Springs consistently has had TDS of 11,000 mg/L (Craig, 1984).

Water samples from five of the mound springs (Fig. 1.16) were analyzed in September 1995. Temperature and pH were measured in the field and analyses for cations, anions and alkalinity (Table 1.1) were completed at the University of New Mexico using procedures recommended by the American Public Health Association (1992). Surface water temperatures range from 20 to 28°C, and the TDS measured ±11,500 mg/L for all but one of the springs. The anomalous spring, with just under 8,000 mg/L TDS, is also the most active, is the only one perched on a known fault, and was reportedly not affected by the drilling of the Kaseman wells (Clark, 1929). Swimming Pool Spring issues from the Pajarito fault in Arroyo Peñasco where the Petrified Forest Formation abuts the Permian Abo Formation. Thus it appears that this spring is receiving a mixture of waters from the San Juan basin and the adjoining Nacimiento Mountain province. The remainder of the springs receive their waters from deep hydrogeologic units of the San Juan basin.

The data presented in Table 1.1 indicate that the spring waters are super-saturated with CO₂ and saturated with respect to CaCO₃. It appears that the mounds are being constructed by inorganic processes. As CO₂ degasses from solution, the pH and the concentration of carbonate ions (CO₃²⁻) increases, which pushes the reaction towards CaCO₃ saturation and precipitation. This degassing process occurs continuously as water flows down slope with calcite and possibly aragonite being deposited until equilibrium with the atmospheric pCO₂ is reached. Biological processes, such as metabolic reactions of algae and bacteria, may also be driving CaCO₃ precipitation. Some flow paths are covered by a reddish brown algal growth; others are not. Flow paths without algal growth did not receive continuous flow during the winter of 1995–1996. Other studies of travertine deposits have found that biologic processes control CaCO₃ precipitation during the spring/summer and inorganic processes dominate during the winter (Irion & Müller, 1968; Chafetz et al., 1991). These seasonal changes in activity were manifested as light/dark laminations, similar in scale to those at the travertine mound springs.

These layers of chemical sedimentation are essentially recorders of the interplay between basin hydrodynamics and the regional climate. Further examination of these travertine mound springs will help deconvolve these signals and may tell us about regional climate change since middle to late Pleistocene time.

We thank the Pueblos of Zia and Jemez for permission to access their lands.

Return to vehicles. Retrace your route 1.8 miles down the Arroyo Peñasco drainage to NM-44. **1.8**

32.8 **Turn left** on NM-44. Retrace route 8 mi to junction with NM-4 in San Ysidro. About 4 mi north of here is “Warm Spring”, discussed in the following minipaper. **1.9**

TABLE 1.1 Water analyses of travertine mound springs.

Site	Depth to Water (ft)	Temp (C)	pH	Ca mg/L	Mg mg/L	Na mg/L	K mg/L	Cl mg/L	SO4 mg/L	HCO3 mg/L	TDS mg/L	Log pCO2 atm	Log IAP/K Calcite	Log IAP/K Gypsum
Pajarito, aka														
Swimming Pool Springs	0	23.5	7.11	273	53.8	2229	54	2223	1812	1241	7886	-0.978	0.6755	-0.2207
Big Mama	60	-	6.36	375	62.0	3382	83	2781	3453	1345	11481	-0.192	-0.0204	0.0467
Big Mama Outflow	0	21.3	6.44	366	62.6	3457	84	2810	3478	1360	11618	-0.267	0.0521	0.0358
Moon Crater	15	19.5	6.80	391	62.6	3397	91	2633	3738	1496	11809	-0.585	0.4452	0.0879
Double Springs	0	27.9	6.34	445	63.1	3146	102	2544	3172	1872	11344	-0.028	0.2644	0.0658
Strike-Slip Springs	67	-	6.43	400	63.1	3472	89	2809	3641	1425	11899	-0.236	0.0893	0.0823

WARM SPRING—THE SPRING THAT WASN'T

T. E. Kelly

Geohydrology Associates, Inc., 4015 Carlisle, N.E., Suite A, Albuquerque, NM 87107

About 12 mi north of San Ysidro, at mile marker 35.6, Warm Spring provided an opportunity for travelers to rest on their trips between Albuquerque and the Four Corners area. The spa was located on the Ojo del Espiritu Santo Ranch, which later became part of Zia Pueblo. Although the spa was very popular for many years, gradually the buildings fell into disrepair and the site was largely abandoned. That didn't stop the nature lovers from bathing, but it caused a minor traffic hazard on NM-44. Finally, Zia Pueblo cleared the site and fenced it off. Nothing remains but concrete slabs and the water tank, but on a cold morning you can see steam rising from the site (Fig. 1.17).

Though this has been dubbed Warm Spring, it is not a spring at all. It is the Kaseman No. 2 oil test that was drilled in 1926. Attempts to plug the well were unsuccessful, and the well was allowed to flow. The well is also called "Zia Hot Well" in various reports (Vuataz and Goff, 1986; Shevenell et al., 1987).

The Kaseman No. 1 had been drilled about a mile south to a depth of 550 ft. The well encountered a strong, artesian flow of salty water from the Poleo Sandstone. According to Renick (1931, p. 82), the well flowed nearly 2500 gpm and had a shut-in pressure of 225 psi. The Kaseman No. 1 was plugged and abandoned at 550 ft and the rig moved to the second location.

The Kaseman No. 2 was drilled to a depth of 2008 ft. Artesian flow was encountered at a depth of 425 ft, and additional flows were found at greater depth. The well was drilled with cable tools, so multiple strings of casing were set to reduce the flow. According to Renick (1931, p. 83), 12-in. casing was set at 486 ft, 8-in. casing set at 940 ft, and 6-in. casing was set at 1810 ft. The well was open hole below the 6-in. casing to total depth.

The two Kaseman wells were drilled on a small anticlinal structure sometimes called the Rio Salado anticline. According to the log published by Renick, the Kaseman No. 2 was spudded in the "Chinle(?)" (=Petrified Forest Formation of Chinle Group) and completed in the Magdalena Group (now Madera Formation). The Poleo Formation (Chinle Group) was encountered at 645 to 870 ft; the Chupadera Formation (=Permian Yeso and Glorieta Formations) from 870 to 1535 ft; the Abo Formation from 1535 to 1890 ft; and the Madera Formation to the bottom of the well at 2008 ft.

With three casing strings reducing the flow, it was estimated by the State Engineer Office that the Kaseman No. 2 was flowing at the rate of 2050 gpm in 1926. The temperature increased with depth, but the total mineralization decreased (Table 1.2). Since the well was completed, the flow has gradually decreased. Craigg (1984, table 1) measured the discharge at 63 gpm in May 1984, and in January 1996, the flow was reduced to 41 gpm. The temperature has remained relatively constant. As shown in Table 1.2, the highest temperature reported by Renick was 142°F (61°C). Trainer (1974, table 1) reported a sample collected in March 1964 had a temperature of 54°C (129°F), and in January 1996, I mea-

sured the temperature at 54°C also. Temperatures and flow rates listed in Shevenell et al. (1987) for samples collected in 1979–1984 are 56 to 53°C and about 40 to 80 gpm. In January 1996 there was an abundance of gas bubbles discharging from the wellhead; there was a strong odor of hydrogen sulfide present.

TABLE 1.2. Water characteristics, Kaseman No. 2 in 1926 (Renick, 1931, p. 83).

Temperature			
Depth (ft)	Temp (°F)	Depth (ft)	Temp (°F)
425	108	1060	125
490	108	1570	125
550	112	1760	142
610	116	1920	142
910	124		
Chemical Data			
Producing Interval	0-940	940-1810	+1810
Total dissolved			
solids	11,760 mg/l	7780	5580
NaCl	5450	3800	2890
CaCO ₃	1130	1510	1710

The TDS in all samples obtained since 1978 are about 12,000, indicating that virtually all flow is now from the zones above 940 ft. The geochemistry of the water is similar to other thermal/mineral springs in the area but unique from fluids in the Valles caldera geothermal system. Sr-isotopes and total Sr show that the water has circulated only in Paleozoic to Mesozoic sedimentary rocks as one would surmise from the local geology (Vuataz et al., 1988, p. 6061). The water is tritium-dead, making the average mean residence time of the water 10,000 yrs (old water). The gas may smell of H₂S but analyses of the well gas and those from nearby springs show a concentration of <0.02 mol-% (Goff, unpubl. data). The gas consists mostly of CO₂ and N₂. Chemical geothermometers indicate a subsurface equilibrium temperature approximately equal to the discharge temperature.

The water presently is being used for stock watering and occasional bathing in pools located in the outfall about 150 ft east of the well. The Zia Pueblo has diverted the flow into three stock tanks. The overflow has formed an apron of mineral deposits before the water enters a tributary to the Rio Salado.

The author appreciates the review comments and suggestions on this manuscript by Dr. Fraser Goff, Los Alamos National Laboratory.

- 34.7 Cross Arroyo Peñasco again. **0.7**
 35.4 MP 29. **0.5**
 35.9 White Mesa (Mesa Blanca) at 12:00. **4.3**
 40.2 San Ysidro Village Limit sign. **0.5**
 40.7 Get in left lane. **0.1**
 40.8 Junction with NM-4. **Turn left** toward Jemez Springs. The next 1.4 mi are through the pastoral village of San Ysidro. On the right, hills of white Zia Sandstone are nearly continuous about a mile east of the town. **0.2**
 41.0 Post Office on right. **0.2**
 41.2 Police and Fire departments on right. As we drive up the northeast-trending Jemez River valley, terrace deposits of the paleo-Jemez River will become more common. Low roadcuts here display gravels of terrace Qt4. **0.6**

HISTORY OF FORMATION AND DRAINAGE OF PLEISTOCENE LAKES IN THE VALLES CALDERA

John B. Rogers, Gary A. Smith, and Harold Rowe

Department of Earth and Planetary Sciences, University of New Mexico,
 Albuquerque, NM 87131

The Valles caldera was created by collapse concurrent with the eruption of the upper Bandelier Tuff at 1.14 ± 0.02 Ma (Spell et al., 1990).



FIGURE 1.17. Kaseman No. 2 well, viewed toward the west, with discharge to the foreground.

San Diego Canyon represents the only drainage outlet from the caldera (Fig. 1.18). The head of the canyon, the breach in the Valles caldera wall, is coincident with the lowest spot on the caldera rim and its location has possible structural control (Bailey and Smith, 1978). Lake beds are known from both surface exposures and subsurface data within the caldera (e.g., Griggs, 1964; Smith and Bailey, 1968; Doell et al., 1968; Smith et al., 1970). The timing and cause of formation and drainage of caldera lakes have been presented differently by previous workers.

Smith and Bailey (1968) proposed that the breaching of Valles caldera resulted from overflow of a lake displaced by the growing resurgent dome (Fig. 1.18) within 100 ka of caldera formation. Evidence for this interpretation, confirmed by our observations, is that Redondo Creek rhyolites (<1.140 and >1.133 Ma; Spell and Harrison, 1993) are interbedded with lake sediments that thin against the resurgent dome and are associated with hydromagmatic tuffs consistent with eruption through a lake. Earliest ring-fracture domes (Fig. 1.18) are associated with pumiceous magmatic pyroclastics rather than hydromagmatic tuffs. These eruptive products exhibit no evidence of eruption through a lake, suggesting drainage of the lake prior to eruption of the 1.13–1.09 Ma (Spell and Harrison, 1993) Cerro del Medio dome complex (Fig. 1.18).

Goff and Shevenell (1987) and Goff et al. (1992) proposed initial caldera breaching as late as <0.5 Ma by headward erosion of the Jemez River. This interpretation of a late initial breach is used to provide a mechanism for the late development of a vapor cap above the liquid-dominated Valles hydrothermal reservoir without appealing to boiling down of the reservoir. In this interpretation, erosional breaching and draining of widespread intracaldera lakes subsequently lowered the hydraulic head on the Valles hydrothermal system, resulting in the formation of the vapor zone (Trainer, 1984). The time of formation of the vapor cap is poorly constrained. A maximum age of 0.66 Ma is based upon K/Ar dating of hydrothermal illite from the molybdenite deposit in the VC-2A core (WoldeGabriel and Goff, 1989; Goff, personal commun., 1994). Goff and Shevenell (1987) proposed that the cessation of hot-spring activity on the highest travertine deposit at Soda Dam (Travertine A) after 0.48 Ma was produced by the hypothesized loss of

head and provides a near-minimum constraint on drainage of caldera lakes in this interpretation.

The evidence of Smith and Bailey for an early breach is compelling. U-Th disequilibrium dates for travertines at Soda Dam (Goff and Shevenell, 1987) indicate 1000 ft of incision within 100 ka of the upper Bandelier Tuff eruption. Rapid downcutting through approximately 800 ft of ignimbrite to prior grade is plausible, but additional incision through 200 ft of Paleozoic bedrock (Goff and Kron, 1980) without a sizable perennial stream seems unlikely. There are no tributaries to the Jemez River except canyon-wall ravines, between Soda Dam and the caldera. To achieve the high incision rates implied by these data, it is likely that San Diego Canyon drainage included the large intracaldera watershed within 100 ka of caldera formation. The ancient Jemez River gravels buried by Travertine A include probable clasts of intracaldera rock types, which argue for a breach earlier than deposition of Travertine A.

Lake terraces are present in Valle San Antonio and Valle Toledo in the northern moat (Fig. 1.18). These terraces are at different elevations in the two valleys and suggest formation in smaller lakes impounded in sectors of the moat following eruption of ring-fracture domes. Exposed lake sediments in Valle San Antonio have normal polarity (Rogers, 1996), indicating an age <0.78 Ma, and on the basis of topographic relationships arguably formed upstream from the 0.557 ± 0.004 Ma (Spell and Harrison, 1993) San Antonio Mountain dome. The lake sediments of the higher terrace in Valle Toledo also have normal polarity and extend up-valley from the 0.915 Ma to 0.787 Ma (Spell and Harrison, 1993) Cerro Santa Rosa dome complex. Griggs (1964) suggested that some lake sediments recovered from core within the Valle Grande, the large eastern valley of the Valles caldera, are as young as 25 ka.

All of the observations are most consistent with the formation and drainage of several lakes in the caldera. The initial, probably caldera-wide, lake was drained within 100 ka of caldera formation by a combination of headward erosion and displacement of water by the growing resurgent dome. Smaller lakes formed later in headwater tributaries within the caldera moat as a consequence of drainage disruption by ring-fracture domes. These lakes may have sustained the liquid-dominated geo-

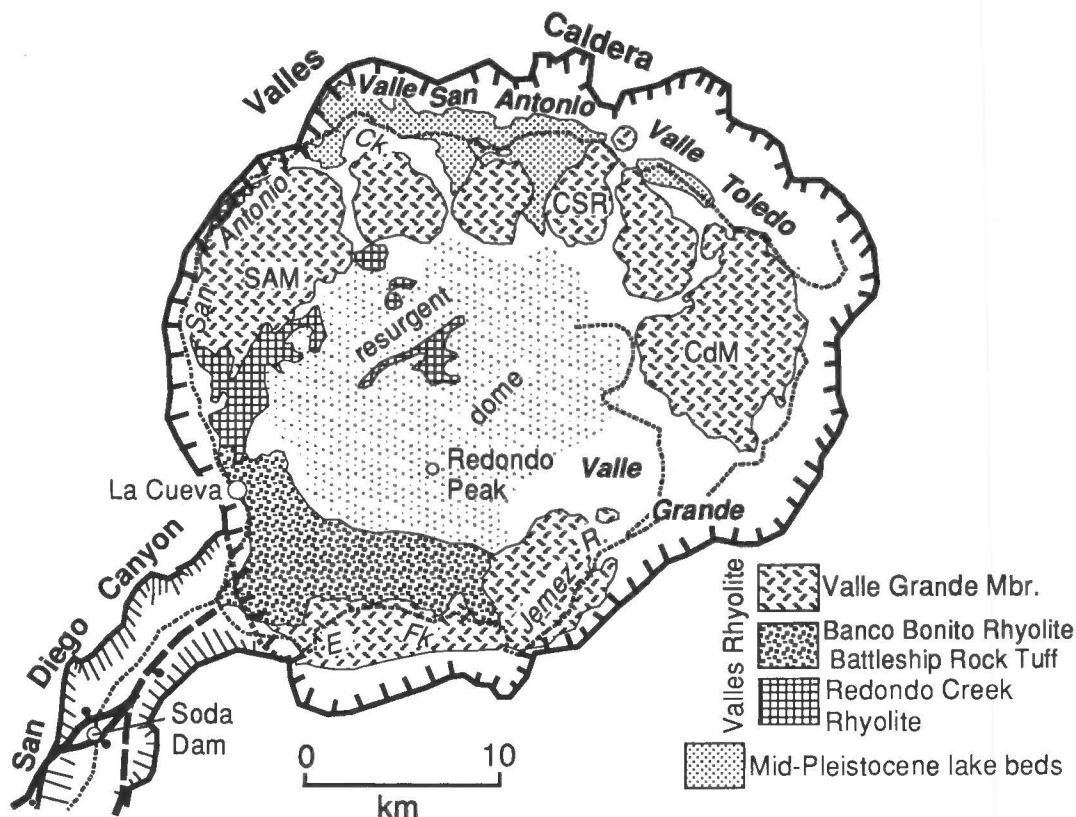


FIGURE 1.18. Generalized map of the Valles caldera and San Diego Canyon (modified from Smith et al., 1970). CdM = Cerro del Medio; CSR = Cerro Santa Rosa; SAM = San Antonio Mountain.

thermal system. Most recently, the breach at the head of San Diego Canyon was filled by products of the Battleship Rock and Banco Bonito eruptions at approximately 50-60 ka (Reneau et al., 1996). Car-sized boulders of Banco Bonito lava found 15 mi downstream of the breach may represent catastrophic overflow of this latest dam. Complete integration of caldera surface waters (i.e., the East Fork of the Jemez River in Valle Grande) with San Diego Canyon was perhaps not completed until post-25 ka.

- 41.8 MP 1. **0.1**
 41.9 Old San Ysidro Catholic Church on right. To left (Fig. 1.19), a good view of the east limb of the southern Nacimiento syncline, exposed as the hanging wall along the north-trending San Ysidro fault. The section exposed here is much the same as that seen at Stop 1 on the western edge of the syncline: Abo, Yeso, Glorieta (Permian), Moenkopi and Agua Zarca (Triassic). Zia Sandstone exposures in foreground, down-dropped along the east side of an unnamed fault east of the San Ysidro fault. Pajarito Peak (9042 ft) rises in the distance above the synclinal strata. **0.8**
 42.7 Cross Jemez River. **0.2**
 42.9 White Zia sandstone exposed in roadcuts for the next 0.9 mi, typically covered with terrace gravels. Cattleguard. Leaving Zia Indian Reservation and entering Jemez Indian Reservation. **0.3**
 43.2 Redondo Peak at 11:30. **0.2**
 43.4 Cerro del Pino, a dacite dome of the Keres Group (Bailey et al., 1968; Gardner et al., 1986) is visible at 12:00. **0.4**
 43.8 MP 3. **0.4**
 44.2 Chamisa Mesa, capped with Paliza Canyon basalt, is visible in near distance at 2:30. **0.5**
 44.7 Zia Sandstone in roadcut to right mantled with Qt4 alluvium. **0.1**
 44.8 Cross arroyo just before MP 4. **0.3**
 45.1 Low, gravel-covered hills in Zia sandstones to right. At 9:00 the view is across the trace of the Jemez fault, which places eroded white pinnacles of Zia (middle distance) against Permian and Triassic strata to west, with Pajarito Peak the highest point in distance. Extensive pediments are developed along the western side of the Jemez Valley, many of which are capped by travertine-cement gravels. **0.1**
 45.2 Enter Jemez Pueblo, which is built on eroded Zia sediments covered with terrace gravels. The pueblo has about 2000 Towa-speaking inhabitants. At the time of Spanish colonization, many of the Jemez people lived 12 mi upstream (Giusewa Pueblo, just north of the town of Jemez Springs), and in smaller villages in the canyon and on mesa



FIGURE 1.19. East limb of the southern Nacimiento Mountains syncline, uplifted along the San Ysidro fault, viewed from the east. Strata are Permian Abo, Yeso and Glorieta Formations, and Triassic Moenkopi and Agua Zarca Formations at top. Down-dropped Miocene Zia Formation sandstones exposed to right.

tops. The Jemez people actively resisted Spanish domination, and sometimes in alliance with the Navajos, fought them before, during and after the Pueblo revolt of 1680, and were ultimately settled in this location early in the 1700s (Chilton et al., 1984). James H. Simpson, one of the earliest explorers of New Mexico after the American conquest, visited Jemez Pueblo in 1849, and recorded his observations (Simpson, 1850; see also Kues, 1992). **0.6**

- 45.8 Jemez Pueblo post office to left; civic center and tribal offices just beyond. **0.3**
 46.1 Quaternary gravels on Zia sandstones to right. **0.2**
 46.3 Jemez Trading Post on left. **0.3**
 46.6 Extensive Zia sandstone exposures at 9:00 across valley in middle distance. Electron spin resonance (ESR) dates on old travertine deposits interbedded with Quaternary alluvium of Qt3 indicate ages of 315 to 180 ka (S. Ikeda, University of Osaka, Japan, unpubl.). **0.2**
 46.8 Zia roadcut to left, and in distance to right. Ahead (12:00) to north in far distance is Mesa de Guadalupe, with reddish Permian Abo and Yeso strata overlain with profound unconformity by thick, tan Pleistocene Bandelier Tuff (Fig. 1.20). Leaving Jemez Pueblo. **0.1**
 46.9 Cross Vallecito Creek. Junction with NM-290, to USFS-10 and Ponderosa, on right. Good Zia exposures covered with terrace gravels are present along the north side of NM-290 here, as well as along the right side of our route, for the next 0.6 mi. **0.5**
 47.4 Zia sandstone roadcut to right (Fig. 1.21) shows sharp con-



FIGURE 1.20. View to north at mile 46.8 along NM-4, just north of Jemez Pueblo; Vallecito Creek and high Zia Formation exposures in mid-distance, to right.



FIGURE 1.21. Zia Formation sandstone capped by Quaternary cemented alluvium at mile 47.4.

tact near top with overlying coarsely conglomeratic, carbonate-cemented, Quaternary alluvial unit. Through this section of the Jemez Valley, the terraces are underlain by an alluvial fill unit dozens of feet thick, locally cemented with travertine. **0.2**

- 47.6 Salmon-colored outcrops of the Mesita Blanca Member of the Yeso to right, overlain with sharp unconformity by white Zia sandstone, which in turn is capped by gray, travertine-cemented alluvial deposit (Fig. 1.22). Both the Quaternary gravels and Zia Formation thin rapidly to the north at this location across a postulated northeast-striking, cross valley fault. **0.3**
- 47.9 Superbly exposed, cross-bedded eolian sandstones of the Mesita Blanca Member of Yeso in roadcuts and small mesa to left (Fig. 1.23), and forming the high cliffs of Mesita Blanca to right. **0.4**
- 48.3 Frybread stalls to right, and store/service station to left; with continued dramatic high cliffs of Mesita Blanca Member to right. **0.3**
- 48.6 Contact between basal, salmon-colored sandstones of Yeso and brick-red Abo Formation in roadcuts, left and right. As we drive by them, the Abo and Yeso Formations may not seem too different, but they represent profoundly dif-



FIGURE 1.22. Slope-forming Mesita Blanca Member of the Yeso, overlain with sharp unconformity by thin white Zia sandstone, capped by gray, cemented Quaternary alluvial unit, mile 47.6, east of NM-4.



FIGURE 1.23. Small butte west of NM-4, composed of eolian cross-bedded sandstones of Mesita Blanca Member of Yeso, mile 47.9.

ferent depositional systems during the Early Permian. Abo deposition occurred during latest Pennsylvanian and Wolfcampian (Early Permian) time in river channels and on floodplains. Paleoflow was to the SSW off of the Precambrian-cored Uncompahgre uplift (Eberth and Miall, 1991). In contrast, Yeso deposition during the Leonardian took place on a broad, shallow marine to evaporitic coastal plain on which eolian deposition occurred locally. Terrace gravels, probably Qt3, overlie Abo bedrock just beyond. **0.3**

- 48.9 Leaving Jemez Indian Reservation; entering village of Cañon. **0.3**
- 49.2 Jemez Valley schools to left are constructed on the Qt4 terrace on Abo Formation. **0.3**
- 49.5 Leaving Cañon; road curves down through Abo Formation covered with thick terrace gravel deposits of Qt4 for the next 0.6 mi. View to west (left) across San Diego canyon shows basal brick-red Abo Formation overlain by salmon-colored Yeso formation along the west side of the canyon. A higher gray plateau beyond is developed in the Pennsylvanian Madera Formation, upthrown along the west side of the Jemez fault. **0.7**
- 50.2 Junction of NM-4 with NM-485. **Turn left** on NM-485 and immediately cross Jemez River near its confluence with the Rio Guadalupe. This road is very narrow in places; be watchful for local traffic. **0.3**
- 50.5 Old adobe and wooden buildings to right, close to road, part of the village of Cañones, whose residences are scattered along both sides of the road for another mile. Sandstones and shales of the Abo Formation are exposed almost continuously along the left side of road nearly to the Guadalupe Box. **0.4**
- 50.9 Good view of southwest side of Guadalupe Mesa, the interfluvium between the Jemez River to the east and Rio Guadalupe to the west, at 1:00. The thick, reddish Permian (Abo, Yeso) section, dipping southeast, is overlain with angular unconformity by the tan, Pleistocene Bandelier Tuff. The thin gray layer at the contact of the Bandelier Tuff and the Permian section is a buried paleo-Jemez River deposit, Qg2, which may contain a reworked lag of Cerro Toledo Rhyolite (Rogers, 1996). Tshirege units A, B, C, and D of Rogers (1995) are present as well as underlying ignimbrite of the Otowi Member. **0.2**
- 51.1 Terrace exposed on hillslope above us to the left is Qt2. The deposit underlying Qt2 contains Lava Creek B ash, which constrains the age of this deposit to about 0.62 Ma (Rogers, 1996). Note large pedestal of Abo Formation sandstone to left of road. **0.7**
- 51.8 Turn-out on right allows a great view of the west side of Guadalupe Mesa. The Tshirege Member overlies tuffs and associated gravels of Cerro Toledo Rhyolite, which overlie the Otowi Member, and Permian red beds. **0.4**
- 52.2 MP 2. Quaternary terrace gravels on left. **0.2**
- 52.4 Road curves to right; prominent peak at 12:30 is Garcia Mesa, which displays Bandelier Tuff stratigraphy. Virgin Canyon is to the right of Garcia Mesa. **0.3**
- 52.7 To left is a field of huge Abo sandstone boulders. **0.4**
- 53.1 Road dips across lower end of Osha Canyon to the left. **0.1**
- 53.2 MP 3. Contact between red Abo Formation and gray, underlying Madera Formation at 3:00. This contact, at the uppermost marine limestone bed of the Madera, is just



FIGURE 1.24. Columnar Bandelier Tuff units overlying Permian red beds (Abo and Yeso Formations), west side of Guadalupita Mesa at mile 53.7.

below the Pennsylvanian–Permian boundary. The mesa behind Garcia Mesa at 2:00 is Virgin Mesa. Mappers in this region report many petroglyphs, some of which could be considered sexually explicit, on the walls of the Bandelier Tuff. **0.2**

- 53.4 Unnamed volcanoclastic unit of DuChene et al. (1981) exposed at the tan, distinctly stratified unit about halfway up the hillside at 11:00. This unit is compositionally transitional between the Abiquiu and Zia formations (Woodward, 1987), and palynological data suggest an early

Miocene age. This unit is 350–450 ft thick, and is bounded on the west by a fault. **0.3**

- 53.7 Another good view of Bandelier Tuff overlying Permian red beds on Guadalupita Mesa at 1–2:00 (Fig. 1.24). General location of former logging town of Gilman. **0.5**
- 54.2 Santa Fe National Forest sign. **0.2**
- 54.4 Yeso Formation exposures to left. To right at 1–2:00, the view shows the west side of Guadalupita Mesa, and a fault that is antithetic to the major Sierrita fault we will cross farther up the valley (Fig. 1.25). The fault in juxta-



FIGURE 1.25. West side of Guadalupita Mesa from mile 54.4, showing fault near center of photo along which salmon-colored Yeso strata south (right) of fault have moved up relative to Yeso to Agua Zarca sequence north of fault; overlying Bandelier Tuff is not offset.

poses Permian Abo, Yeso, and Glorieta Formations, and Triassic Moenkopi and Agua Zarca Formations to the north, against the Abo and Yeso Formations south of the fault. The overlying Bandelier Tuff fills a channel cut along the fault in the Permian beds and is not offset by the fault, indicating that fault displacement occurred prior to the early Pleistocene. Many of the faults through this part of the Jemez Mountains, while rift-related, were apparently most active in earlier phases of rift development, whereas most rift fault activity presently occurs far to the east along the Pajarito fault zone. **0.8**

55.2 Massive exposures of Precambrian gneiss come into view ahead, as we cross the Sierrita fault (Fig. 1.26). The Sierrita fault is normal and listric, with antithetic normal faults that create keystone grabens. Here, the fault juxtaposes Precambrian hornblende, quartz monzonite gneiss to the northwest with Permian Yeso Formation to the southeast. Stratigraphic offset of the Precambrian rocks approaches 2250 ft; the overlying Bandelier Tuff is offset about 50 ft. **0.2**

55.4 Enter canyon carved by Rio Guadalupe through the Precambrian gneiss (Fig. 1.27). The Rio Guadalupe falls more than 100 ft in 0.25 mi, forming a distinct knickpoint as the river traverses the resistant Precambrian rocks (Fig. 1.28).



FIGURE 1.26. Trace of Sierrita fault near entrance to Guadalupe box, mile 55.2. Reddish Precambrian gneiss to left is juxtaposed against Permian Yeso Formation to right.



FIGURE 1.27. Entrance to Guadalupe Box, carved through Precambrian gneiss by the Rio Guadalupe.



FIGURE 1.28. Rapidly descending Rio Guadalupe at knickpoint in Precambrian gneiss of Guadalupe Box.

It is important to point out that all of this incision is post Bandelier Tuff in age, i.e., less than 1.2 Ma. The U.S. Geological Survey maintains a gaging station at the mouth of the canyon. **0.2**

- 55.6 Pass through two tunnels cut through the Precambrian rocks, excavated originally for the narrow-gauge railway that formerly occupied this roadbed. The railroad (Santa Fe Northwestern) was built in the 1920s from Bernalillo into the Jemez area to transport timber for the White Pine Lumber Company's sawmill in Bernalillo. With the decline in residential construction during the Depression, the company went bankrupt, and its successor (New Mexico Lumber and Timber Company) substituted trucking for the logging spurs. The trucks put their timber on the railroad at a loading platform established in Gilman in 1937, but railroad operations ceased entirely in 1941, when the Jemez and Guadalupe Rivers flooded (Myrick, 1970). **0.3**
- 55.9 Pass through Forest Service gate; paved road ends just beyond. To right, across the river, Precambrian rocks are overlain by Mississippian (Arroyo Peñasco, Log Springs) and Early Pennsylvanian (Osha Canyon, Sandia) Formations. Slopes of Holiday Mesa, rising from 1–2:00, are Sandia and overlying Madera Formations, capped with thick Bandelier Tuff (Fig. 1.29). **0.1**
- 56.0 Last Precambrian outcrops, just before dirt road begins.

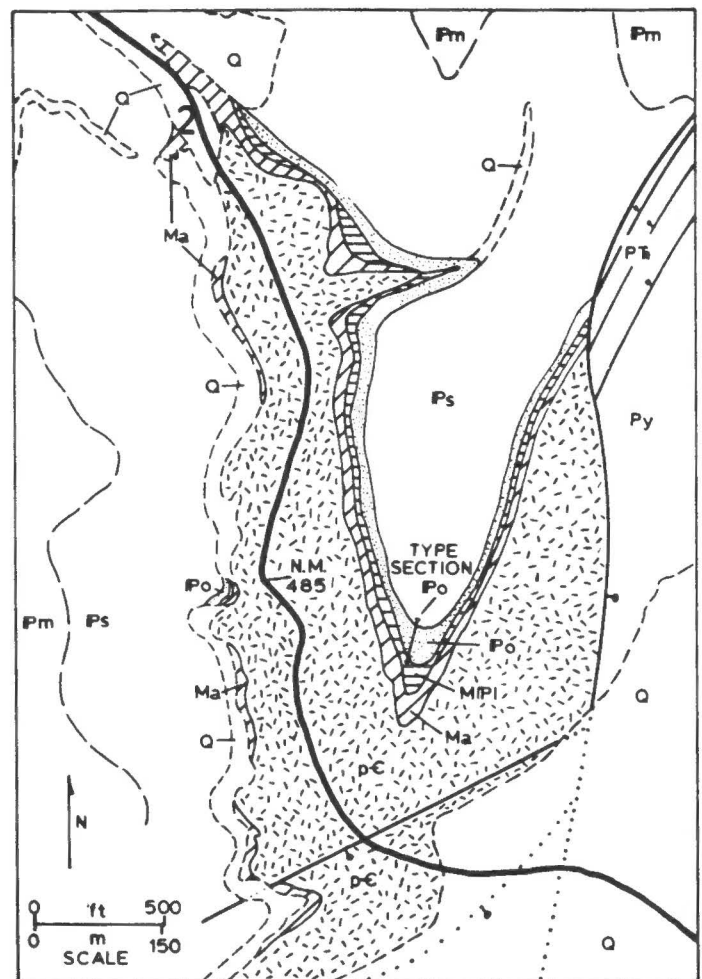


FIGURE 1.29. View northeast from Stop 2, of Holiday Mesa, with slopes of Pennsylvanian Sandia and Madera Formations, capped by columnar Bandelier Tuff.

This is the site of Stop 2, but we will drive up the road a short distance to turn around. **0.4**

- 56.4 To left, roadcuts are through massive brown sandstones and underlying shales of the Sandia Formation, overlain by locally thick colluvial wedges. **0.3**
- 56.7 Turnout on right. Guided by flagpersons, turn around here and head south toward the tunnels. **0.7**
- 57.4 Pavement begins. **0.4**
- 57.8 **STOP 2.** Park along side of road, beginning at turnouts just north of the tunnels. We will examine the Precambrian rocks, the rapidly falling Rio Guadalupe, and the late Paleozoic section at this stop. The Mississippian–Pennsylvanian sequence exposed in Guadalupe Box is one of the most complete in the Jemez–Nacimiento Mountains area, and is known primarily from studies by Armstrong (1955), DuChene (1973, 1974), Armstrong and Mamet (1974) and DuChene et al. (1977). To view part of this section we must cross to the east side of the Rio Guadalupe by rock hopping, and walk south a short distance; refer to the geologic map (Fig. 1.30) for distribution of rock units here. Time will not allow us to hike to the best-exposed section at the end of the large ridge indicated on the map, but an introduction to some of the units will be obtained nearer to Stop 2.

Nonconformably overlying the reddish Precambrian gneiss is the Espiritu Santo Formation (Arroyo Peñasco Group), of Middle Mississippian age. This is predominantly a gray, shallow marine, poorly fossiliferous, ledge-forming dolomitic limestone about 25 ft thick in this area



Q	QUATERNARY/TERTIARY ALLUVIUM
PT	PERMIAN/TRIASSIC UNDIFFERENTIATED
Py	PERMIAN YESO FM.
Pm	PENNSYLVANIAN MADERA FM.
Ps	PENNSYLVANIAN SANDIA FM.
Po	PENNSYLVANIAN OSHA CANYON FM.
MPI	MISS./PENN. LOG SPRINGS FM.
Ma	MISSISSIPPIAN ARROYO PEÑASCO FM.
pC	PRECAMBRIAN GNEISS

FIGURE 1.30. Geologic map of area around Stop 2 (upper left corner, large 2), showing outcrops of Mississippian and Pennsylvanian formations on Precambrian gneiss (after DuChene et al., 1977).

(Fig. 1.31). Above the Espiritu Santo Formation is a discontinuous, thin (2–5 ft), disky red, ferruginous shale unit, the Log Springs Formation, named by Armstrong (1955) from considerably thicker exposures elsewhere in the southern Nacimiento Mountains. This shale, probably a residual soil (DuChene, 1974), lacks fossils and its age is uncertain, but based on stratigraphic position is probably Late Mississippian (Armstrong and Mamet, 1974).

Resting unconformably upon the Log Springs Formation is an approximately 31-ft-thick sequence of white to gray, crystalline limestones and carbonate sands, interbedded with gray calcareous shales, which is overlain by about 40 ft of nodular gray shales. Together these units comprise the Osha Canyon Formation (DuChene et al., 1977), with its type section just to the south (Fig. 1.30).



FIGURE 1.31. Mississippian Espiritu Santo Formation limestone, overlain by slopes composed of Early Pennsylvanian Osha Canyon and Sandia strata, just southeast of Stop 2.

Northrop and Wood (1945) first recognized the Morrowan (earliest Pennsylvanian) age of this interval on the basis of characteristic brachiopods from the lower limestones, and subsequent study (DuChene et al., 1977) revealed a diverse Morrowan fauna consisting of more than 25 species of brachiopods, small solitary rugose corals and tabulate corals, bryozoans, echinoid and crinoid remains, and rare gastropods.

The Sandia Formation, of Atokan (late Early Pennsylvanian) age, overlies the Osha Canyon and attains a thickness of about 225 ft. It consists of massive, coarse-grained quartz sandstones, slope-forming green to gray to tan shales, silty sandstones, and thin-bedded marine limestone beds. The Sandia Formation is widely exposed in the area we are traversing, and is locally very fossiliferous, but little study of these fossils has yet been done. Higher on the slopes of Holiday Mesa, the Madera Formation, up to 760 ft thick here (DuChene, 1974), gradationally overlies the Sandia Formation. The Madera is primarily dense, gray, locally cherty limestones interbedded (increasingly so higher in the section) with gray shales and arkosic sandstones. Modern studies of the biostratigraphy and paleontology of the Madera Formation in this area have not been attempted; Northrop and Wood (1946) indicated the upper Madera here is of Missourian (early Late Pennsylvanian) age. Most workers have divided the Madera in the Jemez and Nacimiento Mountains into a lower gray limestone and upper arkosic member, but facies changes within short distances make these informal terms of dubious value, and their usage is discouraged.

Retrace route 5.5 miles to NM-4. **5.5**

- 63.3 Intersection of NM-485 with NM-44; **turn left** and head north on NM-44. Location of Cañon Landing. Entering Cañon de San Diego, cut by the Jemez River. Sandstones and shales of the Abo Formation appear along right of road from here to Jemez Springs. Bandelier Tuff caps mesas on both sides of canyon. **0.2**
- 63.5 La Junta fishing access on left. **0.2**
- 63.7 MP 10. **0.5**
- 64.2 **OPTIONAL STOP 3:** Turn out to right with bus stop shelter and "Gateway to the Jemez Mountains" information. This stop presents a fine view of the south end of Mesa de Guadalupe, 11–12:00 ahead, with brick-red Abo and



FIGURE 1.32. South end of Mesa de Guadalupe at Optional Stop 3. Abo and Yeso red beds capped by tan Bandelier Tuff.

salmon-colored Yeso Formations overlain by a thick cap of Bandelier Tuff (Fig 1.32). The bright white material locally exposed at the Yeso-Bandelier contact is fluvially reworked, poorly-consolidated fall that preceded deposition of the Bandelier ignimbrites. Locally, stratified gravels and associated floodplain sediments are also preserved at the base of the Bandelier Tuff. At least three levels (Qg1, Qg2, Qg3) of pre-Bandelier Tuff Rio Guadalupe and Jemez River gravels have been observed (Rogers, 1996).

During the war of the Reconquest, in 1692, the Spanish, under the command of De Vargas, pursued Jemez warriors up the cliffs to the top of Mesa de Guadalupe. Overwhelming the Jemez there, survivors were thrown off the cliffs to their death. The path taken by the Jemez and the Spanish for that battle can still be traversed today. **0.5**

- 64.7 Cross cattle guard. Small grocery store is to right and thick beds of Abo formation are just beyond. **0.3**
- 65.0 Entrance to Las Casitas fishing access to left. Just beyond, to left, the Abo-Yeso and overlying Bandelier Tuff are well exposed in high slopes of Mesa de Guadalupe just west of the Jemez River. Columnar jointing of the Bandelier is conspicuous. The low terrace to left is Qt5. This terrace is underlain by alluvial deposits that contain clasts of the Banco Bonito rhyolite flow (Smith et al., 1970), which indicates an age of about 60 ka (Toyoda et al., 1995; Toyoda and Goff, this volume; Reneau et al., 1996) and suggests a genetic relationship to earlier breaching of the southern wall of Valles caldera by the Jemez River as its drainage was integrated through the caldera. See previous minipaper (Mile 41.2 of this road log) by J. Rogers. **1.3**
- 66.3 San Diego day use picnic ground on left. **0.4**
- 66.7 River's Bend fishing access on left. Southern end of Virgin Mesa is to the west across river. Otowi Member of Bandelier Tuff pinches out beneath Tshirege Member on left. **0.3**
- 67.0 Vista Linda Campground to left. **0.5**
- 67.5 Old adobe ruins on left. Landslides and other mass movement deposits are visible on the east flank of Virgin Mesa, at 9:00. **0.2**
- 67.7 Spanish Queen Picnic Area to left. **0.2**
- 67.9 Arroyo Road to right; houses and trailers on Abo Formation slopes next 0.4 mi. Nearly hidden among them are mine dumps of the Spanish Queen copper mine. Legends

of rich treasures from this mine date from the time of early Spanish colonization, but more recent analysis of the ores indicate very low abundances of precious metals. The mine was worked primarily for copper by the Spanish; Simpson (1850) observed copper ore and an old copper-smelting furnace that looked as if it had been abandoned for a long time. The most recent activity was by the Burnett Mining Company in 1926–1929 and 1937, which extracted some 19,200 lbs of copper. Although the company installed a 15-ton Mace furnace, it was not operated, as the ore was shipped to El Paso for smelting.

The sandstone copper deposit here includes chalcocite, malachite and azurite in Abo sandstones and partings of shale, often replacing fossil wood fragments, which also contain minor amounts of uranium. The main ore-bearing horizon is 2.5 ft thick, but a second, lower-grade mineralized zone lies about 40 ft below the main horizon (Kelley et al., 1961; Elston, 1967). The Abo Formation in this area has also yielded Wolfcampian (Early Permian) plant and vertebrate fossils. **0.1**

LATE PALEOZOIC FOSSIL VERTEBRATES FROM THE SPANISH QUEEN MINE LOCALITY AND VICINITY, SANDOVAL COUNTY, NEW MEXICO

Adrian P. Hunt¹ and Spencer G. Lucas²

¹Mesa Technical College, 824 West Hines Avenue, Tucumcari, NM 88401;

²New Mexico Museum of Natural History and Science, 1801 Mountain Road NW, Albuquerque, NM 87104

In 1878, Edward D. Cope announced the first discovery of Permian vertebrates in North America (from Texas) in a lecture at Philadelphia. Unfortunately, his arch rival, Othniel C. Marsh, was in the audience and remembered that years before, David Baldwin had sent him some Permian bones from northern New Mexico. Marsh left the meeting early and published on the New Mexico fossils before Cope published his (Marsh, 1878; Romer, 1960). From then on, north-central New Mexico was an important focus for the collection of Permian vertebrates (Langston, 1953; Romer, 1960; Berman, 1993). Early collecting (1877–1931) was centered in the Cutler Formation of south-central Rio Arriba County. In 1931, A. S. Romer of Harvard discovered a small bonebed in the Abo Formation, at the Spanish Queen Mine locality, south of Jemez Springs. The University of California (UCMP) collected this locality again in 1938 and found another bone bed (named the Johnson bonebed) about 325 ft north of the Spanish Queen copper mine (which is about 1.8 mi north of the “Spanish Queen Mine locality” of Romer). From 1975–1978, D. S. Berman of the Carnegie Museum of Natural History collected in this area and found a partial skeleton of the new sphenacodont *Dimetrodon occidentalis* (Berman, 1977) geographically between the Harvard and UCMP localities.

Romer (1937) named the new pelycosaur *Sphenacodon ferocior* from the Spanish Queen Mine locality, and Langston (1952) described a partial vertebral column of an embolomere amphibian (possibly *Archeria*) that had been collected from this locality by the UCMP. The associated fauna includes diadectids and sphenacodonts.

The fauna of the Johnson bonebed includes unidentified amphibians, an embolomere, and varied elements of small diadectids and sphenacodonts as well as vertebrate coprolites (Langston, 1953). Langston (1953) noted that the fauna from this quarry is distinct from that of the Spanish Queen Mine locality and is more similar to some localities (such as the Welles quarry) in Rio Arriba County.

The paleontology collection of the Department of Earth and Planetary Sciences at the University of New Mexico (UNM) includes some specimens from the Spanish Queen Mine locality, which were presumably given by A. S. Romer to his friend S. A. Northrop. The UNM specimens include a partial, dentulous maxilla of a medium-sized sphenacodont

and other densely packed fragments. The matrix on these specimens is a clay-pebble conglomerate which represents a channel-lag deposit.

All the vertebrate localities in the Abo and Cutler Formations of north-central New Mexico have been conventionally assigned an Early Permian (Wolfcampian) age. However, in the last decade it has become clear that some of the lower portions of these two stratigraphic units are actually Late Pennsylvanian in age (e.g., Fracasso, 1980; Eberth, 1987; Hunt and Lucas, 1992; Eberth and Berman, 1993). Lithostratigraphic correlations of Eberth (e.g., 1987; Eberth and Berman, 1993) suggest that the Johnson bone bed, and presumably the Spanish Queen Mine locality, both of which occur in the lower quarter of the Abo Formation, are late Virgilian or early Wolfcampian in age. The base of the Abo in the Jemez Springs area is late Virgilian (Kues, this volume).

- 68.0 The Bluffs fishing access parking lot to left. **0.7**
 68.7 San Diego Drive on left. **0.4**
 69.1 Entering village of Jemez Springs, population (1990) 413. **0.6**
 69.7 San Diego Bar on left. **1.5**
 71.2 Jemez Springs post office to left. **0.2**
 71.4 Los Ojos Restaurant and Saloon on right; Jemez Springs civic center, police station and bath houses to left, just beyond. By this point, road level has dropped from the Abo Formation into Upper Pennsylvanian reddish clastics and limestones of the upper Madera Formation.
 Several interesting hot springs ($T \leq 75^\circ\text{C}$) occur in the vicinity of the Los Ojos (“The Springs” but literally “The Eyes”) Bathhouse and the quaint gazebo to the left of the road (Goff et al., 1981). In 1978–79, the village of Jemez Springs received a grant from the State of New Mexico to drill a geothermal exploration well (Fig. 1.33). The well struck a hot aquifer identical in temperature and chemical composition to the hottest springs, at the contact of alluvium and Madera Formation (79 ft depth). Another aquifer was encountered in the Madera at 500 ft, but it was more dilute in composition and was only 62°C . Precambrian rocks were intercepted at about 787 ft but no hot waters were found below 500 ft. A small heat exchanger was built and is housed in the little brown shed between the gazebo and the police station but it rarely works correctly due to deposition of calcite from the mineral-rich fluids. Geochemically, the fluids resemble those in the 200–300°C geothermal reservoir inside Valles caldera. **0.3**
 71.7 Low exposures of gray nodular Madera limestone along road to right; just beyond to left are the red-roofed buildings of the Handmaids of the Precious Blood, at MP 18. **0.3**

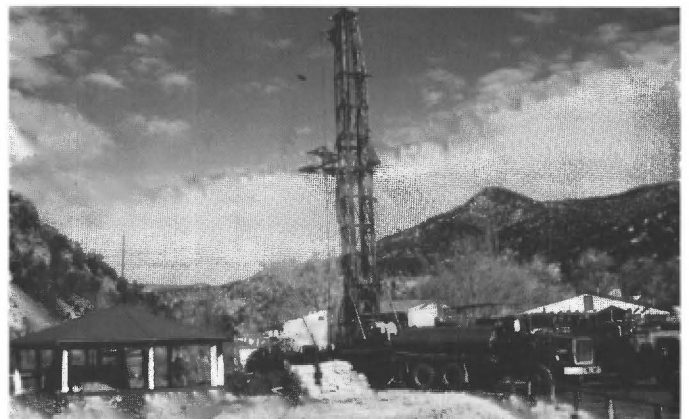


FIGURE 1.33. Drilling an exploratory geothermal well (1978–1979) in Jemez Springs town, mile 71.4.

72.0 Entrance to Jemez State Monument to right; large white church of the Servants of the Paraclete opposite to left. The monument includes the ruins of the Church of San Jose de los Jemez (Fig. 1.34), and various remains, including a kiva, of the Pueblo of Guisewa (Towa for "place at the boiling waters"), which had been a thriving community for 200 years before the entry of the Spanish. The church was founded in 1621–22 by Fray Geronimo Zarate Salmeron but was destroyed during the Pueblo Revolt of 1680, after which the main Jemez settlement was moved to the present site of Jemez Pueblo. Examination of the thick walls of the church reveals blocks of Abo sandstone, Madera limestone, and Bandelier tuff, cemented by a gravelly mud. The church was excavated in 1921–22 and 1935–37. Large piles of selenite found on the floor during partial restoration in 1922 suggest that the thin translucent plates were used as window panes in the church. A small museum is present within the visitor's center, and trails lead to the church and other structures.

The church is located at the mouth of Church Canyon, cut into the upper Madera Formation, and a good section of Madera is exposed just behind the church on the north wall of the canyon (Fig. 1.35). Looking to the west, across

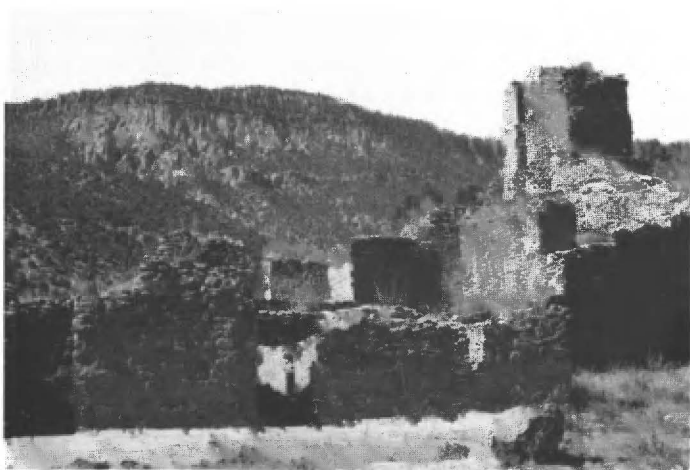


FIGURE 1.34. View to west of ruins of the Church of San Jose de los Jemez at Jemez State Monument; note "tent-rock" erosional features of Bandelier Tuff on upper slopes of Virgin Mesa, along west side of Cañon de San Diego.



FIGURE 1.35. View to northeast of church ruins and slopes of Madera Formation beyond, along Church Canyon.

San Diego Canyon, the Bandelier Tuff capping Virgin Mesa has weathered into a series of overlapping tepee-like structures, or "tent rocks" (Fig. 1.34). **0.1**

72.1 Large deposits of travertine cap bluff on west side of river at 11:00. **0.1**

72.2 Continuous high section of Madera Formation limestones and shales extends to right from Church Canyon to the Jemez Ranger Station, ahead. This sequence is an excellent, albeit steep, exposure of the upper 250 ft or so of the Madera Formation, capped by red shale and sandstone of the Abo Formation near the top of the mesa. The Missourian and part of the Virgilian stage (Upper Pennsylvanian) is represented by the Madera here (Kues, this volume), and numerous beds are profusely fossiliferous. In general, the lower part of the section is composed mainly of gray marine limestones and calcareous shales, whereas the upper 100 ft (Virgilian) is primarily nonmarine to marine red, gray and brown shales with subordinant limestones, representing two or three nonmarine shale to marine limestone transgressive cycles. See following minipaper for additional discussion of cyclicity in the Madera in San Diego Canyon. Sutherland and Harlow (1967), in their study of the brachiopods from high in this section, established the name Jemez Springs Shale Member for a 25 to 40 ft thick reddish shale unit just below the top of the Madera, that is continuously exposed through the canyon north to the Battleship Rock area. For a summary of the diverse marine invertebrate taxa present at this locality, see Kues (this volume). **0.3**

PENNSYLVANIAN CYCLES IN THE UPPER MADERA FORMATION OF CAÑON DE SAN DIEGO

David R. Swenson

Energy Development Corp., 1000 Louisiana, Ste. 2900, Houston, TX 77002

North of Jemez Springs in Cañon de San Diego, the upper 550 ft of the Pennsylvanian Madera Formation consists largely of lithologically asymmetric, limestone/shale cycles that formed on the shallow-marine eastern shelf of the Peñasco uplift (Fig. 1.36).

Here, stratigraphic sections of the Madera Formation with fusulinid distributions were described by Henbest and Read (1944), Northrop and Wood (1946) and Lovejoy (1958). The brachiopod fauna of a shaly unit near the top of the Madera Formation was described in detail by Sutherland and Harlow (1967). Eight stratigraphic sections that form the basis of this report were measured by Swenson (1977). They are located along NM-4 from near Soda Dam to a point 5.1 mi north, where the Madera-Abo contact is exposed in a roadcut on the west side of the highway. Fusulinid identifications by Garner Wilde indicate an age from middle or late Desmoinesian to Virgilian. The upper 400 ft of the studied sections consists of repetitive limestone/shale couplets approximately 30–40 ft thick. This cyclical Missourian and Virgilian part of the section is characterized by a range of carbonate lithologies, thick shales, scarce terrigenous sandstones, and generally conformable bedding relationships. The lower 100 ft of the section is characterized by disconformable boundaries, non-repetitive lithologies, and relatively abundant immature terrigenous sandstones. Northrop and Wood's (1946) division of the Madera Formation into upper arkosic and lower gray limestone members in the Nacimiento Mountains is not useful in the study area, inasmuch as lithologies characteristic of the lower gray limestone overlie those characteristic of the upper arkosic member. Detailed descriptions of the stratigraphic sections with thin section, insoluble residue, and sieve data can be found in Swenson (1977).

Variation of skeletal elements and lithologies in the repetitive upper part of the section leads to a model postulating two basic asymmetric

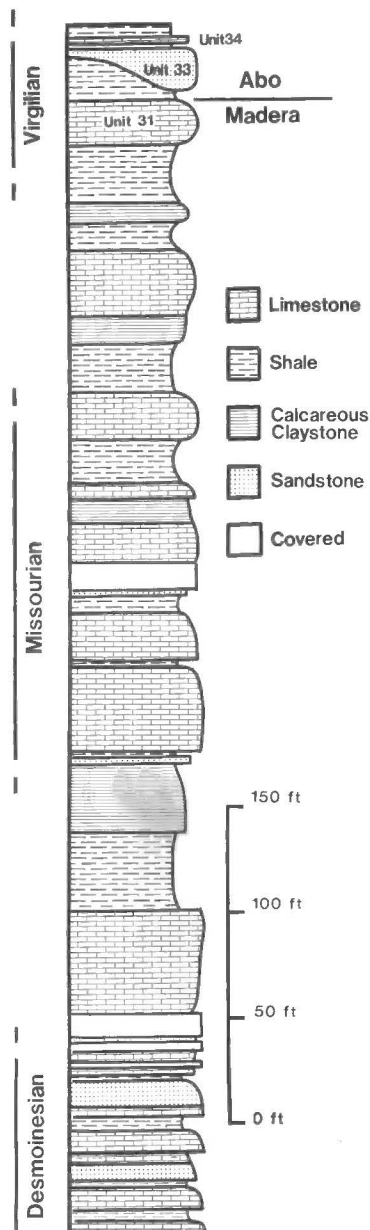


FIGURE 1.36. Generalized composite stratigraphic section of the upper Madera Formation in Cañon de San Diego north of Jemez Springs.

cycles, one faunally diverse and one poorly fossiliferous. The faunally diverse cycle contains skeletal elements of virtually all common Pennsylvanian marine invertebrate phyla and reflects deposition in and adjacent to a normal marine environment, without significant environmental stress. The succession of lithologies in an idealized cycle, starting with the shale facies, gives an indication of the changing environments of deposition during one cycle. The lower part of the clayshale is generally rich in quartz and iron oxides but unfossiliferous. Sparse, thin arkoses are found locally in this shale or at its base. The shale grades upward to calcareous, micaceous, fossiliferous clayshale interbedded with thin, discontinuous molluscan biomicrites and mixed assemblage biomicrudites. Common fossils include echinoids, crinoids, and brachiopods such as *Juresania*, *Neospirifer*, *Composita*, *Antiquatonia* and *Derbyia*. Clayshales apparently represent a range of environments progressing upward from possibly subaerial delta plain or mudflat to normal marine shelf.

Higher in the cycle the shales drop out, leaving thin-bedded mixed-assemblage biomicrudites similar to those below. Many common Pennsylvanian marine invertebrate groups are present, especially brachiopods, bryozoans, and crinoids, and they are commonly unabraded and whole.

The two highest cycles also contain phylloid algae. These limestones were deposited in clear water, on a normal marine shelf probably just below storm wave base.

Succeeding the biomicrudites are variably-bedded, mixed assemblage biomicrites, in which fragmentation of skeletal grains and greater relative abundance of echinoderm grains were observed. These limestones also include crinoid biomicrudites that appear to have accumulated in situ. Comparison of bedding characteristics and lithologic textures of these mixed assemblage facies indicates the biomicrites were deposited in an environment that experienced more bioturbation, bioerosion and/or turbulence than that of the biomicrudites; characteristics of a shallower environment.

Variable intrasparite/dismicrite limestone facies overlie the biomicrites. Some cycles have biosparites below or interbedded with this facies. These limestones occur in moderately thick to massive nodular beds. Many have textures that are apparently variants of the intrasparite or peloidal limestones that are notable in this facies. Poorly fossiliferous micritic limestone with a variably developed fenestral fabric (possibly due to stromatolitic algae) is the characteristic lithology. The biosparites consist of fragmented, abraded, heavily micritized skeletal grains dominated by echinoids, molluscs and ophalimidid and ammodiscid foraminifera. The limited fauna of the intrasparite/dismicrite facies and the low-diversity fauna in the biosparites indicates a stressed environment. The texture of the biosparites indicates a relatively high energy environment. These observations suggest that this part of the cycle records environments ranging from very shallow marine to possibly intertidal mudflats situated along a generally low-energy shoreline.

Capping this cyclical sequence are rocks of the nodular clayshale facies, with sparse interbeds of intrasparite/dismicrite limestones. The sand-to-pebble size micritic nodules are in grain-to-grain contact in a matrix of silty clayshale. Nodules are composed of micrite, microsparite, or dismicrite, and are commonly rounded and reddened along their outer edges. Fossil debris is fragmented and sparse. The origin of these micrite nodules may be due to pedogenic processes, such as in the lower Abo and Hueco Formations (Crabaugh, 1988; Mack and James, 1986), or cannibalization of intrasparite/dismicrite facies just up dip. The oxidized, rounded rims suggest subaerial exposure and/or deposition. The matrix clayshale is very similar to the unfossiliferous, quartz-rich clayshale that overlies the nodular clayshale, which was deposited near or above sea level.

The poorly fossiliferous cycle contains a restricted marine fauna, probably indicating that long-term environmental stresses limited the presence of many genera. The cycle starts similarly to the normal marine cycle, with an unfossiliferous clayshale, and grades upward into fossiliferous clayshale containing thin discontinuous beds of molluscan and fusuline biomicrudite grading upwards into more evenly bedded limestone. Common fossils include pelecypods, gastropods, echinoids, fusulinids, and a few brachiopod genera such as *Derbyia*, generally whole and unabraded. As in the normal marine cycle, this progression indicates a deepening marine environment but with fewer crinoids, phylloid algae, and productid and spiriferid brachiopods. The moderately diverse faunal assemblage suggests a thriving marine community in an environment that was apparently somewhat stressed.

Overlying the fossiliferous limestones are thin beds of poorly fossiliferous micrite, commonly microlaminated with fine-grained, unidentifiable skeletal fragments and iron oxides. Generally the only fossils are sparse ostracods and the foraminifera *Syzrania*, although scattered brachiopods, pelecypods, and echinoderm ossicles can be found also, especially high in the cycle. The textural evidence suggests quiet deposition below wave base in a stable environment. Microlaminae imply intermittent transport of slightly coarser material into this environment and a scarcity of benthic animals. The general scarcity of fossils, on outcrop and in thin section is striking, and may indicate severe environmental stress, such as poorly oxygenated bottom waters. These poorly fossiliferous micrites comprise a large part of the limestone of this cycle (as does the biomicrite in the normal marine cycle), are commonly overlain by variably-bedded molluscan and mixed assemblage biomicrites (as in the normal marine cycle) and similarly record a shallowing environment. The remainder of the cycle follows the pattern of the normal marine cycle.

The Desmoinesian section seems generally cyclical, and is characterized by coarse-grained, lithic-rich arkoses, a lack of fossiliferous offshore clayshales or limestones, and sharp contacts at the base of several units. The arkoses contain mainly granitic/gneissic rock fragments, appear to be developed in place of much of the shale of the upper cycles, and are increasingly marine in nature upwards, i.e. fossiliferous and interbedded with limestones. Whether this section is composed of abbreviated cycles or not, accommodation space was limited but regularly augmented as it filled, and progradational pulses of Precambrian rock fragments regularly buried shales and limestones alike.

The Madera-Abo contact is also exposed throughout the study area. Woodward (1987) defined the top of the Madera Formation in the Nacimiento Mountains to be at the top of the highest thick limestone unit. Swenson (1977) used the highest thick limestone in Cañon de San Diego (Unit 31) as the top of the Madera Formation (Fig. 1.36), although unit 34, albeit thin, is also easily identifiable and mappable throughout the canyon. Regardless of semantics, the transition to Abo-like continental sedimentation occurs between units 31 and 34. As unit 34 contains Virgilian fusulinids and unit 31 has been dated as Virgilian also (Sutherland and Harlow, 1967), the base is dated as Virgilian. The first Abo sand, unit 33, is a medium-grained, crossbedded, arkosic channel sandstone with an underlying laminated arkosic marine sandstone where exposed in the roadcut that is the northernmost exposure of the Madera Formation in the canyon. In the southwest only a thin, very coarse, calcithic arkose remains, apparently a splay sand or a local stream deposit. Considering also that this is the only section with an even higher limestone developed, this spatial distribution is consistent with the derivation of the lower Abo sands from the Uncompahgre uplift to the north (Adams, 1980; Baars and Stevenson, 1984; Crabaugh, 1988) rather than from the Peñasco Uplift.

Comparison of vertical variation among and within the cycles aids in their interpretation. The Desmoinesian section's reduced accommodation space and common arkosic sandstones argue for quite different influences on deposition than those of the upper section. Evidence in the Nacimiento Mountains (Cordell, 1962; Adams, 1980) for tectonic activ-

ity of the Peñasco uplift in the Desmoinesian is consistent with the study area's Desmoinesian characteristics. Apparently the Peñasco uplift was relatively quiescent in the Missourian and early Virgilian.

Asymmetry of individual cycle lithologies indicates the continuing influence of tectonic highlands, although not necessarily the Peñasco uplift. Shales record relative sea levels progressing upward from lowstand to highstand with increasing amounts of limestone. The uppermost shales or immediately overlying limestones were deposited in the deepest marine environment, which then slowly shallowed through the biomicrite facies into the biosparite and intrasparite/dismicrite facies. Perhaps enlargement of the surrounding highlands during lowstand provided a ready source of siliciclastics which inhibited carbonate deposition while sea level rose. When reduction of land area during highstand allowed the waters to clear, limestones mantled much of the seafloor and then inhibited erosion of siliciclastics while sea level fell. These cycles were probably due to eustatic sea level oscillation, considering the ample evidence in the Pennsylvanian for glacially-driven eustasy (e.g., Heckel, 1986). The large number of major and minor cycles recognized by Heckel (1986) in the Midcontinent are not obvious in the study area but may be obscured by effects of tectonism, the area's position on the paleoshelf, or loss of part of the marine Virgilian to onset of Abo deposition.

- 72.5 Jemez Ranger Station (U.S. Forest Service) on right; cross Jemez River just beyond. Fault to right juxtaposes Madera Formation against Precambrian granitic/gneissic rocks to north. 0.2
- 72.7 Alluvium in roadcut to left, then grayish-orange Precambrian rocks. 0.2
- 72.9 **STOP 4. Soda Dam and Jemez fault zone.** Park in turnout on right; a second larger turnout occurs 300 ft farther to left. The travertine dam across the Jemez River is about 300 ft long and 50 ft high and was built by carbonated thermal waters that discharge from a strand of the Jemez fault zone (Fig. 1.37). There are presently about 15 springs

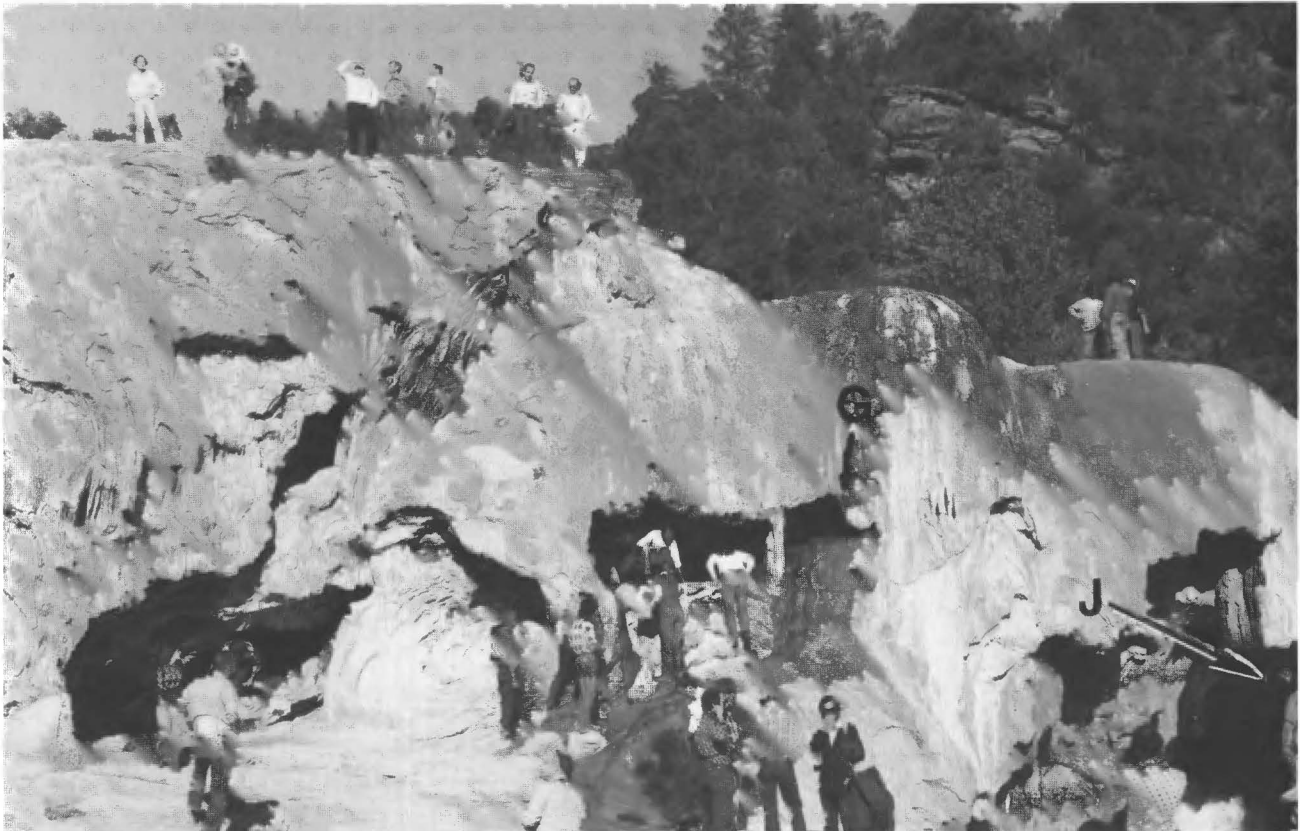


FIGURE 1.37. Travertine deposits of east end of Soda Dam. J, location of Jemez River, below east tip of Dam; G = Grotto spring.

and seeps in this area having a maximum temperature of 48°C. About 25 years ago water flowed along the central fissure at the crest of the dam, but the New Mexico State Highway Department eliminated the hump in the paved road by dynamiting a notch in the west end of the dam. This forever changed the plumbing of hot-spring water and today Soda Dam is slowly disintegrating (Goff and Shevenell, 1987).

The hot springs at Soda Dam and at Jemez Springs have been known since prehistoric times, and were among the most-studied geologic features of north-central New Mexico after the American occupation, beginning with Simpson's (1850) observations. Summers (1976) summarized previous studies of the Soda Dam and other nearby hot springs. Trainer (1984) conducted investigations on the geohydrology of the springs and calculated total thermal discharge at about 1200 l/min.

Thermal/mineral waters at Soda Dam contain about 1500 ppm Cl, 1500 ppm bicarbonate, and substantial quantities of As, B, Br, Li, and other trace elements typical of high-temperature geothermal fluids. They are composed of about 50% geothermal reservoir fluid from Valles caldera and about 50% cold meteoric waters. ^{36}Cl and ^3H isotopes indicate that the water is relatively old, at least a few thousand years (Rao et al., this volume; Shevenell and Goff, 1995; this volume). Several people have claimed that

the hot waters follow a trace of the Jemez fault zone out of the caldera and mix with dilute groundwater (Dondanville, 1971; Trainer, 1975; Goff et al., 1981). By combining geochemical data on hot spring waters and hot aquifers throughout the southwestern perimeter of the caldera with other geologic, geophysical, and drill hole data, Goff et al. (1988) showed that a major subsurface tongue of reservoir water flows out of the caldera along the Jemez fault zone (Fig. 1.38).

The travertine deposits of Soda Dam proper have been dated by the U-Th disequilibrium technique and have a maximum age of about 7 ka (Goff and Shevenell, 1987; Goff and Gardner, 1994). Two older deposits at slightly higher elevation occur across the Jemez River (age 60–110 ka). On the west side of the road roughly 100 ft above the road, occurs an extremely large deposit of travertine that has an age range of about 0.48–1.0 Ma by evaluation with the U-U dating method (Goff and Shevenell, 1987). These older deposits do not overlie Bandelier Tuff; instead they lie directly on Paleozoic and Precambrian rocks. A discontinuous deposit of ancestral Jemez River gravels can be seen beneath the travertine and a large cave is found along the contact. The travertine deposits show that hydrothermal fluids have discharged at the Soda Dam area for the last 1 Ma or about as old as formation of Valles caldera.

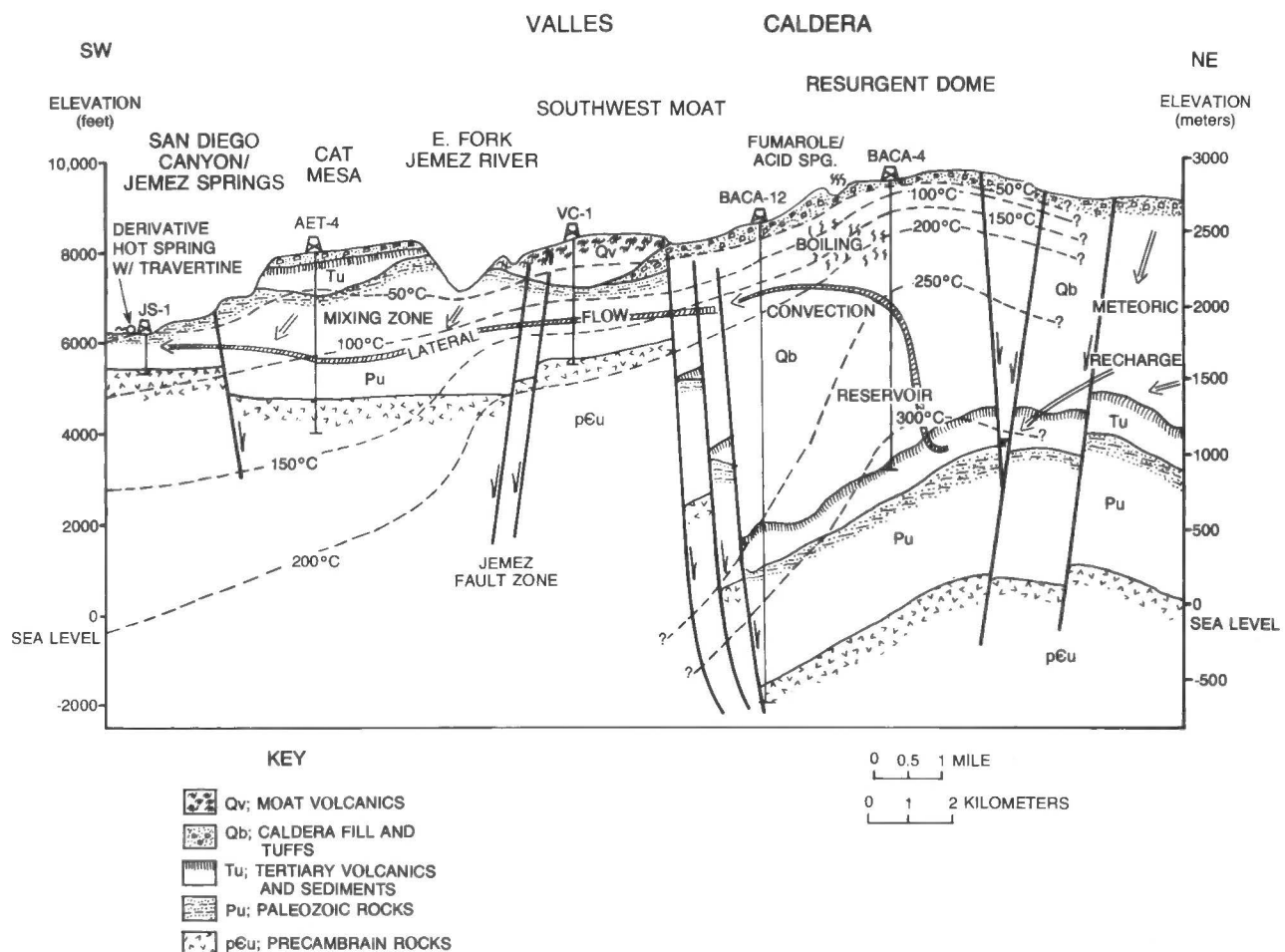


FIGURE 1.38. Cross section of southwest margin of Valles caldera showing general configuration of the active hydrothermal system (modified from Goff et al., 1988). Surface geology, well bore data, geophysics, and fluid geochemistry provide tight constraints on this model. Soda Dam is at far left side of diagram.

The Jemez fault zone is very complex in this area. The main trace trends northeast across the highway and creates a 50 ft scarp along the north side of the older travertine. Generally, displacement along the fault in Paleozoic rocks is about 650–825 ft, down to the east. At Soda Dam, a local horst of sheared Precambrian granite-gneiss is uplifted and overlain by distorted Paleozoic rocks. The granite-gneiss is hydrothermally altered and contains secondary chlorite, barite, galena, and sphalerite in veins and fracture fillings. The Jemez fault zone continues to the southwest and displaces the Tshirege Member of the Bandelier Tuff by about 160 ft in the canyon wall.

If you gaze carefully at the upper east wall of San Diego Canyon (Fig. 1.39), you can see a white band of Abiquiu Formation (late Oligocene) overlying orange Permian Yeso Formation sandstone and shale. The Abiquiu is overlain by basalt flows and an andesite flow/flow breccia sequence (8–10 Ma?) of the Paliza Canyon Formation, and the mesa is capped by a thin layer of Tshirege Member, Bandelier Tuff. Looking northwest, the canyon wall is composed of Pennsylvanian Madera Formation, Permian Abo Formation, Abiquiu Formation, Paliza Canyon Formation, and both members of the Bandelier Tuff. The canyon is partly controlled by erosion along the Jemez fault zone and the stratigraphy is different on either canyon wall.

Late Paleozoic strata near Soda Dam rest upon uplifted Precambrian rocks along the Jemez fault zone. These strata have been measured and briefly discussed by Henbest and Read (1944), Northrop and Wood (1946), Armstrong (1955), Lovejoy (1958), and Armstrong and Mamet (1974). In contrast to the Upper Pennsylvanian Madera strata that are widely exposed along most of Cañon de San Diego, the faulted sequence near Soda Dam consists of Mississippian to early Middle Pennsylvanian rocks. About 35 ft of dolomitic limestones and sandstones of the Mississippian Espiritu Santo Formation rest directly upon the Precambrian, and some microfossils, mainly foraminifers,

have been reported from these units (Armstrong and Mamet, 1974). Above this is a heterogeneous, 119-ft-thick sequence of shale, limestone and minor sandstone assigned questionably to the Sandia Formation, of Atokan (late Early Pennsylvanian) age (Henbest and Read, 1944; Lovejoy, 1958). The Sandia(?) is overlain by about 100 ft of locally cherty limestones of the basal Madera Formation, of early Desmoinesian (early Middle Pennsylvanian) age (Lovejoy, 1958). Some of the Sandia and Madera beds contain marine invertebrate fossils, mostly brachiopods, but these have not yet been studied. If time and interest at Stop 4 allow, some of these fossiliferous units just east of Soda Dam may be inspected.

Return to vehicles and continue northeast on NM-4. **0.2**

73.1 Slopes and roadcuts to left along highway are in the Madera Formation for next 5 mi, and the Madera is extensively exposed to the right (forested slopes) east of the Jemez River. Crossing main trace of the Jemez fault zone. **0.5**

73.6 Servants of the Paraclete, Catholic rehabilitation facility, grounds and buildings to right. **0.1**

73.7 MP 20. **0.3**

74.0 Landslide on right, across Jemez River. **0.1**

74.1 Good exposures of Madera Formation limestones and shales to left. **0.9**

75.0 Spectacular cliffs of Bandelier Tuff in distance at 11–12:00, above Abo Formation and underlying Madera Formation slopes. **0.7**

75.7 Entrance to Hummingbird Music Camp on right. Just beyond to left is a thick and fossiliferous sequence of the upper Madera Formation, described by Corrao and Kues (1996); see also Kues (this volume). Old travertine deposits are present in the lower part of the section. Fossil collecting may be pleasantly done here, in the shade of the pine trees, with music of variable quality wafting up from the camp. H₂S from the Hummingbird fumarole (on both sides of road) adds a distinctive aroma when the wind is right. **1.0**



FIGURE 1.39. Stratigraphy of upper wall of Cañon de San Diego, looking east from Soda Dam.

- 76.7 Entrance to Battleship Rock picnic ground and Camp Shaver on right. The East Fork of the Jemez River runs between them. The Madera roadcut across and a little south of the entrance is abundantly fossiliferous.

Battleship Rock (Fig. 1.40) is a spectacular outcrop of columnar-jointed ignimbrite of post-Valles caldera age formed by small eruptions of rhyolitic ash that flowed down an ancestral Jemez River. Subsequent erosion by later streams has formed canyons on either side of this beautiful example of reversed topography. San Antonio Creek drains the western caldera while the East Fork, Jemez River drains the eastern caldera; the streams combine at Battleship Rock.

The ignimbrite is about 260 ft thick and is composed of two main flow units that comprise a single cooling unit (Bailey and Smith, 1978). Although the base is poorly consolidated, the center is densely welded and very striking in appearance, having black fiamme as long as 8 in. Abundant lithic and crystal fragments are found in the matrix of the ignimbrite with glass shards and pumice. Chemical analyses of the pumice show it contains about 73 wt % SiO₂. Sr 87/86 values are about 0.704, more primitive than most rhyolites in the caldera (Vuataz et al., 1988). The age of the Battleship Rock ignimbrite has been difficult to determine, but recent electron spin resonance dates indicate an age of about 55-60 ka (Toyoda et al., 1995; Toyoda and Goff, this volume).

- 76.9 Roadcuts to left in Madera Formation, locally obscured by red Abo slump debris and sandstone boulders, and by alluvium. Battleship mineral seep issues here. 0.4

LATE PALEOZOIC CHONDRICHTHYANS FROM THE ABO FORMATION, SANDOVAL COUNTY, NEW MEXICO

Adrian P. Hunt¹, Spencer G. Lucas² and Jiri Zidek³

¹Mesa Technical College, 824 West Hines Avenue, Tucumcari, NM 88401;

²New Mexico Museum of Natural History and Science, 1801 Mountain Road NW, Albuquerque, NM 87104;

³New Mexico Bureau of Mines and Mineral Resources, Socorro, NM 87801

New Mexico yielded the first described Early Permian vertebrates from North America (Marsh, 1878) and subsequently became an important source of late Paleozoic nonmarine tetrapod fossils. These fossils derive



FIGURE 1.40. View to north of Battleship Rock, from entrance to Camp Shaver at mile 76.7.

from a lithosome of fluvial redbeds, most of which are included in the Abo or Cutler Formations. However, the extensive paleontological studies of these redbeds have failed to discover many fish fossils. The following few fossil fishes are known from the Pennsylvanian-Permian redbeds of New Mexico (Berman, 1993; Zidek and Kietzke, 1993; this paper): Cutler Formation, Rio Arriba County (Rio Puerco area)—*Xenacanthus* sp. cf. *X. texensis* (Cope), *Progyrolepis* sp.; Cutler Formation, Rio Arriba County (El Cobre Canyon)—*Gnathorhiza* sp.; Sangre de Cristo Formation, Santa Fe and San Miguel Counties—*xenacanthid* indet., *Gnathorhiza* sp.; Abo Formation, Sandoval County—*Xenacanthus* sp., *Gnathorhiza* sp., *Deltodus* sp., *hybodont* indet.; Abo Formation, Valencia County—*Gnathorhiza bothrotreta* Berman; Abo Formation, Socorro County—*palaeoniscoid* indet.; Bursum Formation, Socorro County—*Petalodus* sp., *Deltodus* sp., *Orthacanthus* sp.; and Laborcita Formation, Otero County—*xenacanthid* indet., *Acanthodes* sp., *palaeoniscoid* indet. (more than one taxon), *rhipidistian* indet.

This paucity probably reflects the research interests of the vertebrate paleontologists who have collected in New Mexico (e. g., E. C. Case, S. W. Williston, A. S. Romer, D. S. Berman), all of whom searched for and studied tetrapod fossils. Fossil fish require different excavation strategies than tetrapod fossils. The best fish remains are collected by careful splitting of shaly rocks that often exhibit no exposed bones. Fish fossils most often occur in strata of aquatic origin that contain few, if any, tetrapods. Therefore, the scarcity of known fish is partly due to collecting bias. Another important factor is that most of the strata of the Abo-Cutler lithosome represent well-drained fluvial environments, so there are few examples of the lacustrine environments that favor the preservation of fish fossils.

Here we report on two chondrichthyan teeth from the Abo Formation of Sandoval County that hint at a diversity of fish that is not apparent in previous museum collections from the Abo-Cutler of New Mexico. These fossils came from New Mexico Museum of Natural History and Science (NMMNH) locality 348, which is in a ledge of reddish brown conglomeratic sandstone of the upper part of the Abo Formation at UTM 39665885N, 351010E, zone E in San Diego Canyon about 0.6 mi northwest of Battleship Rock. Dan D'Andrea discovered this locality and collected the fossils reported here.

Two teeth which represent distinct taxa were collected from NMMNH locality 348. NMMNH P-25067 (Figs. 1.41 A-B) represents two thirds of a crown. A large central cusp is gently rounded and ornamented by crenulations. A portion of one low, accessory cusp is preserved, and it is separated from the central cusp by a shallow saddle. The accessory cusp is also rounded with crenulations. Maximum width is 3.6 mm, and the maximum preserved length is 8.3 mm.

NMMNH P-25067 is difficult to classify. The ornamentation pattern is suggestive of *hybodonts* (e.g., "*Hybodus*" *allegheniensis*: Lund [1968], fig. 5; *Polyacrodus*: Johnson [1979], pls. 51-62; [1981], figs. 47-145). However, in overall morphology, the New Mexico specimen more closely resembles the caseodontid *Fadenia* (e.g., Nielsen, 1932, pls. 3-6) or the edestoid *Agassizodus* (e.g., Nielsen, 1932, pl. 7, figs. 4-17, pl. 8). Nevertheless, the ornamentation pattern of the New Mexico specimen is more distinctive than in these taxa, so we tentatively identify the specimen as an indeterminate *hybodont* shark.

NMMNH P-25066 (Fig. 1.41 C-D) is a larger (maximum length = 18.2 mm, maximum width = 6.9 mm) and more complete tooth. The crown in occlusal view is a rounded rectangle covered with tiny, ovoid pores. In lateral view, the crown is asymmetrically convex with the highest point offset from the center. No root is preserved, but the visible tooth crown base is a convex surface.

NMMNH P-25066 is a *cochliodontid* tooth plate (cf. Zidek, 1988, fig. 4; Zidek and Kietzke, 1993, fig. 3). Such tooth plates are difficult to identify at the generic level, partly because of variability and partly because of the antiquity of most of the relevant literature. The Abo specimen is similar to material assigned to *Deltodus* (Newberry, 1897, pl. 24, figs. 1-7; Ossian, 1974, pl. 7, figs. 1-7), so we tentatively assign it to this genus.

The Abo Formation of Sandoval County is Virgilian (Late Pennsylvanian) at its base (Eberth, 1987; Kues, this volume). The fish teeth de-

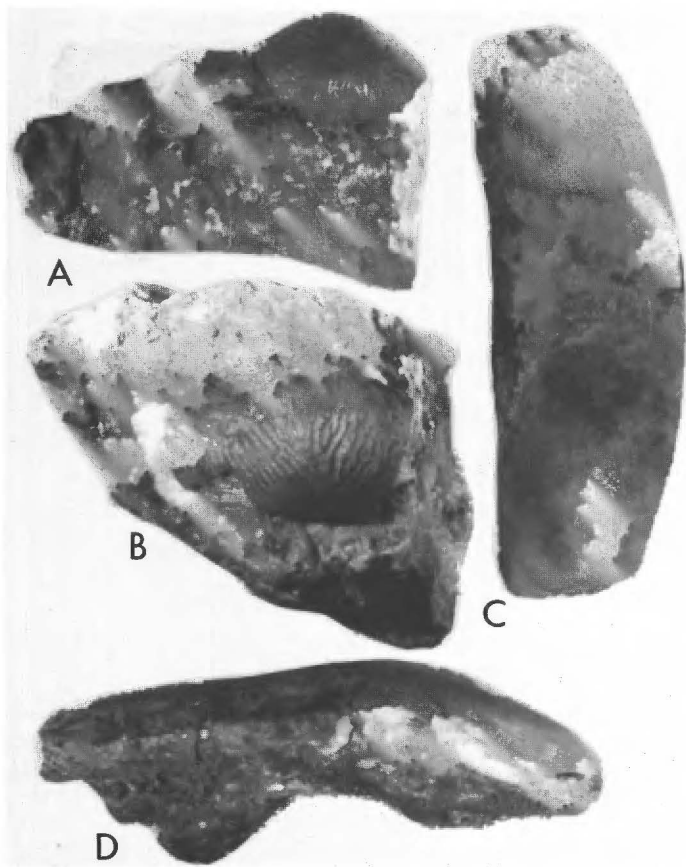


FIGURE 1.41. Chondrichthyan teeth from the Early Permian Abo Formation near Battleship Rock. A, B, *Hybodont?* indet. (NMMNH P-25067), x 4.5. C, D, *Deltodus* sp. (NMMNH P-25066), x 4.



FIGURE 1.42. Section of upper Madera Formation (Jemez Springs Shale Member and overlying marine limestone unit) at mile 77.8. Contact between these units and overlying basal Abo Formation is at road level about 0.1 mi to north.

scribed here derive from high in the formation and are thus presumably of Early Permian (Wolfcampian) age. The presence of a hybodont and *Deltodus* in this portion of the Abo is consistent with, but not demonstrative of, a Wolfcampian age (Johnson, 1992). *Cochliodontids* are not otherwise known from nonmarine deposits, so the *Deltodus* occurrence high in the Abo is somewhat anomalous. Perhaps the tooth plate was brought there by a scavenger or predator. Hybodontids, however, are well known from both marine and freshwater deposits.

- 77.3 View of Bandelier Tuff overlying Keres Group andesite flow/flow breccia to right. **0.2**
- 77.5 Entrance to Rincon fishing access on right; ahead to left is red-stained upper Madera strata, including the Jemez Springs Shale Member. **0.3**
- 77.8 To left, a section of the upper Madera, partly obscured by vegetation (Fig. 1.42). The red-stained shale slope is Jemez Springs Shale Member, overlain by a cliff-forming limestone unit. Brachiopods and fusulinids in these uppermost Madera Formation units indicate a Virgilian (Late Pennsylvanian) age. **0.1**
- 77.9 Contact between uppermost limestone of Madera and overlying red sandstones of Abo in roadcut to left. The boundary between the two formations slightly predates the beginning of the Permian Period. Abo Formation sandstone and shale units in left roadcuts, next 1.0 mi. **0.5**
- 78.4 Large parking area for Spence hot spring on right. Several springs (T 42°C) flow from the contact of Abo Formation and overlying Battleship Rock ignimbrite and Banco Bonito flow along a small bench about 100 ft above the east side of the Jemez River. The largest pool is a favorite des-

tinuation for bathers. In contrast to the mineralized thermal waters down-canyon, Spence hot spring is one of a group of dilute thermal waters that issue in the southern and western moat of Valles caldera (Goff and Grigsby, 1982). Silica and trace element contents of these springs are relatively low. ³⁶Cl isotope work indicates that Spence hot spring may contain a few percent of geothermal reservoir water from the caldera (Rao et al., this volume). Heat flow in this sector of the caldera is high due to proximity of the youngest post-caldera eruptions and the underlying reservoir (Sass and Morgan, 1988). **0.3**

- 78.7 Dark Canyon fishing access to right, MP 25 just beyond. Banco Bonito obsidian over Battleship Rock Tuff in cliffs to right. **0.2**
- 78.9 Red Abo Formation roadcuts end on left, overlain by gray colluvium from volcanic units. **0.4**
- 79.3 View of large cave in cliffs ahead at 1:00, at the contact between flow units of the Battleship Rock Tuff. **0.5**
- 79.8 La Cueva ("the cave") campground to right. **0.1**
- 79.9 Stop sign; La Cueva. Junction of NM-4 and NM-126. Confluence of San Antonio Creek and Sulphur Creek. **Turn right** on NM-4 towards Los Alamos. Road now following Sulphur Creek on right. **0.5**
- 80.4 Forest Hill Road on left. **0.1**
- 80.5 Redondo Creek Rhyolite (about 1 Ma) on left in roadcut; a vertical fracture zone in east end of this outcrop may be a manifestation of the Valles caldera ring fracture. **0.2**
- 80.7 On left, junction with Sulphur Creek Road, Forest Service

Road 105. On right, confluence of Sulphur Creek and Redondo Creek. Redondo Border on skyline at 12:00 and Redondo Peak at 1:00 are composed primarily of intracaldera Bandelier Tuff. **0.3**

- 81.0 Redondo Creek Road on left goes to Redondo Creek graben in resurgent dome of caldera. We will spend much of Day 2 on this road. Ascend post-caldera rhyolitic deposits. **0.3**
- 81.3 El Cajete pumice fall on left; begin to climb up on to surface of Banco Bonito flow. **0.6**
- 81.9 Now driving on surface of Banco Bonito obsidian flow; road cuts expose Banco Bonito through pressure ridges. **0.2**
- 82.1 Redondo campground on left. **0.1**
- 82.2 Turnout on right for San Diego Canyon (Jemez Canyon on some maps) overlook. **0.5**
- 82.7 Dirt road to right goes to Continental Scientific Drilling Program (CSDP) corehole VC-1 (Figs. 1.43, 1.44). The hole was drilled in August 1984 on the southern side of the Banco Bonito obsidian flow on strike with the southwestern projection of the Redondo Creek graben. Objectives were (1) to intersect the hydrothermal outflow plume of the Valles geothermal reservoir relatively near source, (2) to study the structure and stratigraphy near the intersection of the ring-fracture zone and the pre-caldera Jemez fault zone, and (3) to study the petrology of the youngest moat volcanics in the caldera (Goff et al., 1986). Total depth is 2809 ft and the bottom hole temperature is about 185°C. Fluid geochemistry of aquifers at 1300 to 2000 ft depth in VC-1 resembles, but is more dilute than, reservoir waters in the caldera. A model of the hydrothermal outflow plume is shown in Fig. 1.38 (Goff et al., 1988). VC-1 core is altered and structurally disrupted below 1100 ft, particularly the lowermost interval of brecciated Precambrian rocks and Sandia Formation (Hulen and Nielson, 1988). Molybdenite was found in this breccia zone along with chalcocopyrite, sphalerite, galena, pyrite and barite. Fluid inclusion work indicates that the molybdenite was deposited from dilute liquid water at temperatures as high as 280°C (Sasada, 1988). Geissman (1988) found that the paleomagnetic character of Paleozoic rocks in the corehole was overprinted by a reversed magnetic signature and concluded that major hydrothermal activity occurred between 1.4 and 0.97 Ma at about 300°C. K-Ar dates on hydrothermal illites have dates as young as 1.21 Ma (WoldeGabriel, 1990).



FIGURE 1.43. VC-1 core and drill rig.

Sturchio and Binz (1988) obtained ages of 95 to >400 ka on calcite veins using the U-Th disequilibrium technique. The moat volcanic sequence contained several surprises, including an obsidian flow (VC-1 rhyolite) with no surface expression (Goff et al., 1986). Compositionally, the youngest moat rhyolites are amazingly similar in major/trace element chemistry and phenocryst assemblages and composition (Gardner et al., 1986). Several interpretations of the moat sequence based on VC-1 core have been presented but no interpretation is universally accepted (Goff and Gardner, 1987; Self et al., 1991; Wolff and Gardner, 1995; Wolff et al, this volume; Toyoda et al., 1995; Toyoda and Goff, this volume). **0.3**

- 83.0 Leaving Santa Fe National Forest; entering Baca Ranch. **0.3**
- 83.3 Crest of Banco Bonito flow; road to El Cajete vent area on left. **1.1**
- 84.4 Descend off the Banco Bonito flow surface. Pyroclastic El Cajete deposits begin to appear in roadcuts, mostly to left. Flow-banded Banco Bonito rhyolite overlies El Cajete

VC-1 Stratigraphy

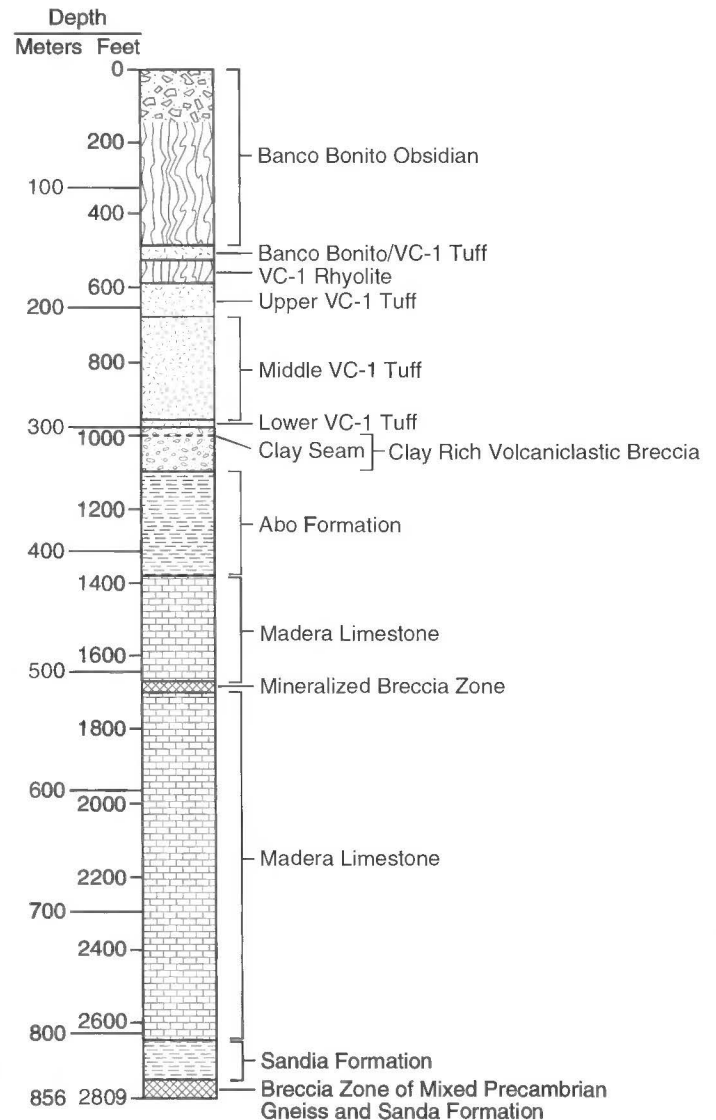


FIGURE 1.44. Diagram showing generalized stratigraphy of VC-1 core.



FIGURE 1.45. Roadcut at mile 85.5 displaying three late Pleistocene rhyolite units, reflecting the youngest eruptions in the Valles caldera.

- pumice. At 12:00 is Los Griegos, a pile of Paliza Canyon andesites capped with 8 Ma (?) dacite. South caldera rim is at 3:00. **0.9**
- 85.3 USFS-133 to Jemez Falls and Banco Bonito campground on right. **0.2**
- 85.5 On left can be seen Banco Bonito obsidian overlying El Cajete rhyolite fall, flow, and surge deposits, overlying South Mountain Rhyolite (Fig. 1.45). This is the famous "Three Rhyolites Stop" of many previous field trip guides. The El Cajete deposits fill in old channels of the ancestral Jemez River which cut into the South Mountain Rhyolite. The outcrop displays vitrophyric blocks of colluvium and stream reworked fragments of Banco Bonito, but in-place material is found higher in the slope. The deposits at this site show so much variation that this stop is a favorite of student field trips. The Banco Bonito flow is the youngest eruption in the Valles caldera and forms a 4-mi-long sequence of several flow units that fills a paleovalley in the southern moat of the caldera (Manley and Fink, 1987; Goff et al., 1986; Self et al., 1991). Recent age determinations on the El Cajete deposits using ESR, TL, and carbon-14 methods show that they are about 55–60 ka (Toyoda et al., 1995; Reneau et al., 1996). $^{40}\text{Ar}/^{39}\text{Ar}$ dates on the South Mountain Rhyolite are about 521 ka (Spell and Harrison, 1993). **0.2**
- 85.7 Cross East Fork of Jemez River. On left, mouth of El Cajete Canyon and parking area; leaving Baca Ranch and entering Santa Fe National Forest. **0.1**
- 85.8 El Cajete pumice fall beneath pink ignimbrite on left. **0.7**
- 86.5 Old log cabin on left. **0.3**
- 86.8 On right, USFS-134 to Vallecitos de los Indios. **0.2**
- 87.0 On right, long row of mailboxes is junction with USFS-10 to Vallecitos de los Indios and village of Ponderosa. **0.2**
- 87.2 Trilobite Trail on right. **0.5**
- 87.7 Las Conchas Peak, composed of Paliza Canyon Formation rocks, at 12:00. **0.1**
- 87.8 MP 34. **0.5**
- 88.3 Roadcuts through fall and flow units of El Cajete pumice. **0.6**
- 88.9 On left, surge E between Fall D (lower) and Fall F (upper); surge E is brownish band and has this appearance due to inclusion of vitrophyre debris (Wolff et al, this volume). **0.4**
- 89.3 On left, road to Copar Pumice's Las Conchas mining pit. **0.2**
- 89.5 **STOP 5. El Cajete pyroclastic deposits.** Pull off road into turnout on right. Roadcut on left (Fig. 1.46) shows several fall and surge beds in El Cajete pumice. The youngest sequence of eruptions from the Valles caldera, consisting of the El Cajete, Battleship Rock, and Banco Bonito Members of the Valles Rhyolite, happened about 50–60 ka (Toyoda et al., 1995; Reneau et al., 1996). Given the new age constraints on these eruptions, taken in the context of post-caldera volcanic history, there are previously unrecognized implications for future volcanism in the caldera area and volcanic hazards in northern New Mexico (Wolff and Gardner, 1995).



FIGURE 1.46. Roadcut at Stop 5, through fall and surge beds of the El Cajete pumice.

The main center of vents for these young units lies about 2.5 mi northwest of this stop, and exposed in this roadcut are the basal fall and pyroclastic surge deposits of the earliest phases of the sequence of eruptive events. The lowest fall units are massive to crudely bedded pumice lapilli and bombs, and are draped over a paleomound of South Mountain Rhyolite (521 ka; Spell and Harrison, 1993). The fall deposits blanketed topography, burying a conifer forest with 16 to 20 ft of pumice. In these lower fall units, vertical molds of standing trees can be found, some of which have been evident in this roadcut in the past. Over these lower fall deposits lies a thin light brown surge deposit of mostly sand to very fine sand pyroclasts and lithic fragments. This surge had surmounted the paleohill, blanketed with the pumice fall, and was flowing pretty much right out of the roadcut towards us. The surge deposits exhibit interesting thickness and textural variations that correlate with the topography that the flow encountered. Within the surge deposit, many holes are evident. These holes, although animals have pirated some in this roadcut, are not animal burrows, but are rather molds of the snapped off tree tops that still were exposed above the early pumice fall deposits. The surge was energetic enough to snap tree tops up to 1 ft in diameter, and was hot enough to carbonize the wood. Consequently, these molds contain abundant charcoal. In contrast, the earlier pumice fall was not hot enough to carbonize the standing trees and the vertical parts of the trees rotted, resulting in preferential preservation of the trees as the carbonized snapped off tree tops within the surge. The paper by Wolff et al. (this volume) presents a great deal of new information on these youngest volcanic products of the Valles caldera. 0.4

PUMICE DEPOSITS IN THE JEMEZ MOUNTAINS, NEW MEXICO AND PUMICE MINING IN THE JEMEZ NATIONAL RECREATION AREA

Michael A. Linden¹ and Diane N. Tafuya²

¹Forest Service, Southwestern Region, 517 Gold Ave. SW, Albuquerque, NM 87102;

²Forest Service, Santa Fe National Forest, 1220 St. Francis Dr., Santa Fe, NM 87504

New Mexico is one of the largest producers of pumice in the U.S., due to the Quaternary volcanic rocks of the Jemez Mountains. These volcanics are composed primarily of silicic tuff, air fall pumice and rhyolitic flows. The Jemez volcanic sequence includes three pumice deposits of distinctly different character, and the economic value of each deposit is largely determined by these characteristics. The Bandelier Tuff is composed of two rhyolite ash-flow units erupted from the Toledo and Valles volcanic centers, respectively. The Guaje pumice and the younger Tsankawi pumice are air fall pumice units at the base of each ash flow. The El Cajete pumice is part of a younger eruptive sequence and is the most economically important pumice unit in the Jemez Mountains. Due to their physical differences, the three pumice deposits are processed into very different end-product uses.

The Guaje pumice is subrounded, grayish white, and generally under 2 cm in size. The pumice deposit ranges from 7 to 17 m in depth and reserves appear to be substantial. Its size, color and lack of staining make it an excellent construction-grade pumice. It is mined by Copar Pumice Company, of Española, New Mexico, at their Guaje Canyon mine, east of Los Alamos, by front-end loaders and loaded as run-of-pit material for minimal screening at an off-site mill. The pumice is used as an aggregate for building blocks and concrete, and in roofing and landscaping. Until recently, Guaje pumice was also mined by General Pumice Company, of Santa Fe, New Mexico, at their Rocky Mountain mine, west of Española. They sold their pumice to American Pumice Company, in Santa

Fe, where it was milled to very fine grain sizes for specialty applications including cosmetics, paints, compounders, chemicals and dental polishing.

The Tsankawi pumice is a subrounded, white-stained lapilli pumice, generally under 1.3 cm. Currently, this deposit is mined exclusively by Utility Block Company, in Paliza Canyon, north of Ponderosa, to feed their "cinder block" manufacturing plant in Albuquerque. The pumice is excavated with bulldozers, screened through a single grizzly at the mine, and trucked directly to the block manufacturing plant. The Tsankawi pumice is suitable for other construction uses, but its smaller size and stained coloration make it less desirable on the open market. The deposit is relatively thin, ranging from 2 to 8 m in depth. The Tsankawi deposit was substantially depleted by mining in the 1950s and '60s, the profitable new areas on this deposit are limited.

The El Cajete pumice is a subangular, grayish-white pumice deposit with fragment sizes as large as 25 cm in diameter. The deposit ranges to 24 m in depth, is laterally extensive, and has been mined on a moderate scale only in the last 10 years. Stratigraphically, the deposit varies from layers of ash and surge deposits to layers of block-sized pumice bombs. Between 30% to 60% of the pumice deposit is composed of fragments larger than 19 mm. The portion of the El Cajete pumice deposit over 19 mm in size is suitable for use as stone-wash pumice in the garment-finishing industries, primarily in El Paso and Los Angeles. Copar Pumice Company mines the El Cajete pumice at its Las Conchas mine and is planning to mine it at their newly proposed El Cajete and South Pit mines as well (see Fig. 1.47). The coarse-sized fraction sells at four or more times the value of common, construction-grade material. As opposed to construction-grade pumice, stone-wash pumice has been determined by the courts to be a "locatable" mineral. The El Cajete pumice is screened at the mine to discard pumice smaller than 19 mm. The presence of desirable fragment sizes, along with the absence of staining and the volume and homogeneity of the deposit, make this pumice deposit very attractive economically.

The Jemez National Recreation Area (NRA), outlined in Figure 1.47, was signed into law on October 12, 1993. The 57,000 acre NRA was created to "conserve, protect, and restore the recreational, ecological, cultural, religious, and wildlife resource values of the Jemez Mountains." Among other things, the Act banned any future patenting of federal land under the 1872 Mining Law and does not allow mining or extraction of minerals, except on valid, pre-existing mining claims. The Act directed the U.S. Forest Service to examine all mining claims in the NRA, in order that a validity determination can be made. Mining claims for pumice, staked several years prior to the enactment of the law, cover roughly 3400 acres of the NRA. In essence, if the pre-existing pumice mining claims are found to be valid under the 1872 Mining Law, then mining for "locatable" pumice will be allowed to proceed. However, the Act also stipulates that strict reclamation standards be applied to any approved mining plans.

Copar Pumice Company currently operates the Las Conchas mine, where their reserves are severely depleted and reclamation operations are underway. The company has proposed the opening of their El Cajete mine, also within the NRA and the watershed for the East Fork of the Jemez Wild and Scenic River. Copar has submitted an operating plan to the Forest Service and an Environmental Impact Statement has been prepared for the El Cajete mine. Start-up for the 83 acre mine is projected for mid-late 1996. If approved, the El Cajete mine will produce 100,000 tons over a ten-year period of coarse-sized pumice, 19 mm or more in diameter, which is used in the garment-finishing industry. All other pumice less than 19 mm in diameter must be wasted on site because "common variety" pumice extraction is not allowed under any circumstances under the NRA Act. The pumice claims in the NRA are located proximal to the El Cajete crater, the postulated source for the El Cajete volcanics, and is the primary reason why coarse-grained pumice is so abundant in the area.

A key aspect of the validity determination involves characterizing the deposit in terms of homogeneity, fragment size and reserves. After examining existing exploration data from the company, we initiated a drilling, trenching, and mapping program on the claims. Between 1989 and 1996, a total of 58 auger-core holes and 9 deep trenches were completed

Vicinity Map
Jemez Area
Santa Fe National Forest

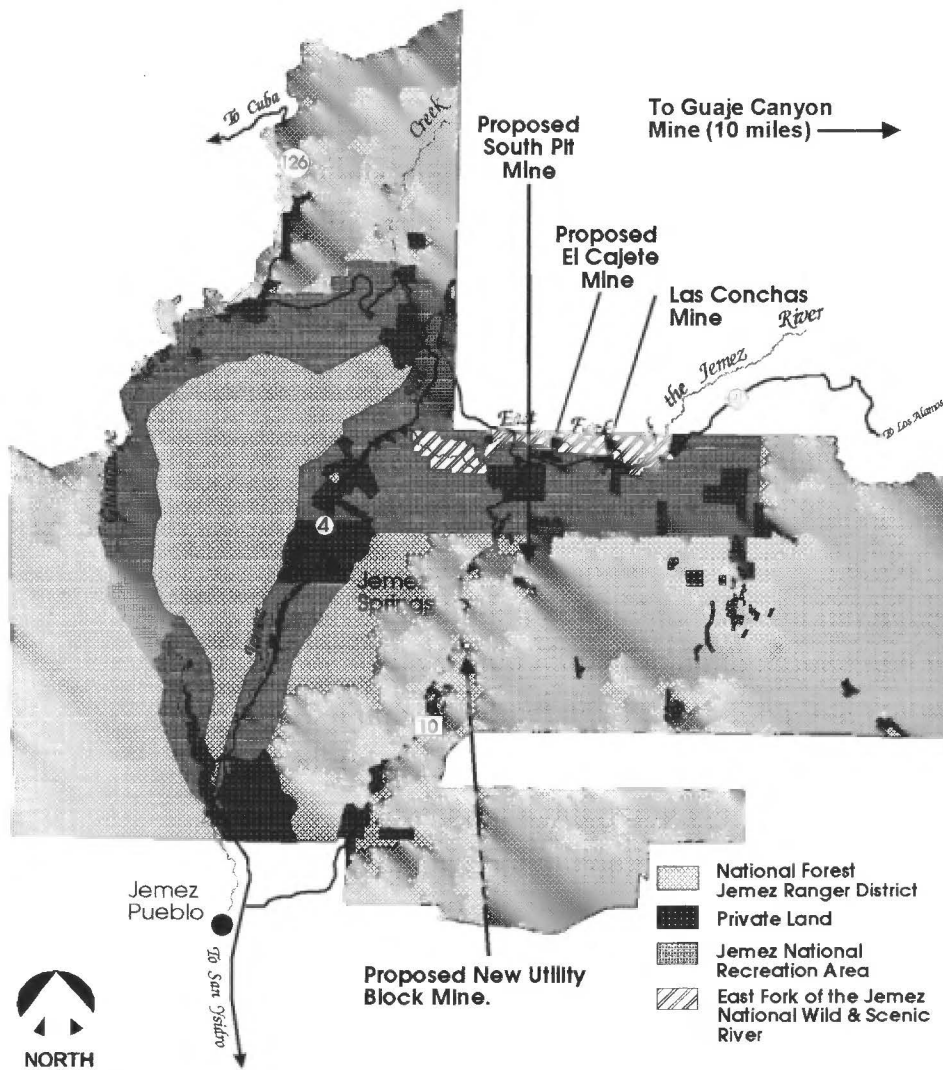


FIGURE 1.47. Map of Jemez Ranger District, land use, and locations of existing and proposed pumice mines.

by Copar and the Forest Service in this area. Auger-cores were recovered using a large-bore core barrel in order to recover the coarse-grained pumice as nearly intact as possible for the validity examinations. The latest auger-core drilling conducted in 1995 used a 25 cm diameter core barrel and a 15 cm diameter sampler tool. Recovered samples were hand-sieved to determine the percentages of various size fractions. These exploration attempts yielded important information on some of the stratigraphic characteristics of the El Cajete pumice. The base of the deposit, in many cases, is marked by a 1–6 cm thick, sandy-clay zone that grades into weathered rhyolite. This zone is interpreted as a paleosol resting on the South Mountain Rhyolite. Cross-sections drawn from core hole information strongly suggest that the original surface on which the El Cajete air-fall pumice was deposited was similar to present topography in the area. On a gross scale, layers containing the coarser-sized fragments occur more frequently with increasing depth and distinct, ash-surge deposits occur in the upper and basal sections of the deposit.

As part of a geohydrologic assessment for the proposed El Cajete mine area, 10 auger-core holes (of the 58 total), plus 3 water-monitoring wells,

were completed by Copar in 1994. Based on this assessment, two separate aquifers occur in the area; a shallow, “perched” aquifer above the clay paleosol and a deeper, more productive aquifer 65–100 m below the surface, within fractures in the rhyolite. Tritium dating by Los Alamos National Lab of the water in the deep aquifer indicates that the water has been underground for at least 30 years and is thought to have originated in deep-seated fractures in the Valles caldera region.

Forest Service geologists estimate an excess of 1.7 million tons of stone-wash pumice (>19 mm) at the El Cajete mine area. Millions more tons of stone-wash pumice exist on the surrounding mining claims as well. Currently, Copar is applying to the State of New Mexico, Mining Act Reclamation Bureau for a mining permit at the El Cajete and South Pit mines. All “hardrock” mining operations in New Mexico, which excludes phosphate, coal, sand and gravel, and other aggregate (quarry) producers, must acquire a mining permit in order to mine. The State has defined stone-wash pumice as a mineral covered under the new regulations. Examination of the mining claims in the NRA is presently continuing and a final determination is expected in the near future.



FIGURE 1.48. Landslide block of hydrothermally altered basalt from Valles caldera wall. Age of alteration is about 8 Ma.

- 89.9 On right, road to Triple H Ranch. Cross East Fork of Jemez River; South Mountain rhyolite cliffs at 10:00 are favorite of rock climbers. **0.2**
- 90.1 On left, pyroclastic flow from South Mountain is overlain by South Mountain rhyolite flow. **0.3**
- 90.4 Cross East Fork of Jemez River again. On right, clays from hydrothermally altered Paliza Canyon basalt in landslide block from caldera margin (Fig. 1.48) have a formation age of about 8 Ma (WoldeGabriel, 1990). The eruption age of the basalt is estimated at 10 Ma. **0.1**

- 90.5 Las Conchas campground on left. **0.2**
- 90.7 Outcrops of South Mountain rhyolite on left. **0.3**
- 91.0 Rabbit Mountain, a post-Toledo caldera rhyolite dome (1.43 Ma; Stix et al, 1988) appears at 12:00. **0.5**
- 91.5 Roadcuts through El Cajete pumice fall deposits; no vitrophyre fragments are contained in deposits at this location. **0.1**
- 91.6 Old corral on left. Behind the corral can be seen South Mountain at 9:00 with Redondo Peak on skyline. **0.6**
- 92.2 USFS-280 on right to Peralta Canyon. Leaving Santa Fe National Forest; entering Baca Ranch. **0.1**
- 92.3 Valle Grande, the largest valley in the caldera at 11:00. **0.2**
- 92.5 Cerro la Jara, a small, post-Valles caldera rhyolite dome, at 9:00. **0.5**
- 93.0 Baca Ranch main gate on left. **0.1**
- 93.1 On right, USFS-268, Paso del Norte Road, to Bland Mining District and Cochiti Lake. Exposures show hydrothermally altered Paliza Canyon andesites. Alteration is dated at about 6.5 Ma (WoldeGabriel and Goff, 1989). **0.7**
- 93.8 MP 40. **0.8**
- 94.6 Valle Grande gate where we will enter Baca Ranch on Day 2 (Fig. 1.49). Valles caldera formed 1.21 Ma during catastrophic eruption of ca. 70 mi³ of the Tshirege Member of the Bandelier Tuff (Smith and Bailey, 1968; Isett and Obradovich, 1994). By comparison, the amount of ash released during the May, 1980 eruption of Mount St. Helens is estimated at 0.5 mi³. To the west, we can gaze across Valle Grande, the eastern portion of the caldera moat, to-



FIGURE 1.49. View to west of the southern Valle Grande. RP = Redondo Peak; R = Redondito knob; SM = South Mountain; LJ = Cerro La Jara; B = Baca Ranch headquarters.

ward the broad mountain of Redondo Peak (11,352 ft) forming the eastern segment of the resurgent dome. This segment is really a northeast-trending ridge that includes the knob of Redondito. To north, from right to left, are the post-caldera rhyolite domes of Cerro Medio at 10:00, Cerro del Abrigo at 9:30, and Cerro Santa Rosa. If you look northwest through the low spot between these domes and Redondo Peak, you can see the northwest wall of the caldera, about 11 mi distant. **0.7**

- 95.3 N.M. Highway Department Historic Marker for the Valle Grande. **0.8**
- 96.1 Roadcuts through Tschicoma dacite on right. **0.5**
- 96.6 Leaving Baca Ranch; entering Bandelier National Monument. Eastern topographic rim of Valles caldera. **0.8**
- 97.4 On right, USFS-289, Dome Road, to St. Peter's Dome and Cochiti Lake. We will take this route on Day 3. This area was devastated by a large fire in May 1996, which makes the following minipaper of unusual interest. **0.3**

OVERVIEW OF FIRE HISTORY IN THE JEMEZ MOUNTAINS, NEW MEXICO

Craig D. Allen¹, Ramzi Touchan² and Thomas W. Swetnam²

¹National Biological Service, Jemez Mountains Field Station, Bandelier National Monument, Los Alamos, NM 87544;

²Laboratory of Tree-Ring Research, University of Arizona, Tucson, AZ 85721

Fire is a key determinant of the ecological structure and function of many southwestern forests (Allen, 1989). Fire can also have significant effects on geomorphic processes (Swanson, 1981; Meyer et al., 1995; White, in press). Accurate information on the spatial and temporal variability in past fire regimes is important to ecologists and earth scientists who seek to understand past and present landscape patterns and processes.

We used dendrochronological (tree-ring) methods to reconstruct fire occurrence patterns covering the last several hundred years across a variety of vegetation types, topographic situations, and geographic locations in the Jemez Mountains (Touchan et al., in press). We dated over 3000 fire scars from 354 trees, snags, logs and stumps at 25 sites located around an arc 30.8 mi in diameter that circumscribes the Jemez Mountains (Fig. 1.50). Elevations of sampled sites ranged between 6560 and 9840 ft.

Each scar was dated to its precise year of formation, and in most cases to the season in which the fire occurred. Samples from a single tree recorded as many as 30 fire events. We used these data to develop fire histories at multiple spatial scales, building up from individual trees through clusters of trees at sites, and then aggregating to the scale of watersheds (Allen, 1989), the entire mountain range (Touchan et al., in press), and even the whole Southwest (Swetnam and Betancourt, 1990; Swetnam and Baisan, in press).

Ponderosa pine (*Pinus ponderosa*) dominates most sample sites, although we also sampled mixed conifer forests that contained Douglas fir (*Pseudotsuga menziesii*), white fir (*Abies concolor*), and Engelmann spruce (*Picea engelmanni*). We collected aspen (*Populus tremuloides*) cores from pure stands adjacent to some mixed conifer sites and crossdated them to determine postfire establishment dates. We also used dendroclimatic methods to reconstruct December-June precipitation back to 1653 A.D. using ring-width chronologies from nine sites in northern New Mexico.

The fire scar chronologies show that fire was frequent and widespread in the Jemez Mountains prior to the 1890s (Fig. 1.51). For example, fire scar samples in Bandelier record 115 different fire years between 1480 and 1899 A.D. Surface fires burned in primarily grassy fuels from the lowest elevation mesa-top stands of ponderosa pine at 6660 ft to the summit of the Frijoles Creek watershed at over 9840 ft, with average intervals between widespread fires ranging from 5 to 15 yrs. In many years climate-synchronized fires burned throughout the Jemez Mountains (and even throughout the Southwest; see Swetnam and Betancourt, 1990); in other years, smaller, patchier fires occurred. We believe that lightning caused the vast majority of these fires, as lightning strikes and lightning-ignited fires are very abundant in this region (Gosz et al., 1995). Like elsewhere in the Southwest, the widespread surface fires ceased throughout the Jemez area in the late 1800s (Fig. 1.51), apparently because intense grazing by large numbers of free-ranging livestock reduced the grassy fuels through which most fires spread (Allen 1989; Swetnam and Baisan, in press; Touchan et al., in press).

The network of 25 fire scar sample sites reveals significant spatial variations in past fire regimes across the Jemez Mountains. Ponderosa pine forest sites exhibited a range of high-frequency surface fire patterns, with reduced frequencies observed (1) at low elevation sites, which

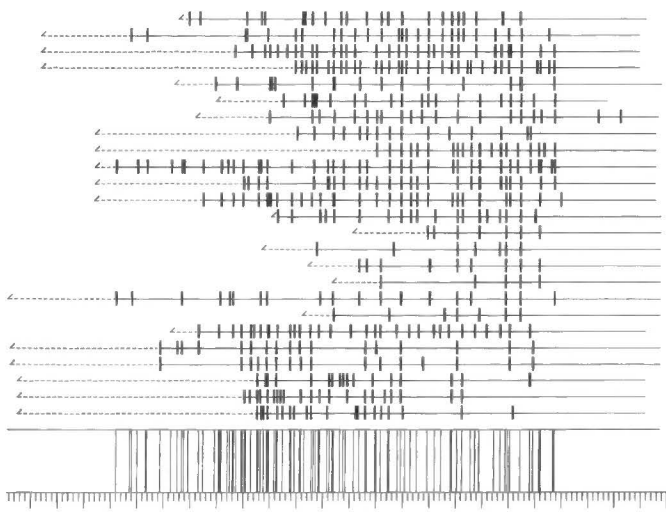
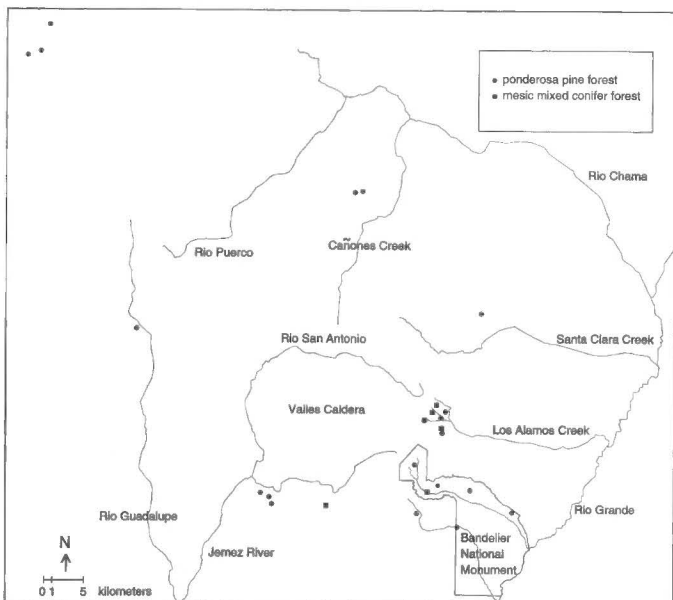


FIGURE 1.51. Composite fire history chart for major fires in the Jemez Mountains. Horizontal lines represent individual sites located in Figure 1.50; each line covers the maximum life spans of trees within a site. From top to bottom, site time lines are arranged sequentially relative to the site map, starting from the west-central site in Figure 1.50 counterclockwise around to the cluster of three sites in the northwest corner. Vertical bars are composite fire dates recorded by scars on at least 25% of the trees within each site; thin vertical lines indicate fire dates on the time line when at least 10% of the sites recorded a major fire. Note the synchrony of fire events between sites, and the cessation of widespread fires in the late 1800s.

FIGURE 1.50. Map showing location and general forest type of sites sampled for fire scars in the Jemez Mountains.

have inherently lower potentials for producing fine fuels; (2) at places that are topographically isolated from the larger matrix of pine forests; and (3) during times that livestock grazing likely reduced the quantity and continuity of local surface fuels. Past fire regimes in mesic mixed conifer forests included a combination of surface fires and patchy crown fires at 15-30 yr intervals. Historical lightning fire records from Bandelier National Monument indicate that in most years middle-elevation ponderosa pine forests have a greater propensity for sustaining fires than other vegetation types.

Other significant findings include (1) some of the first quantitative reconstructions of fire history from several southwestern forest types, including riparian mixed conifer, ponderosa pine/piñon-juniper ecotone, and spruce-fir; (2) surprisingly frequent fire occurrence from several moist or high elevation forest types; (3) proof that essentially all paleofires occurred in spring or early summer, whereas much prescribed burning today occurs in the fall for control reasons; (4) indications of possible Native American enhancement of fire frequencies in a few, particular time periods and places; and (5) demonstration of the long-term coexistence of the endemic Jemez Mountains salamander (*Plethodon neomexicanus*) with fire.

Major changes in southwestern fire regimes over the past century (Swetnam and Betancourt, 1990; Swetnam and Baisan, in press) are having correspondingly large ecological effects on southwestern forests, including those of the Jemez Mountains of northern New Mexico (Allen, 1989). Fire suppression during this century has allowed the buildup of unnaturally high densities of trees and amounts of ground fuels that were formerly thinned by frequent surface fires. Thus fire suppression has promoted conditions that today threaten forests in the Jemez Mountains with increasingly large, intense, and uncontrollable crown fires. In 1977, one such fire, the La Mesa fire, burned through the heart of Bandelier's ponderosa pine forests. This was the largest and most intense fire to burn in the Jemez Mountains this century. Diverse studies have been conducted on the ecological effects of the La Mesa fire (Foxy, 1984; Allen and Eskew, in press), including fire effects on avifauna and nitrogen-cycling to cultural resources.

Fires certainly affect geomorphic processes in the Jemez Mountains. For example, White and Wells (1984) studied the geomorphic effects of the La Mesa fire in six small watersheds that burned with varying intensities in Bandelier National Monument. Water runoff in the Frijoles watershed became "flashier" after the fire due to the loss of vegetation and litter ground cover. The amount of post-fire erosion depended upon upslope catchment area, slope steepness and shape, amount of vegetation regrowth, and most importantly, the degree to which impermeable ash layers developed. They found that the higher elevation sites had largely stabilized within 2 yrs due to the more rapid recovery of vegetation cover. White (in press) has followed the recovery of these burned watersheds into the 1990s, finding that log dams (from fallen trees) and the development of cryptogamic crusts have also contributed to more stable surface conditions.

Other evidence indicates that fires have been important in the Jemez Mountains for thousands of years. Stearns (1981) extracted a single core, 12.3 ft in length, from Alamo bog in the central Jemez Mountains. The core had a basal radiocarbon date of 4595 ± 105 yr B.P. This core contained 12 charcoal lenses accounting for 21 % of the total core length. Charcoal lenses were particularly prominent in the lower 40% of the core (ca. pre-3330 yr B.P.), where 6 lenses comprised over a third of the core length. About 3500 yr B.P. two "volcanic ash" layers were observed atop thick charcoal lenses, perhaps indicating redepositions of older "ash" (pumice?) deposits from nearby slopes.

Fire has affected ecological and geological systems in the Jemez Mountains for several thousand years. About two thousand historic fires recorded by the U.S. Forest Service as far back as 1906 are being mapped to allow GIS analyses of fire occurrence patterns, and fire-scar sampling is taking place at additional sites, as efforts continue to refine our knowledge of fire's role in shaping this landscape.

97.7 MP 44. **0.5**

98.2 Densely welded Bandelier Tuff on left; sharp curve through head of Frijoles Canyon. **1.6**

- 99.8 Sandia Crest at 12:00; Frijoles Canyon on right; begin descent of long, steep grade . . . nurse your brakes. **0.4**
- 100.2 St. Peters Dome and San Miguel Mountains at 1:30. **0.1**
- 100.3 Bandelier National Monument boundary sign. **0.2**
- 100.5 Los Alamos County line. **0.3**
- 100.8 MP 47. Tschicoma Formation dacite dated at about 3.8 Ma on left (Dalrymple et al., 1967). **0.2**
- 101.0 Sangre de Cristo Mountains forming eastern side of Rio Grande rift on skyline at 12:00. **0.4**
- 101.4 West Gate pullout (former Girl Scout camp and ski area) on left. **0.6**
- 102.0 USFS-181, road to American and Armstead springs, on left. **0.3**
- 102.3 Bandelier Tuff unit F (Rogers, 1995) on left. **0.2**
- 102.5 Contact between Bandelier Tuff units F and unit E on left. **0.1**
- 102.6 Sangre de Cristo Mountains and Española basin at 12:00. **0.2**
- 102.8 Pajarito fault scarp; road curves sharply to left. **0.3**
- 103.1 10 mph U-shaped switchback on fault scarp. **0.2**
- 103.3 El Cajete pumice on right. **0.2**
- 103.5 Junction of NM-4 and NM-501; **turn left** onto NM-501. Road is in a narrow, wedge-shaped graben filled with fan deposits, material shed off main fault, and El Cajete pumice. Structure dies out as we cross Water Canyon. **0.3**
- 103.8 Bottom of Water Canyon, one of the few canyons that heads in the Sierra de los Valles, crosses the Pajarito Plateau, and empties into the Rio Grande. The canyon gets its name from a large cold spring that discharges about 1 mi upstream of this point. **0.3**
- 104.1 Quaternary fan deposits on both sides of road. **0.3**
- 104.4 Road to Los Alamos National Laboratory (LANL) Technical Areas (TA) 11, 16, 28, 37 on right. **0.1**
- 104.5 Two water tanks on left. Trenches in this area attempted to cut through the trace of the Pajarito fault (Olig et al., this volume; Wong et al., this volume). **0.4**
- 104.9 Crossing fan deposit from Cañon de Valle. **0.5**
- 105.4 Faulted Tshirege unit D on left. Road is crossing fan deposits. **0.5**
- 105.9 Approximate beginning of a high-angle, northeast-trending, reverse fault, which separates the Pajarito Plateau and Sierra de los Valles, from here to the south side of Los Alamos Canyon. **0.1**
- 106.0 Cross Pajarito Canyon and enter a fan-deposit filled trough bounded by high-angle faults, reverse on west and normal on east. This structure dies out on the south side of Los Alamos Canyon. **0.2**
- 106.2 Two Mile Mesa road to LANL technical areas on right. **0.2**
- 106.4 Turn left at Ski Area sign onto Camp May Road, USFS-1. **0.1**
- 106.5 Outcrops of Tshirege unit F on right. **0.2**
- 106.7 Stay on paved road by turning left. Begin to climb Pajarito fault scarp. Road is built on fan deposit. **0.1**
- 106.8 El Cajete pumice in colluvium on left. Road is ascending through Tshirege unit E. **0.2**
- 107.0 Surge deposit on left is contact between Units E and F. Stop 6 is just beyond on the left. **0.6**
- 107.6 Dirt road on left. **0.1**
- 107.7 Cross under power lines. **0.1**
- 107.8 Turnaround in turnout on right and return to Stop 6 turnout. **0.8**

108.6 **STOP 6. Pajarito fault scarp and plateau overlook (“the ocean”).** We are perched atop a 200 ft scarp, developed in Bandelier Tuff, on the Pajarito fault (Fig. 1.52). The Pajarito fault zone is one of a system of faults that form the local, active western boundary of deformation in the Española basin of the Rio Grande rift. The gross geometry of the Española basin is asymmetrical, with rift-fill sediments pinching out altogether against the Sangre de Cristo Mountains on the east and as much as 1 mi of Tertiary and younger rift-fill sediments and volcanics immediately east of the Pajarito fault (Kelley, 1978; Goff and Grigsby, 1982). We believe that referring to the Española basin as a “half-graben” is erroneous, and oversimplifies the basin’s complicated structure. Combining geophysical and drill hole data, Dransfield and Gardner (1985) developed a structure contour map of the pre-Bandelier surface beneath the Pajarito Plateau. The map reveals that, at least for the western part of the basin, the asymmetrical geometry is caused by a series of north-trending down-to-the-west normal faults that effectively stair-step the basin down to its deepest part here on the west. Thus, the area between the westernmost of these smaller faults and the Pajarito fault is a large, deep graben which has been recognized in numerous geophysical studies (Budding, 1978; Cordell, 1978; Goff and Grigsby, 1982; Ferguson et al. 1995). Furthermore, there is some evidence from microseismicity that most of the faults of the area are high angle to seismogenic depths (10 mi); thus, if any of the faults develop into listric faults with depth, it happens at mid-crustal levels, rendering the popular “half-graben” model, for at least the Española basin, moot.

The 10-to-15-mi wide, 30-mi-long Pajarito Plateau is bounded by the Pajarito fault zone on the west, the Rio Grande on the east, the Puye escarpment on the northeast, and the Cañada de Cochiti fault on the southwest. The eastward-sloping plateau is cut in the Tshirege Member of the Bandelier Tuff. The surface largely conforms to the dip-slopes of flows in Units C and D (eastern half) and in Units D, E, and F (western half). The distal edges of flows in Units E and F probably did not extend eastward farther than mid-plateau. The southeast-trending stream dissection of the plateau is strongly influenced by the dip-slopes of the Tshirege units and by jointing and faulting trends. In the Los Alamos area, the two major faulting trends are NNE and WNW (Rogers, 1995). Generally, displacements along the NNE faults are greater than on the WNW ones.

In the western third of the plateau, gentle NNE-trending anticlinal and synclinal folds reverse the dip of Tshirege units as the Pajarito fault zone is approached, giving a broad reverse-drag effect. The overall slope of the plateau does not change because of the increased number of flows in the western part. The easternmost fold is the Los Alamos Canyon arch (Rogers, 1995), which can be seen from here as it crosses Los Alamos Canyon. It dies out to the SSW as it crosses Cañon de Valle. The arch determines the western limits of exposure for the lower stratigraphic units of the Tshirege. The Water Canyon arch (Rogers, 1995) dies out to the NNE, after crossing Pajarito Canyon, into the synclinal fold which can be seen just this side of the Los Alamos Canyon bridge. Facies changes in the Tshirege units occur immediately east or west of the arch.



FIGURE 1.52. View of “the ocean”, with city of Los Alamos and Omega bridge in right foreground.

Los Alamos Canyon is fault-controlled in the western part of the plateau. The west-trending Los Alamos Canyon fault (Rogers, 1995) extends eastward down the canyon from the left-bend in the canyon, under the Omega bridge, to the Los Alamos Canyon arch. It is downthrown to the north. This allows the synclinal fold axis to be much deeper on the north side of the canyon. We are looking at the southern end of a structure that becomes graben-like to the north and is fault-bounded on the east by the Los Alamos (Rendija Canyon) fault before Pueblo Canyon, the next canyon north, is reached. An enclon fault, which appears (photo-interpretation) to be a high-angle reverse fault, runs up Los Alamos Canyon from the left-bend through the Pajarito fault zone. Displacement is down to the south. The displacement accommodates the change in structural style of the Pajarito fault zone from the north to the south side of the canyon. Looking north across the canyon, you see a faulted, monoclinical fold. The north-trending faults are closely spaced, small-displacement, down-to-the-west normal faults. On this side of the canyon (south side), down-to-the-east displacement is accomplished by large-displacement faulting. Immediately below us (to the east) is a small graben.

We are standing on the highest stratigraphic unit of the Tshirege Member that crops out on the Pajarito Plateau, Unit F. In the roadcut right below us, is the contact between Units F and E denoted by a surge deposit. Lithologic descriptions for units of the Tshirege Member recognized by Rogers (1995), are given at Stop 3, Day 3 (units A–D), and below, for units E and F.

Unit F (0 to 50 ft)—gray, pink or orange, moderately welded to densely welded tuff, which weathers with thin orange or black rind, contains rare lithics up to 4 in. long. Pumice fragments, frequently flattened with vapor-phase crystallization throughout unit, are commonly 0.4–0.8 in. long but may be as long as 1.75 in.; color same as matrix or gray, lavender, pink, orange or red-brown. Unit F contains 1–2% iron-bearing crystals that weather as pin-head size rust spots, a phenocryst content overall of approximately 6%, and has a vertical profile. A sandy parting (of probable surge origin) separates it from underlying unit E. At places, the top surface of unit F has fumarole vents and spectacular differential weathering of joints. Unit may represent more than one ash flow, its depositional limit was approximately 2.5 mi east of plateau western edge. Unit F can be identified using U, Fe, Th and Cs content in 73.3% of cases.

Unit E (0 to 300 ft)—pink, light orange, light to dark gray, nonwelded to densely welded tuff that weathers with thin light-brown, orange, or black rind. Lithics, 0.4–4.0 in., present in upper part locally. Pumice fragments, commonly 0.4–1.0 in., but up to 9.0 in. long, generally rare or confined to stringers, show vapor-phase crystallization throughout unit. Unit top in places is pumice-rich, as is some rock in the ‘horizontal fracture’ facies (Rogers, 1995). Even in densely welded rock, pumice may not show much collapse. Pumice color may be same as matrix or light to dark gray, tan, red-brown, or red. Unit contains 1–8% iron-bearing crystals that weather as pin-head size and larger rust spots, least common at top; phenocryst content overall is 15–20%. Sandy partings (of probable surge origin) separate unit E from unit D below and unit F above. Unit E may form slopes even where welded, and represents four or more ash flows; depositional limit was approximately 5 mi east of plateau western edge. Unit can be identified using U, Fe, Th, and Cs content in 41.2% of cases, but number of cases used was probably insufficient to characterize, given unit complexity.

Return to NM-501. **0.6**

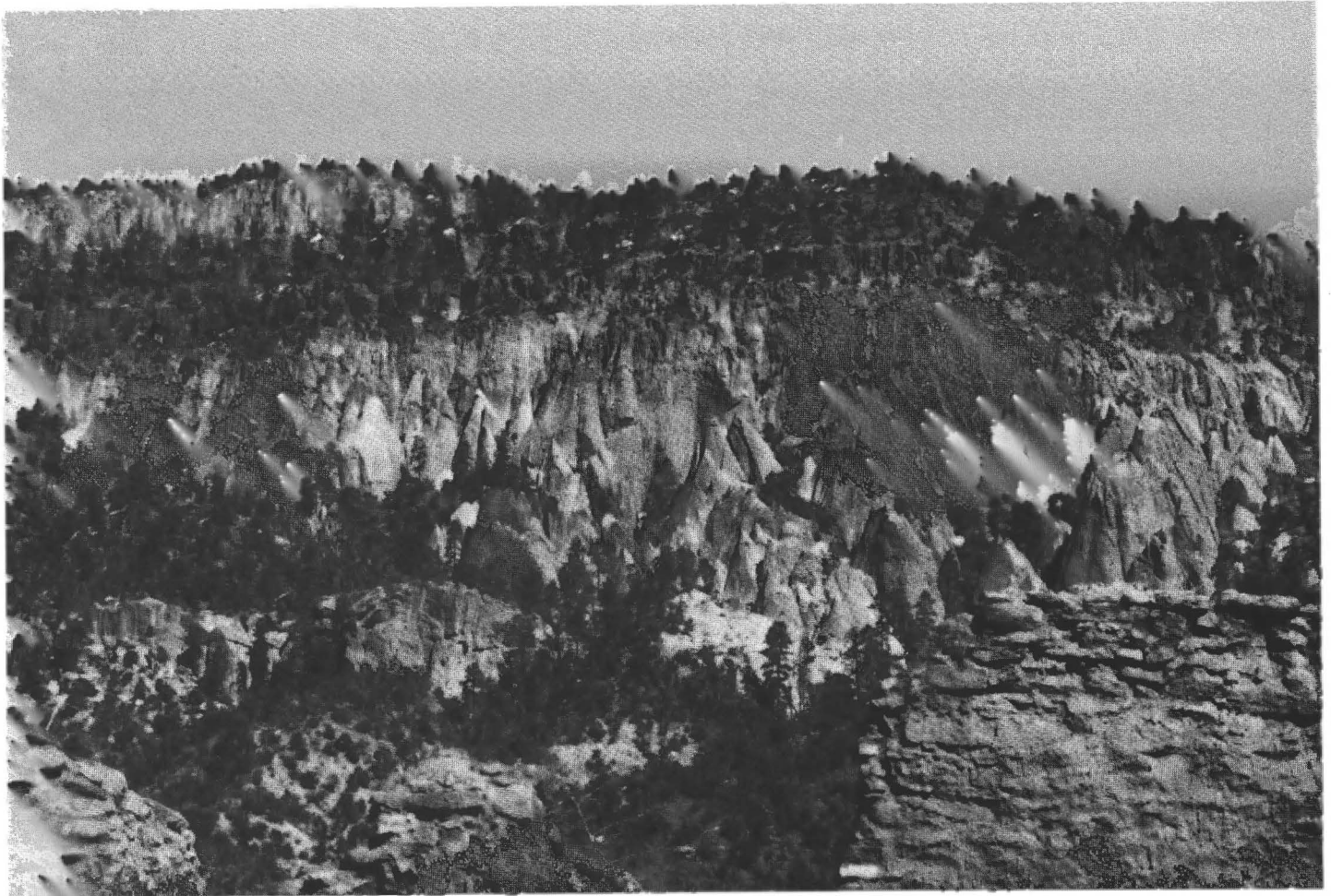
- 109.2 Junction with NM-501. **Turn left. 0.1**
- 109.3 MP 3. **0.1**
- 109.4 Roadcuts expose Unit F on top and Unit E at base. Road follows the dip-slope on contact between these units. **1.2**
- 110.6 Junction with West Road into Los Alamos Canyon on left. **0.2**
- 110.8 Traffic light at Pajarito Road on right. **0.2**
- 111.0 Traffic light at Diamond Drive. **Turn left** and move into right lane as you cross the bridge. **0.1**
- 111.1 Omega Bridge crosses Los Alamos Canyon and was built in 1951 to connect the new, post-World War II expanding lab “campus” with the new, burgeoning residential and commercial community of Los Alamos. **0.3**
- 111.4 Traffic light. Emergency entrance to Los Alamos Medical Center on right. The original hospital was located near Ashley Pond during the Manhattan Project. The present hospital serves a great part of northern New Mexico in addition to Los Alamos. **0.1**
- 111.5 **Bear right** onto Trinity Drive (NM-502). Trinity Drive was named after the first atomic test detonated 255 mi south of Los Alamos near Socorro, New Mexico on July 16, 1945, demonstrating the success of the frantic 2.5 year secret work during the Manhattan Project. **0.7**
- 112.2 Traffic light at Oppenheimer Drive. **0.1**
- 112.3 Police Station and Los Alamos County Building on left. **0.1**
- 112.4 Ashley Pond on left; Los Alamos Inn on right. Ashley Pond was originally a low, marshy area which collected rain and snow-melt. When Los Alamos was a Ranch School (a private prep school for boys), the pond served as a place for year-round recreation. Ice was cut from it and stored in an ice house where today’s historic marker sits in a small shelter at the pond’s southern edge. The pond was named Ashley Pond in honor of the founder of the Los Alamos Ranch School whose name was also Ashley Pond (The geographical pun was irresistible, it seems). **0.1**
- 112.5 20th Street. Turn left to reach Fuller Lodge. **0.1**
- 112.6 Traffic light at 15th Street. **0.2**
- 112.8 Los Alamos County Annex on right. Get in left lane. **0.2**
- 113.0 DP Road splits to right. Hilltop House, on left, has undergone many interesting face-lifts and renovations. It was originally a gas station until the entire first floor was lifted hydraulically to become the second floor, allowing a drive-through entrance to the lobby. The dining room on the top floor was originally a campus chapel in Texas. The owners, the Waterman family (doing business as TRK Management), have been in construction and house-moving projects since the post-war years, when their firm moved many Manhattan Project structures all over northern New Mexico to serve other purposes. **0.1**
- 113.1 **Turn left** on 4th Street. **Then left again** onto Central Avenue. **0.4**
- 113.5 Traffic light at 15th Street. Bradbury Science Museum on right. **0.2**
- 113.7 Los Alamos Post Office on right. During World War II, mail to Los Alamos residents at the top-secret project was simply addressed to P.O. Box 1663, Santa Fe, New Mexico. The “Secret City” acquired a post office only after the war, when its existence was made known to the outside world. The Post Office opened in this facility in November 1948. **0.1**
- 113.8 Fuller Lodge on right is just past intersection with 20th Street to the left. Continue until you reach 20th Street on the right. Turn right and park.

Fuller Lodge, today’s cultural center for Los Alamos, was one of two major log buildings constructed for the Los Alamos Ranch School. When it was built in 1928, it served as a dining hall, quarters for some of the staff, and

one room served as an infirmary. It was designed by famed southwestern architect John Gaw Meem, whose most notable buildings are La Fonda, the Pueblo-revival style hotel in Santa Fe, and Zimmerman Library on the UNM Campus in Albuquerque, New Mexico. Fuller Lodge was Meem's only log structure. Today one can also find remnants of the boys' school in the buildings known as "Bathtub Row," private houses to the north of Fuller Lodge. The most famous resident of "Bathtub Row" after the Ranch School was taken over by the Manhattan Project was J. Robert Oppenheimer, whose house was at the corner of today's 20th and Peach Streets. It is a private residence, but one can drive or walk by the exterior.

Fuller Lodge was named for Edward P. Fuller, a staff member of the Ranch School. It is made of 771 massive pine logs, personally chosen by architect John Gaw Meem and Ranch School Director A. J. Connell. Today the Lodge is used for social gatherings and meetings, and houses County offices, the Fuller Lodge Art Center, the archives of the Historical Museum and the Los Alamos Cultural Arts Council. Between 1946 and 1966 it served as a hotel and restaurant. The Lodge, nicknamed, "Your Host on the Hill," was the only hotel until the Los Alamos Inn opened in 1966.

The banquet this evening will be held at Fuller Lodge.
End of First-Day road log.



West wall of San Diego Canyon from Jemez State Monument (note ruins in foreground; see mile 72, First-day road log). These "tent rocks" are developed from the slightly welded Otowi Member of the Bandelier Tuff. Cliff-forming units above the tent rocks are welded tuffs of the Tshirege Member.